Coordination Chemistry Reviews 254 (2010) 832–875

Contents lists available at ScienceDirect

Coordination Chemistry Reviews

journal homepage: www.elsevier.com/locate/ccr

Review

An overview of the chemistry of homo and heteropolynuclear platinum complexes containing bridging acetylide (μ-C≡CR) ligands

Jesús R. Berenguer, Elena Lalinde*, M. Teresa Moreno

Departamento de Química-Grupo de Síntesis Química de La Rioja, UA-CSIC, Universidad de La Rioja, Madre de Dios 51, 26006 Logroño, Spain

Contents

ARTICLE INFO

Article history:
Received 2 October 2009
Accepted 3 December 2009
Available online 11 December 2009

Keywords:
Platinum
Bridging acetylide ligands
Polynuclear complexes
Photoluminescence

ABSTRACT

Different aspects of transition metal alkynyl chemistry have been widely studied over the past decades because of their interesting structures, chemical reactivity and properties. This review describes the chemistry of homo and heteropolynuclear platinum complexes containing bridging ligands, with special emphasis in synthetic routes, structural aspects and photoluminescence properties.

1. Introduction

Since the overall review of transition metal alkynyl chemistry by Nast in 1982 [1], there has been a much growth in the development of this topic. In this period, excellent reviews and monographs dealing with different aspects related to this type of complex have been published [2–19]. The interest in alkynyl metal complexes stems not only from their rich structural diversity [5,6,9,11,18–22] and interesting chemical reactivity [2,4,8,14,23–28], but also from their increasing potential in Material Science [15–17,29–31]. In particular, the favourable electronic and structural features of the alkynyl units, and their ability to interact with metal centers *via* significant pπ–dπ overlap (which can be modulated by introduction of aromatic conjugated spacers or variation of the metal), have made versatile building blocks of these ligands for the preparation of carbon rich oligomeric and polymeric materials with unique properties, such as optical non-linearity, electrical conductivity and liquid crystallinity [15–17,30,32–39]. This field has recently been stimulated by the attractive photochemical and photophysical (luminescence) behaviour associated with some of these complexes with promising applications in light emitting diodes, optical

Abbreviations: cod, 1,5-cyclooctadiene; cy, cyclohexyl; dmbpy, 4,4′-dimethyl-2,2′-bipyridine; dppa, bis(diphenylphosphino)acetylene; dppb, 1,4-bis(diphenylphosphino)butane; dppe, 1,2-bis(diphenylphosphino)ethane; dppet, *cis*-1,2-bis(diphenylphosphino)ethylene; dppm, bis(diphenylphosphino)methane; dppp, 1,3-bis(diphenylphosphino)propane; Fc, ferrocenyl; nb, norbornadiene; $(OBET)H_2$, *o*-(bisethynyl)tolane; OTf, triflate; phen, 1,10-phenanthroline; py, pyridine; R_f, pentafluorophenyl; thf, tetrahydrofurane; tht, tetrahydrothiophene; trpy, 2,2′,6′,2″-terpyridine.

* Corresponding author. Fax: +34 941 299 621.
E-mail address: elena.lalinde@unirioja.es (E. Lalinde).

0010-8545/$ – see front matter © 2009 Elsevier B.V. All rights reserved.
doi:10.1016/j.ccr.2009.12.010

sensors, molecular devices, etc. [36,40–48]. Furthermore, acetylide-functionalized oligopyridine bifunctional ligands with favourable electronic conjugation have been also utilized for the construction of heterometallic arrays involving d and/or f metal centers, which exhibit peculiar photophysical and electrochemical properties [40,49–51].

On the other hand, the ability of the MC≡CR entity to model the bonding capabilities of the alkyne ligand by using the triple bond of the alkynyl fragment is well documented. Its structural properties have been used to produce bi-, tri- and multi-nuclear aggregates and also a series of cluster complexes. Recent comprehensive reviews related with alkynyl metal complexes include advances in homo and heteropolynuclear alkynyl bridging complexes [8,9,11,12,15–19,21,22,36,42–47].

The scope of this article is confined to the synthesis and properties of homo and heteropolynuclear platinum complexes containing μ-C≡CR ligands, with particular attention to structural aspects and the photoluminescence behaviour of some of these systems.

2. Homometallic complexes

In polynuclear platinum complexes the alkynyl bridging coordination bonding modes shown in Chart 1 have been reported.

Complexes included in this group can be divided in bi- and polymetallic derivatives containing additional ancillary bridging groups (Section 2.1) and systems bearing μ-C≡CR groups as unique bridging ligands (Section 2.2).

2.1. Complexes with ancillary bridging groups

The 30 valence electrons diplatinum complex [(PCy_3)(C≡CPh)Pt(μ-κC^{α}:η^2-C≡CPh)(μ-$SiMe_2$)Pt(PCy_3)] (**1**) containing a κC^{α}:η^2 phenylethynyl bridging ligand, and reported by Stone et al., was the first example of this type of complex. This and two other related derivatives were prepared from silicon–carbon bond cleavage of $SiMe_2(C{\equiv}CPh)_2$ with [Pt(η^2-$C_2H_4)_2$L] (L = PCy_3, $PMeBu^t$, $PPr^i{}_2Ph$) [52]. Since then, different types of complexes have been reported. One notable type of alkynyl-bridged complexes in this group is the so-called A-frame diplatinum derivative, containing bis(diphenylphosphino)methane (dppm) ligands. The first report concerned on the isolation of a series of dimethyl compounds [MePt(μ-κ$^2C^{\alpha}$–C≡CR)(μ-dppm)$_2$PtMe]BF_4 (**2**, Eq. (1)), which were assumed to contain the rare 1e$^-$ type **A** (Chart 1) symmetrically bonded μ-κ$^2C^{\alpha}$–C≡CR ligand, as was confirmed by X-ray diffractometric methods in the propynyl complex (R = Me) [53]. Unfortunately, the ν(C≡C) expected bands are extremely weak or absent.

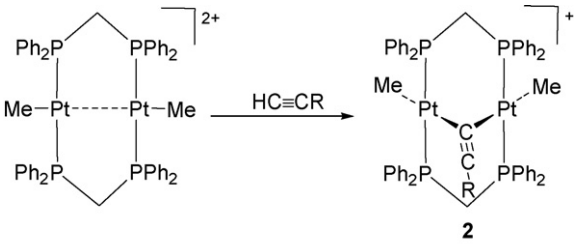

R = Me, H, Ph, C(OH)EtMe, -C-(OH)-$(CH_2)_5$ (1)

As suggested by Shaw and co-workers [53], electronic factors presumably control the alkynyl bonding mode with the high *trans* influence of the methyl groups disfavouring the more usual κC^{α}:η^2 (σ,π, type **B**, Chart 1) bonding mode. In fact, treatment of [$PtCl_2$(dppm)] with LiC≡CBu^t [54], or [Pt(dppm)$_2$]Cl_2 with HC≡CR (R = Ph, *p*-C_6H_4OMe, *p*-C_6H_4OEt, *p*-C_6H_4Et, *p*-C_6H_4Ph) in the presence of $Hg(OAc)_2$ (ethanol, reflux) [55,56], rendered the A-frame diplatinum acetylide cationic derivatives [Pt_2(μ-dppm)$_2$(μ-κC^{α}:η^2-C≡CR)(C≡CR)$_2$]$^+$ (**3**, Scheme 1), containing one bridgehead σ,π(κC^{α}:η^2) alkynyl ligand. Attempts to obtain the tert-butylacetylide derivative by this latter method failed, yielding the related asymmetrical complex [Pt_2(μ-dppm)$_2$(μ-κC^{α}:η^2-C≡CBu^t)Cl(C≡CBu^t)]$^+$ (**4**) crystallized as the ClO_4^- salt (Scheme 1). The Pt···Pt bond distances range from 3.117(3) to 3.236 Å, slightly longer to that found in [MePt(μ-κ$^2C^{\alpha}$–C≡CMe)(μ-dppm)$_2$PtMe]BF_4 (**2**) (3.025(2) Å). These complexes are fluxional even at low temperature (233 K), involving both a κC^{α}:η^2-alkynyl bridging exchange and a pseudoboat inversion and, upon raising the temperature above 298 K, an easy terminal to bridging alkynyl exchange is also observed [55–57]. However, three distinct ν(C≡C) stretches were observed in FT-Raman and IR spectra of [Pt_2(μ-dppm)$_2$(μ-κC^{α}:η^2-C≡CPh)(C≡CPh)$_2$]PF_6 (2125, 2062 and

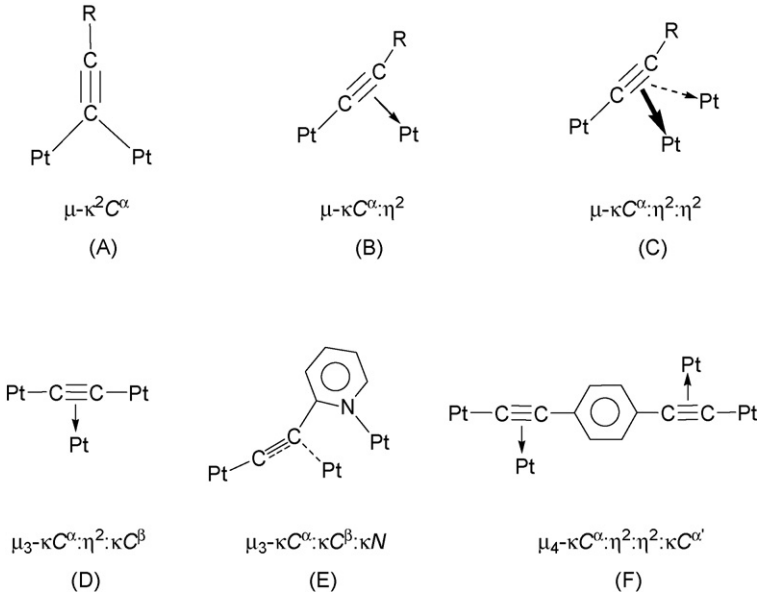

Chart 1.

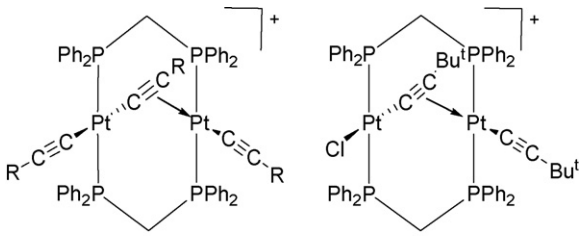

Scheme 1.

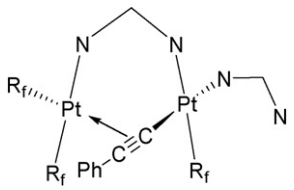

Chart 2.

2027 cm^{-1}) corresponding to three different acetylide environments. All derivatives exhibit rich long-lived photoluminescence in both solution and solid state [55–57]. On the basis of the variation of the alkynyl substituents, the Pt···Pt distances and resonance Raman experiments [58], the emissions were assigned as derived from states metal–metal-to-ligand charge transfer (^{3}MMLCT).

The reaction of [*cis*-Pt(R_f)$_2$(napy)] (R_f = C_6F_5, napy = 1,8-naphthyridine) with HC≡CPh affords a neutral asymmetrical complex [(R_f)$_2$Pt(μ-C≡CPh)(μ-napy)PtR_f(napy)] (**5**, Chart 2), stabilized with two different bridging ligands: the acetylide in a κ$C^α$:η^2-coordination and one 1,8-napy ligand [59]. In agreement with the higher *trans* influence of the C_6F_5 groups with respect to the terminal napy group, the alkynyl is κ$C^α$ bonded to the Pt$R_f N_2$ fragment and η^2 to the Pt(R_f)$_2$N one.

In this section, our group has shown that the bis(pentafluorophenyl) disolvento complex [*cis*-Pt(R_f)$_2$$S_2$] (S = tetrahydrofuran) is an excellent precursor to isomeric diplatinum complexes with a mixed (μ-hydride) (μ-acetylide) bridged system (Scheme 2). Thus, the diplatinum *gem* isomers [*cis*,*cis*-(PPh$_3$)$_2$Pt(μ-H)(μ-C≡CR)Pt(R_f)$_2$] (**6**) are accessible *via* direct C–H activation of terminal alkynes, when the η^2-alkyne Pt^0 complexes [Pt(η^2-HC≡CR)(PPh$_3$)$_2$] interact with the solvento [*cis*-Pt(R_f)$_2$$S_2$] [60–62] (Scheme 2, *i*). The reaction takes place in very mild conditions, and has a notable group functionalization tolerance. However, the reaction with [Pt{η^2-HC≡CC(OH)Ph$_2$}(PPh$_3$)$_2$] is sensitive to the presence of traces of water, also leading to the formation of the (μ-hydroxy)(μ-vinyl) [*cis*,*cis*-(PPh$_3$)$_2$Pt{μ-κ$C^α$:η^2-CH=CHC(OH)Ph$_2$}(μ-OH)Pt(R_f)$_2$] (**7**, Scheme 2, *ii*) as a by-product, as was confirmed by X-ray [61]; and we observed a competitive process between C–H and P–C(PPh$_3$) bond activations with [Pt(η^2-HC≡CR)(PPh$_3$)$_2$] (R = Bu^t, SiMe$_3$) (Scheme 2, *iii*) [62]. Control of some of these reactions at low temperature suggests the formation of an alkyne bridging mixed valence Pt^0···Pt^{II} (Scheme 2, **A**) as intermediate species.

Curiously, the related reactions with the corresponding Pt^{II} isomers [*trans*-PtH(C≡CR)(PPh$_3$)$_2$] (CH_2Cl_2, 30 min) evolve with an easy ligand redistribution process, giving rise to the isomeric *trans* complexes [*trans*-(PPh$_3$)R_fPt(μ-H)(μ-C≡CR)PtR_f(PPh$_3$)] (**9**,

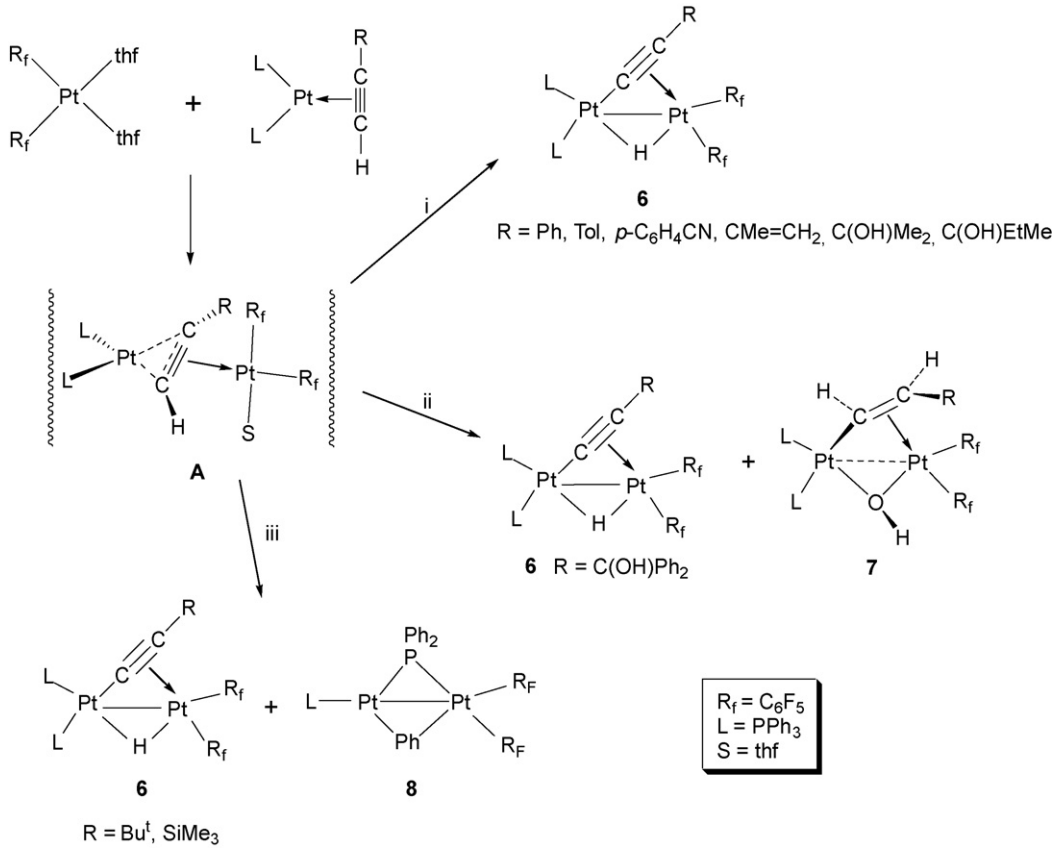

Scheme 2.

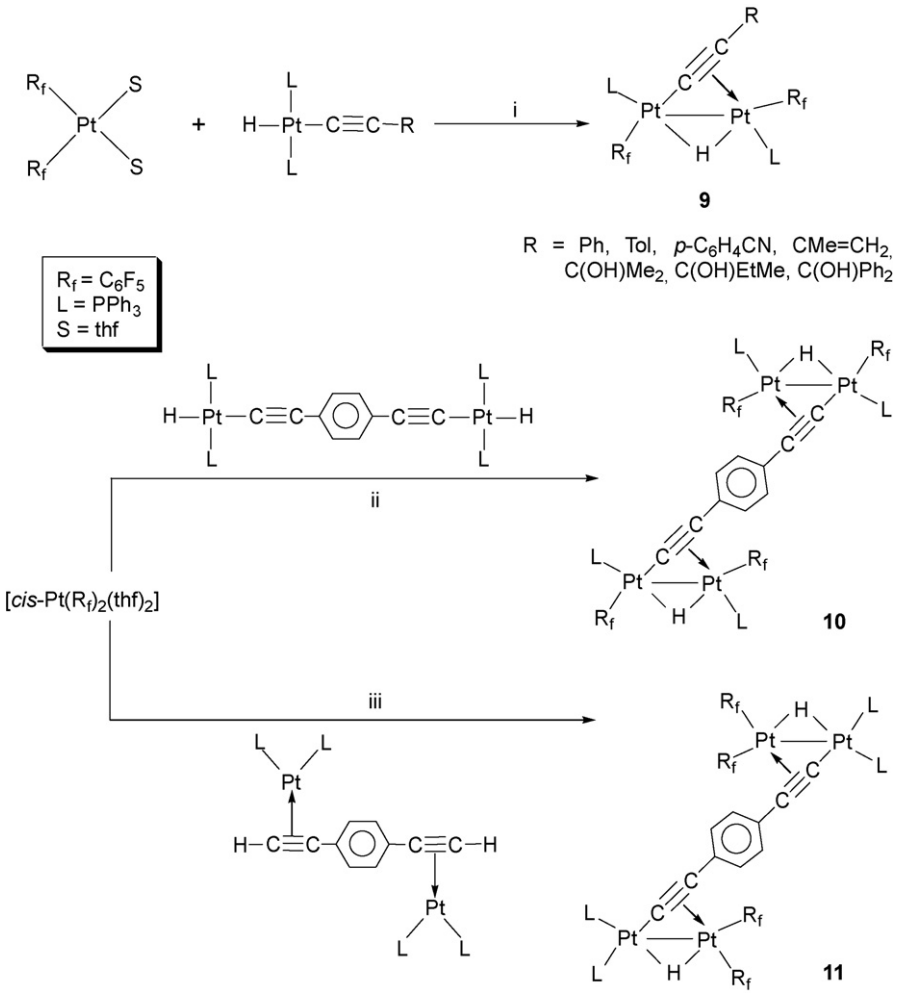

Scheme 3.

Scheme 3, *i*) [60,61,63]. X-ray crystal structures of *gem* (**6**, R = Ph, Tol, CMe = CH_2, C(OH)EtMe, $SiMe_3$) and *trans* (**9**, R = Tol, *p*-C_6H_4CN) derivatives reveals the presence of planar diplatinum cores, having very short Pt···Pt distances (2.8293(5)–2.8459(9) Å), in agreement with a total count of 30 valence electrons, and the alkynyl ligand bonding in a κC^{α}:η^2 fashion. Although some differences could be expected in the κC^{α} (Pt–C_{α}, 1.935(15)–2.024(10) Å) and η^2 (Pt–C_{α},C_{β} 2.172(11)–2.354(12) Å) distances in both types of isomers, due to the different *trans* influence of the C_6F_5 and PPh_3 ligands, the observed bond distances are essentially identical within experimental error. Extension of both processes to the dihydride diplatinum [{*trans*-$PtHL_2$}$_2${μ-κC^{α}:$\kappa C^{\alpha'}$-(1,4-C≡C)$_2C_6H_4$}] (Scheme 3, *ii*) and the isomeric diine [{PtL_2}$_2${μ-η^2:η^2-(1,4-HC≡C)$_2C_6H_4$}] (Scheme 3, *iii*) (L = PPh_3) precursors affords the corresponding tetranuclear bis(μ-hydride)(μ-diethynylbenzene) complexes [60]. The crystal structure of [{*trans*-(PPh_3)R_fPt(μ-H)PtR_f(PPh_3)}$_2${μ_4-(1,4-C≡C)$_2C_6H_4$}] (**10**) confirms the presence of the central *p*-diethynylbenzene, which is attached to two diplatinum units *via* the alkynyl fragments (κC^{α}-bonded to one Pt and η^2 to the other, Fig. 1).

Complexes [*cis*-Pt(C≡CR)$_2$(PPh_2C≡CR′)$_2$] (R, R′ = Ph, Bu^t; R = *p*-C_6H_4–C≡CPh; R′ = Tol, *p*-C_6H_4–C≡CPh) [64,65], having polyfunctional alkynylphosphines as auxiliary ligands, are useful precursors for the synthesis of interesting triplatinum complexes. The final outcome of their reactions with [*cis*-Pt(R_f)$_2$$S_2$] depends on the molar ratio (see Section 2.2) and the alkynyl substituents. In a 1:1 molar ratio, exclusive coordination of the "Pt(R_f)$_2$" unit to the alkynyl ligands, with formation of chelating type 1:1 adducts [*cis*,*cis*-(PPh_2C≡CR′)$_2$Pt(μ-κC^{α}:η^2-C≡CR)$_2$Pt(R_f)$_2$] (**12**) takes place [64,65]. However, in 1:2 molar ratio the results strongly depend on the substituents. Thus, the *tert*-butyl and ethynyltolan derivatives evolve with formation of symmetrical triplatinum complexes (**13A**, Chart 3), having two mixed alkynyl/phosphinoalkynyl bridging systems, as confirmed by spectroscopic means and X-ray crystallography. The related [*cis*-Pt(C≡CPh)$_2$(PPh_2C≡CBu^t)$_2$] derivative affords an unusual symmetrical complex (**13B**, Chart

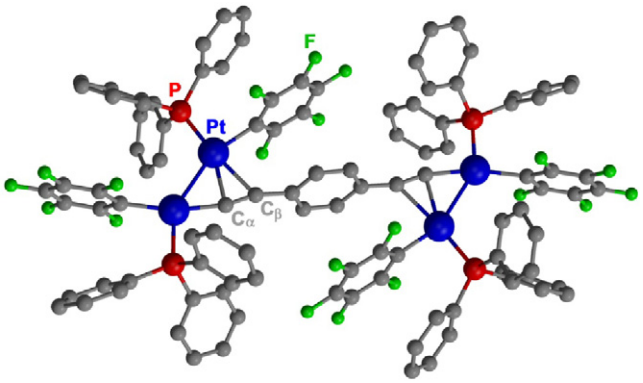

Fig. 1. X-ray structure of [{*trans*-(PPh_3)R_fPt(μ-H)PtR_f(PPh_3)}$_2${μ_4-(1,4-C≡C)$_2C_6H_4$}] (**10**) (Ref. [60]).

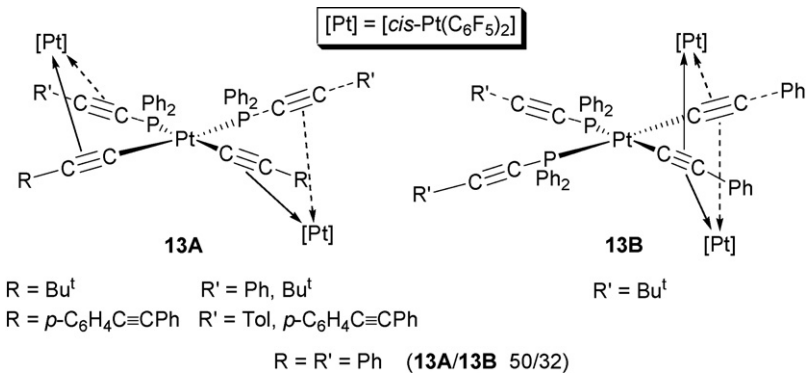

Chart 3.

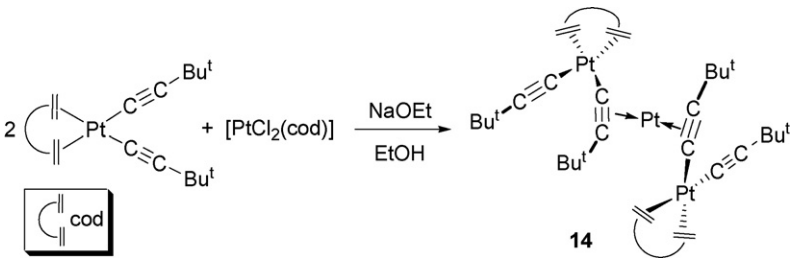

(2)

3), with the phenylethynyl entities acting as six-electron μ_3-κC^{α}:η^2:η^2 bridging ligands, due to the poor η^2 donor capabilities of the *tert*-butylethynylphosphine $PPh_2C{\equiv}CBu^t$, as confirmed by X-ray. However, a mixture of both types of isomers (50:32, **13A**:**13B**) is observed in the 1:2 reaction system [*cis*-$Pt(C{\equiv}CPh)_2(PPh_2C{\equiv}CPh)_2$]/$Pt(R_f)_2$; thus indicating the following η^2-bonding capability to the *hard* Pt^{II} *ion*: alkynyl > P-bonded phosphinoalkyne and C≡CPh > C≡C–C_6H_4–C≡C–Ph > C≡CBu^t fragments. However, the soft $PPh_2C{\equiv}CR$ ligands are always the preferred bonding ligands to the *low valent* "$Pt(PPh_3)_2$" unit [64,65].

2.2. Systems with alkynyl groups as unique bridging ligands

A good number of platinum complexes containing one or two alkynyl groups as unique bridging ligands have been reported. Typically, the preparation of these species is achieved by (a) reaction of a platinum σ-alkynyl complex with a platinum substrate containing labile ligands, and (b) by chloride alkynide exchange process.

The coordination of an alkynyl platinum(II) complex [Pt]–C≡CR to a Pt^0 center in η^2-manner is still quite rare. An interesting example was the trinuclear complex Pt^{II}–Pt^0–Pt^{II} [{(cod)(C≡CBu^t)Pt(μ-κC^{α}:η^2-C≡CBu^t)}$_2$Pt] (**14**), generated by treatment of [*cis*-$Pt(C{\equiv}CBu^t)_2$(cod)] with $[PtCl_2(cod)]$ (2:1 molar ratio) in the presence of NaOEt (Eq. (2)), or more straightforward by direct reaction of the Pt^{II} complex with $[Pt(\eta^2\text{-nb})_3]$ (nb = norbornadiene) [66].

A similar trinuclear complex [{Pt(PN)($SiMe_3$)(μ-κC^{α}:η^2-C≡CPh)}$_2$Pt] (**15**) (PN = $(Pr^i)_2PCH_2CH_2NMe_2$) has been recently detected as an intermediate species in the thermal Si–C(sp) bond activation of [Pt(PN)(η^2-$Me_3SiC{\equiv}CPh$)] to give [Pt(PN)($SiMe_3$)(C≡CPh)] [67]. η^2-Complexation of $Pt(PPh_3)_2$ to the remote alkyne fragment, rather than the inner alkynyl group, in [*trans*-PtH(C≡CRC≡CH)$(PPh_3)_2$] affords very stable hydride–alkynyl–alkyne Pt^{II}–Pt^0 complexes **16** (Eq. (3)) [68]. These complexes are emissive in frozen solutions, with emissions, on the basis of simple extended Hückel calculations [68], ascribed to ^{3}MLCT transitions located on the Pt^0 fragment.

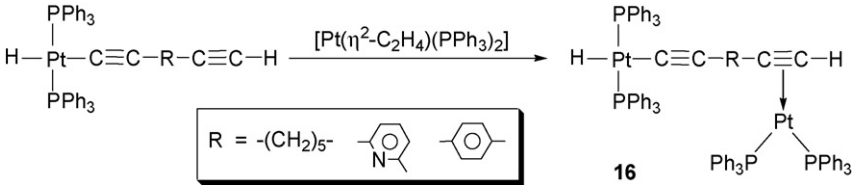

(3)

Complexation of a platinum(II) metal fragment to platinaalkynyl entities has been found more frequently. Reaction of anionic [*trans*-$Pt(R_f)_2(C{\equiv}CR)_2]^{2-}$ with 2 equiv. of the hydride cationic solvento complex [*trans*-$PtHL_2$(acetone)]$^+$ (L = PPh_3, PEt_3) forms the neutral trinuclear zwitterionic hydride platinum derivatives **17** (Eq. (4)) [69]. The crystal structure of the complex with R = Ph and L = PEt_3 confirms that the reaction takes place with retention of the σ-coordination of the alkynyl groups, which are η^2-bonded to the cationic "$PtHL_2$" units. This behaviour can be attributed to the very electrophilic nature of the "*trans*-$Pt(R_f)_2$" unit. A σ-migration of the alkynyl fragments would produce the less polar trinuclear com-

plexes [{*trans*-PtH(μ-κC^{α}:η^2-C≡CR)L_2}$_2${*trans*-Pt(R_f)$_2$}].

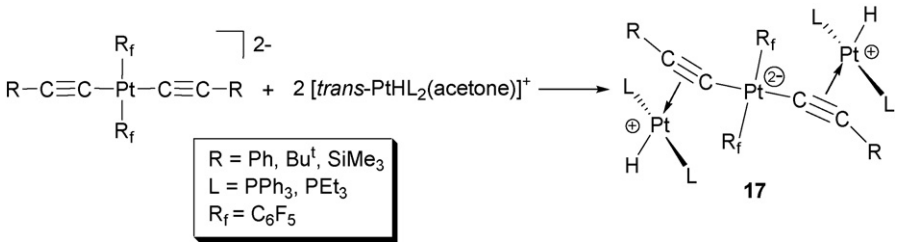

(4)

In contrast to this behaviour, neutral bis(alkynyl)platinum(II) complexes react with the solvento carbonyl substrate [*cis*-Pt(R_f)$_2$(CO)S] (S = thf) to give, after alkynyl transfer to the neutral fragment "*cis*-Pt(R_f)$_2$(CO)", the μ-κC^{α}:η^2 acetylide-bridged zwitterionic compound [*cis*,*trans*- *or cis*,*cis*-(CO)(R_f)$_2$Pt$^-$(μ-κC^{α}:η^2-C≡CR)Pt$^+$(C≡CR)L_2] **18** (Eq. (5)) [70–72]. The driving force for the alkynyl migration is the electrophilic nature of the bis(pentafluorophenyl)(carbonyl)platinum(II) unit, which determines a strong preference for the σ-coordination to the C_{α} alkynyl carbon atom. The crystal structure of the complexes [*cis*,*trans*-(CO)(R_f)$_2$Pt$^-$(μ-κC^{α}:η^2-C≡CR)Pt$^+$(C≡CR)L_2] (L = PPh$_3$; R = Ph [70], C(OH)EtMe [71]) **18** show that the Pt–C≡CR unit is oriented essentially perpendicular to the local coordination plane of the cationic platinum center. The η^2-alkynyl interaction is rather stable, but the trimethylsilyl derivatives interact easily with alcohols (EtOH, MeOH) to form the final (μ-ethynediyl)(methylalcoxycarbene) diplatinum complexes **19** (Eq. (6)), as it has been confirmed by X-ray crystallography [72]. Their formation is suggested to proceed by an initial desilylation of the alkynyl bridging ligand, and probably *via* (μ-ethynediyl)(vinylidene) species, which can undergo addition of ROH to afford the final carbene products [72].

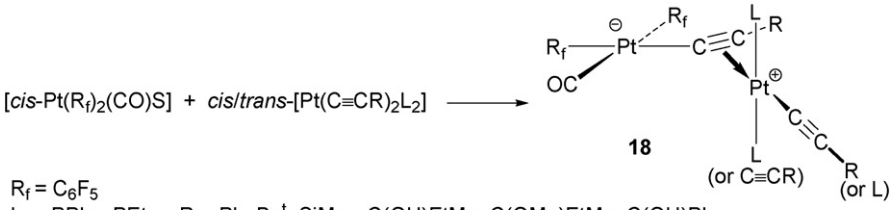

(5)

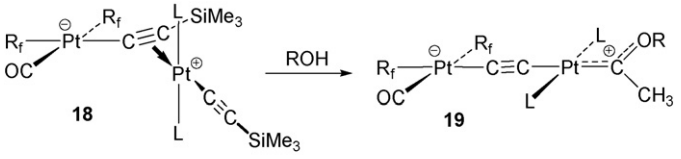

(6)

We have recently found that the reactions of the solvate [*cis*-Pt(R_f)$_2$(CO)S] with hydride–alkynyl platinum(II) complexes in CH_2Cl_2 provide an easy entry to final (μ-vinylidene)diplatinum compounds (**20**, Scheme 4, *i*) [73,74]. The reactions take place *via* initial alkynyl transfer to afford binuclear μ-acetylide compounds **21** (Scheme 4, *ii*), isolated at low temperature (−40 °C). The crystal structure of the complex with R = CMe=CH_2 reveals that the reaction takes place with initial stereoretention, confirming that the cationic "*trans*-PtH(PPh$_3$)$_2$" unit is η^2-bonded to the alkyne fragment of the alkynyl group of the monoanionic "*cis*-Pt(R_f)$_2$(C≡CCMe=CH_2)(CO)" fragment [73]. Complexes **21** evolve in solution at room temperature to the final (μ-vinylidene)diplatinum compounds **20** (Scheme 4, *iii*), and their structures have been confirmed by X-ray crystallography [73]. Their formation is presumed to proceed *via* an initial *trans* to *cis* isomerization of the cationic "PtH(PPh$_3$)$_2$" fragment, followed by a fast regioselective *cis*-1,2-addition of the Pt–H bond across the C≡C triple bond of the alkynyl bridging ligand. As shown in Scheme 4 (*iv*), the presence of one donor N atom in the aromatic ring of [*trans*-PtH(C≡CC_5H_4N-2)(PPh$_3$)$_2$] modifies the outcome of the reaction. In this case, the initial 1:1 adduct **22** evolves to a final zwitterionic derivative **23** (Scheme 4, *v*), with a bridging pyridylacetylide ligand bonded in a κC^{α}:κ*N* bonding fashion as confirmed by X-ray [73].

A different behaviour is found when this alkynyl-hydride [*trans*-PtH(C≡CC_5H_4N-2)(PPh$_3$)$_2$] reacts with the disolvate [*cis*-Pt(R_f)$_2$(S)$_2$] (Scheme 5). In this case, the initial adduct formed **24** (Scheme 5, *i*), containing a bridging κC^{α}:η^2:κ*N* pyridylacetylide ligand, slowly evolves (Scheme 5, *ii*) to an equimolecular mixture of the zwitterionic binuclear platinum complex **25** and a very unusual tetranuclear complex (**26**), which can be described as a formal zwitterionic cationic Pt_3 cluster alkynyl platinate complex [Pt]$^-$(μ$_3$-κC^{α}:κC^{β}:κ*N*-C≡CC_5H_4N-2)[Pt_3]$^+$, as confirmed by X-ray studies [75].

An interesting luminescent trinuclear platinum(II) terpyridyl complex ([{Pt(Bu^t$_3$-trpy)}$_3$(μ$_3$-κC^{α}:η^2:κC^{β}–C≡C–)]X$_4$, X = OTf, PF_6, **27**, Chart 4) has been prepared, by reaction of the ethynediyl complex [{Pt(Bu^t$_3$-trpy)}$_2$(μ-κC^{α}:κC^{β}–C≡C)]$^{2+}$ with 1 equiv. of the nitrile derivative [Pt(Bu^t$_3$-trpy)(NCMe)]$^{2+}$ [76]. The crystal structure shows that the naked $C\equiv C^{2-}$ moiety coordinates in a κ$C^{\alpha,\beta}$ fashion to two Pt^{II} atoms, and connects to the third one in a η^2-bonding fashion. However, the complex exhibits an easy topomerization in solution, even at −80 °C, which is suggested to arise from rotation of the C≡C unit through a σ–π exchange process among the triangle of the three Pt atoms. η^2-complexation of the third Pt(Bu^t$_3$-trpy)$^{2+}$ unit to the binuclear fragment {[Pt]–C≡C–[Pt]}$^{2+}$ ([Pt] = [Pt(Bu^t$_3$-trpy)]) shifts to shorter wavelengths both the absorption and phosphorescent emission bands, assigned to a mixed ^{3}MLCT/^{3}LL′CT {dπ(Pt) → π*(Bu^t-trpy)/π(C≡C) → π*(Bu^t$_3$-trpy)} transition, on the basis of theoretical calculations.

Many di- and triplatinum complexes in which the platinum(II) centers are stabilized by double bridging alkynyl systems have been reported. Only complexes with the alkynyl ligand acting as

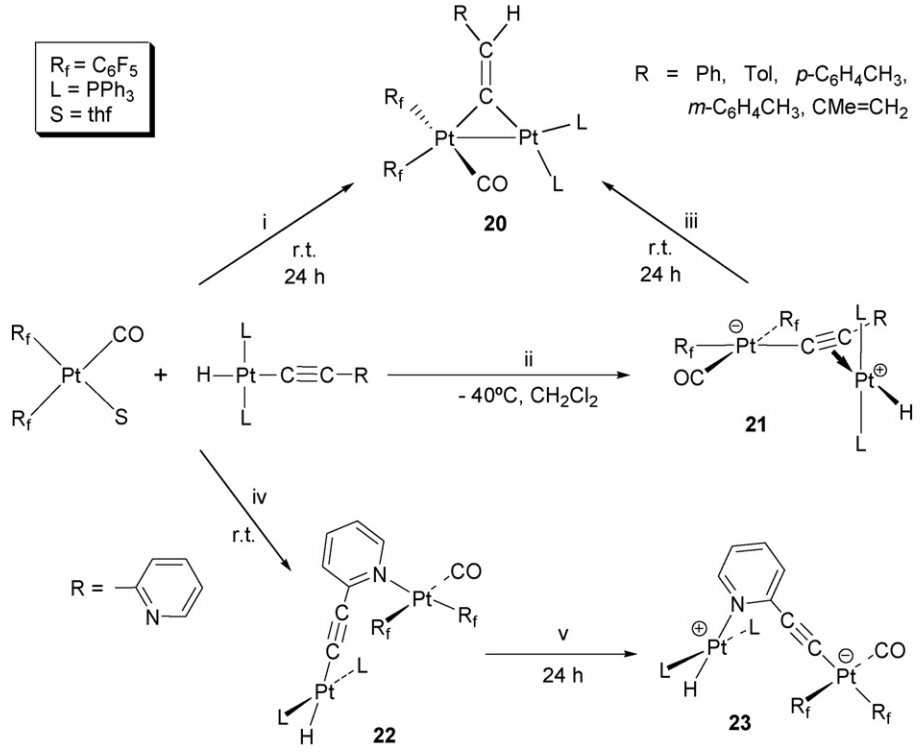

Scheme 4.

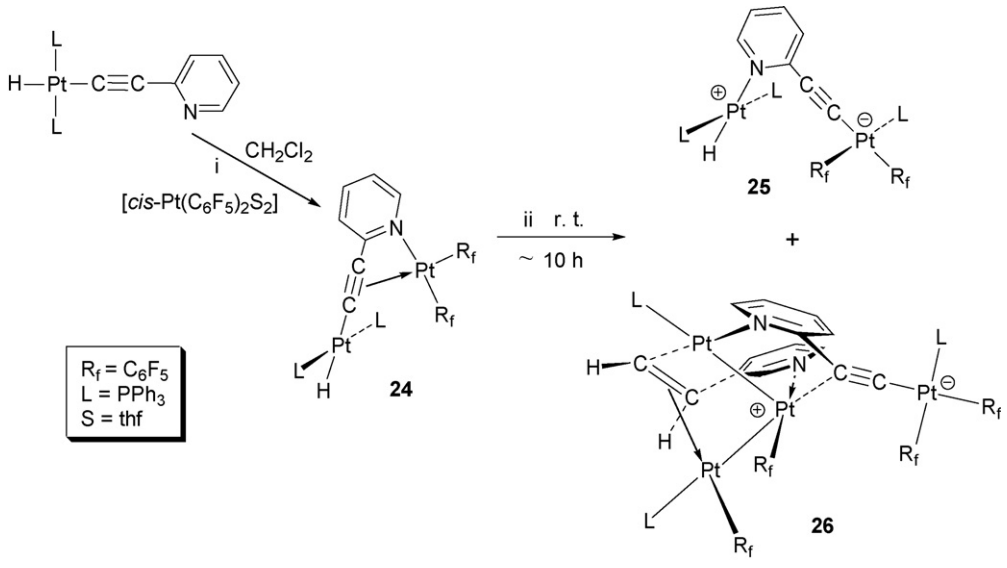

Scheme 5.

four (**B**, Chart 1) or six (**C**, Chart 1) electron donor are known. These complexes exhibit conformations of the types **A**–**E** shown in Chart 5.

Complex [*cis*-Pt(R_f)$_2$$S_2$] (S = thf), with two weak donor tetrahydrofuran ligands, is an excellent precursor to the synthesis of bi- and triplatinum complexes stabilized by double-alkynyl bridging systems (Scheme 6). The reactions with *cis*-bis(alkynyl)platinum(II) complexes render asymmetrical diplatinum complexes **28** (Scheme 6, *i*), having V-shaped bridges in which the "*cis*-Pt(R_f)$_2$" unit is η^2:η^2-coordinated to the neutral chelating 3-platina-penta-1,4-diyne (**C**, Chart 5) [77]. Despite the presence of alkynylphosphine groups ($PPh_2C{\equiv}CR$; R = Ph, Bu^t, Tol, *p*-C_6H_4–C≡CPh **28**), or indeed the alkynediphosphine $PPh_2C{\equiv}CPPh_2$ (**29**, Scheme 6, *ii*), with potential η^2-bonding capability, exclusive coordination of the acidic Pt(R_f)$_2$ unit to the alkynyl fragments takes place [64,65,78]. An unusual triplatinum complex [{*cis*-($PPh_2C{\equiv}CBu^t$)$_2$Pt(μ-κC^{α}:η^2:η^2-C≡CPh)$_2$}{Pt(R_f)$_2$}$_2$] (**30**), with the precursor acting as a chelating tetradentate bridging ligand (**D**, Chart 5), is generated by using a 2:1 molar ratio (Scheme 6, *iii*), as confirmed by X-ray crystallography [65]. All these V-shaped alkynyl bridging complexes exhibit fluxional behaviour, the activation energies of which have been determined.

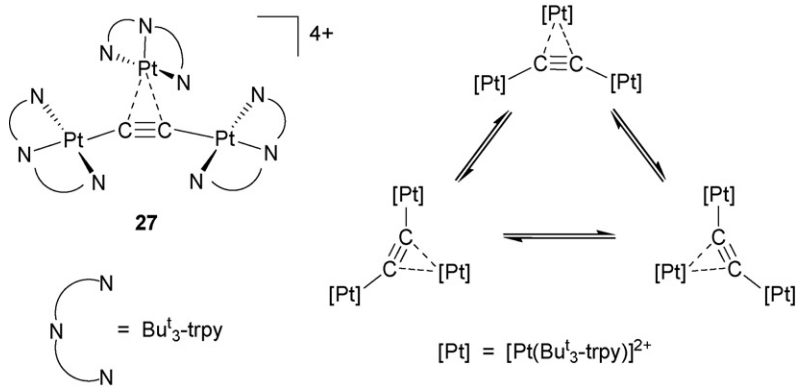

Chart 4.

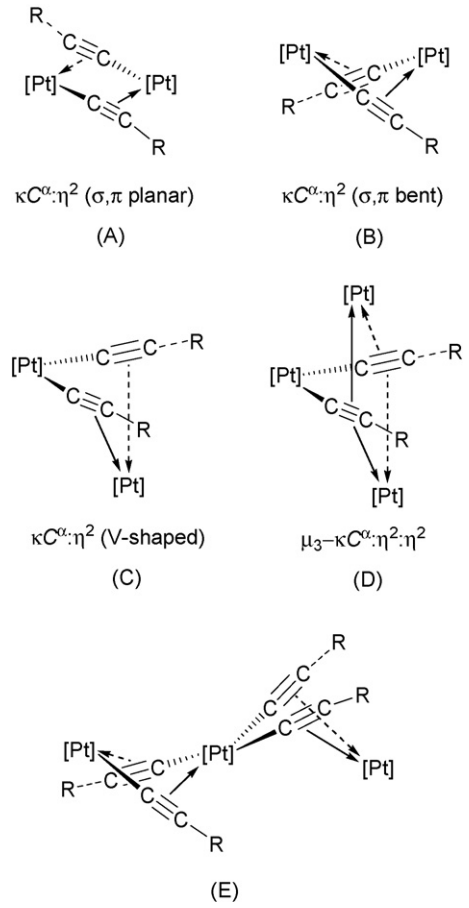

Chart 5.

However, the reaction of *trans*-configured derivatives [*trans*-Pt(C≡CR)$_2$L$_2$] with [*cis*-Pt(R$_f$)$_2$S$_2$] yields stereoselectively the *trans* diplatinum complexes [*trans*-Pt(μ-κ*C*^{α}:η^2-C≡CR)(R$_f$)L]$_2$ (**31**, L = PPh$_3$ [71,79], PPh$_2$H [80]), the formation of which requires a redistribution of the ligands (Scheme 6, *iv*) [71,79,80]. Their crystal structures and spectroscopic data confirm that, in all the cases, the isomer selectively formed has the PPh$_3$ ligand *cis* to the σ-alkynyl groups, thus avoiding steric phosphine···R-alkynyl substituent repulsions. In agreement with theoretical calculations [81], a clear preference for a bent conformation (**B**, Chart 5) is observed [82] (confirmed by X-ray for complexes with R = SiMe$_3$, Bu^t, C(OH)Ph$_2$, C(OH)Me$_2$, C(OMe)EtMe, Fc), except for complex [*trans*-Pt(μ-κ*C*^{α}:η^2-C≡CPh)(R$_f$)(PPh$_3$)]$_2$, which displays a planar central dimetallacyclic PtC$_4$Pt core (**A**, Chart 5). As expected, the Pt···Pt distance in this derivative (3.653(1) Å) is longer than the values observed in the bent analogues (3.2238(4) Å for R = Fc to 3.5108(8) Å for R = SiMe$_3$) or in the V-shape compound [{(dppe)Pt(κ*C*^{α}:η^2-C≡CPh)$_2$}Pt(R$_f$)$_2$] (3.27 Å). In solution, the κ*C*^{α}:η^2 pairwise intramolecular exchange of the acetylide ligands and fast inversion of the central ring (for bent conformations), presumably *via* intermediate bis(μ-κ^2*C*^{α}) (**A**, Chart 1) and/or unsymmetrical mixed (μ-κ^2*C*^{α})(μ-κ*C*^{α}:η^2) species, are also common features for this type of complex. The ν(C≡C) stretching vibration always occurs at lower wavelengths for rectangular σ,π-diplatinum complexes (**31**) (<2000 cm^{-1}, **A** and **B**, Chart 5) than for compounds with chelating V-shape arrangements (**28**–**30**) (>2000 cm^{-1}, **C**, Chart 5).

In [*trans*-Pt(μ-κ*C*^{α}:η^2-C≡CR)(R$_f$)L]$_2$ (**31**, L = PPh$_3$ [71,79], PPh$_2$H [80]), the η^2-alkynyl interaction is displaced by PPh$_3$ and py or PPh$_2$H, to give bridge-cleaved mononuclear complexes [71,79,80]. However, treatment of the diastereomeric mixture for R = C(OH)EtMe with HSPh (Eq. (7)) causes the coupling of the two alkynyl ligands to afford the novel diplatinum complex **32**, bridged by a mixed thiolate/cyclobutenediylidene bridging system [83].

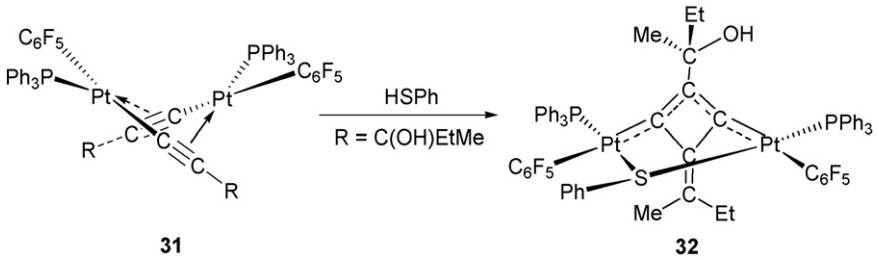

(7)

Similar binuclear cycloplatinate neutral complexes displaying bent σ,π-alkynyl bridging systems (**33**, **34**, Scheme 7) have been prepared by halide–alkynyl exchange reactions [84,85]. The isomers obtained with the κ*C*^{α}(alkynyl) *trans* to N or to the C carbon

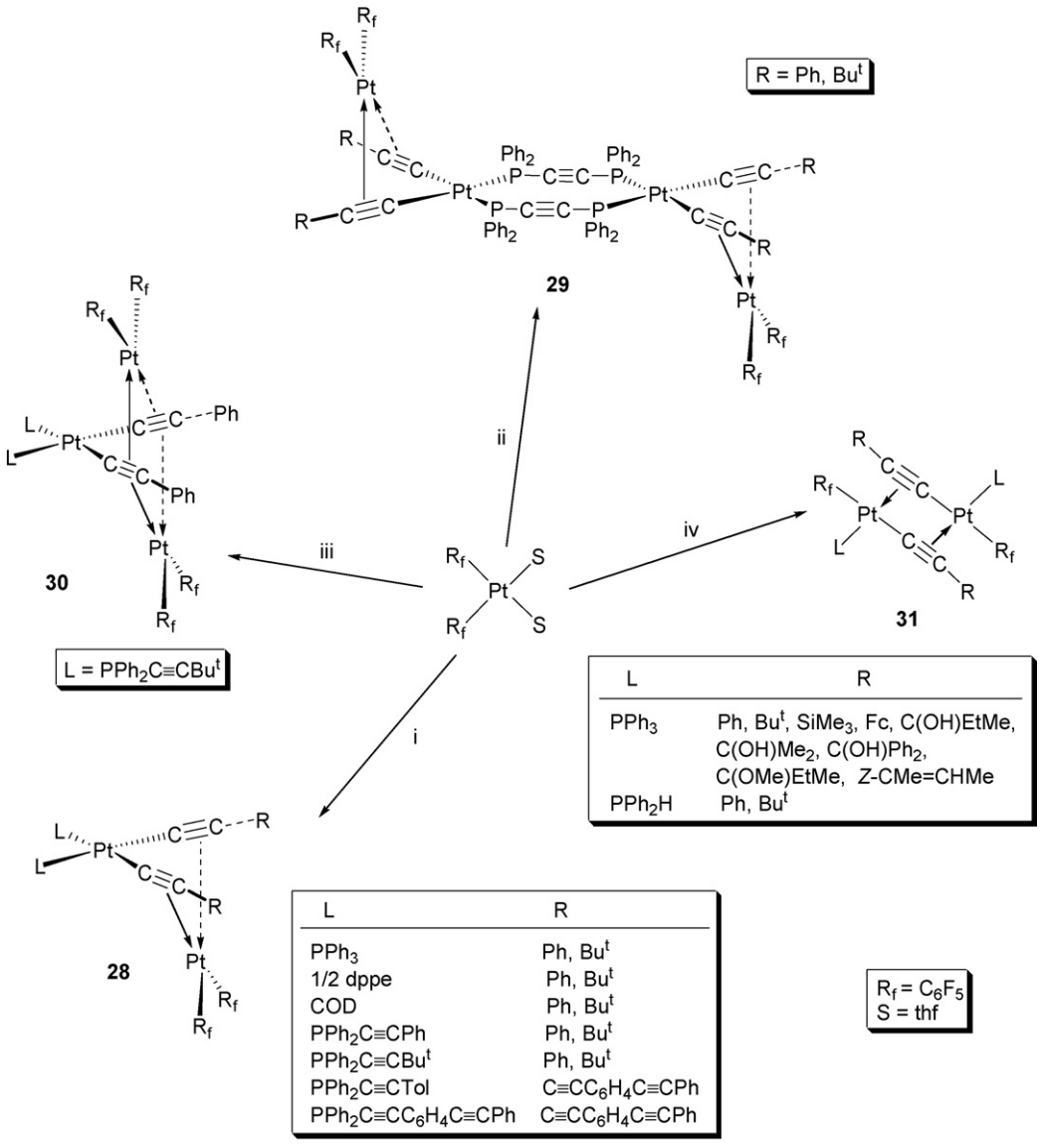

Scheme 6.

metalated seems to be determined by electronic (*transphobia*) and steric hindrance, respectively. As shown in the Scheme 7, the (C∧P) derivative **34** is also generated by neutralization reaction between the anionic *cis*-bis(alkynyl) complex $[Pt(C\wedge P)(C{\equiv}CPh)_2]^-$ with the solvate $[Pt(C\wedge P)(thf)_2]^+$, as a consequence of an alkynylating process [85]. This dimer **34** is quite labile and reacts with several ligands (PPh_3, CO, py, tht) to give mononuclear complexes [85].

Anionic mixed $[PtX_2(C{\equiv}CR)_2]^{n-}$ or homoleptic $[Pt(C{\equiv}CR)_4]^{2-}$ derivatives also react with $[cis\text{-}Pt(C_6F_5)_2S_2]$ (S = thf), acting as monoalkynylating agents to afford related rectangular σ,π-(C≡CR) diplatinum complex (**35**, **36**, Chart 6) [77,85,86]. These complexes were suggested to be formed *via* V-shape intermediate species $[\{[Pt](\mu\text{-}\kappa C^{\alpha}{:}\eta^2\text{-}C{\equiv}CR)_2\}Pt(R_f)_2]^{n-}$ (**C**, Chart 5), that subsequently transfer one alkynyl group from the more to the less charged platinum center. In the case of complexes **36**, the migration of one of the alkynyl ligands seems to decrease the alkynylating capability of the Pt center, and these bimetallic complexes interact with a second "$Pt(R_f)_2$" unit by simple η^2-complexation, giving rise to complexes **37** (Chart 6), having both a bent σ,π and a chelating V-shaped double-alkynyl bridging systems as confirmed by X-ray (R = Ph) [86]. Curiously, in spite of the fact that these trimetallic species have formally two negatively charged adjacent Pt centers, and they are highly fluxional in solution (formal D_{2h} symmetry at room temperature), no evidence of further rearrangement under thermal conditions has been found [86]. Similarly, simple complexation of the cation "$Pt(\eta^3\text{-}C_3H_5)^+$" takes place in the final zwitterionic anionic derivative **38** (Chart 6), generated by reaction of $[cis\text{-}Pt(R_f)_2(C{\equiv}CSiMe_3)_2]^{2-}$ with $[Pt(C_3H_5)Cl]_4$ in 4:1 molar ratio [87].

3. Heterometallic complexes

Some of the complexes included in this section have been examined in different reviews, and therefore they will be more briefly discussed.

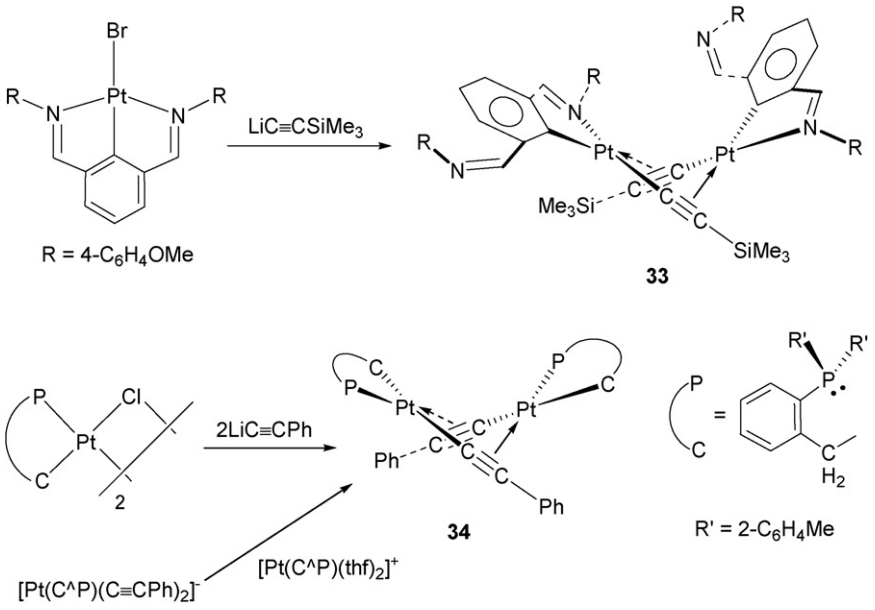

Scheme 7.

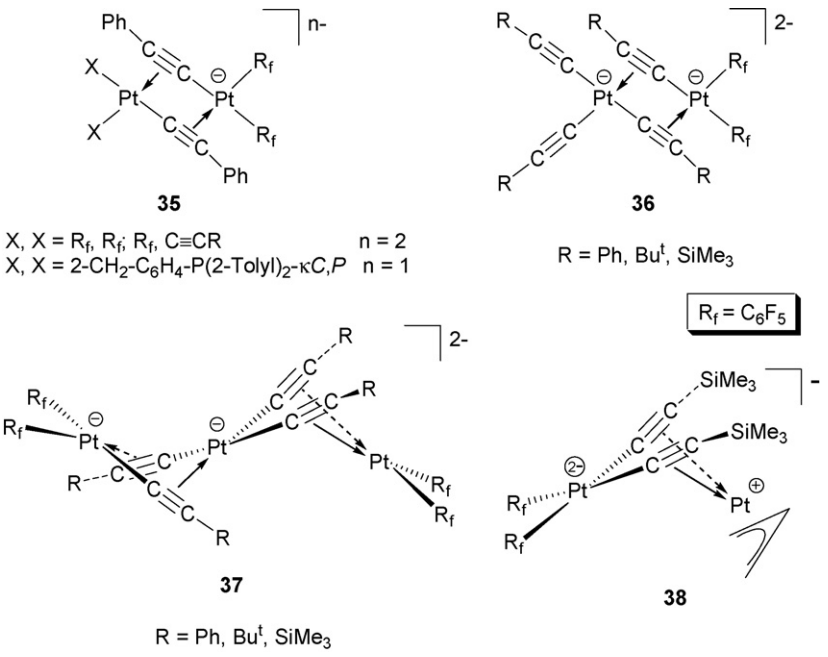

Chart 6.

3.1. Heteronuclear platinum-group 3–8 metal acetylide complexes

In a similar manner to organic 1-alkynes, interaction of $[Pt(\eta^2\text{-}C_2H_4)(PPh_3)_2]$ with the butadiynyl complex $[WCp(C{\equiv}C{-}C{\equiv}CH)(CO)_3]$ causes simple η^2-complexation of the low valent "$Pt(PPh_3)_2$" moiety to the uncoordinated alkyne fragment [88]. However, early-late titanium–platinum complexes with double-alkynyl bridging systems have been prepared starting from bis(alkynyl)titanocene precursors (Scheme 8). In the final complexes, the κC^{α}:η^2-alkynyl bonding preferences of the metal centers depend on the alkynyl substituents and the metal fragment. Thus, reaction of the phenylacetylide $[TiCp_2(C{\equiv}CPh)_2]$ [52] or the diyne complex $[Ti(\eta^5\text{-}C_5H_4SiMe_3)_2(C{\equiv}C{-}C{\equiv}CEt)_2]$ [89] with $[Pt(\eta^2\text{-}C_2H_4)_2L]$ or $[Pt(\eta^2\text{-}C_2H_4)L_2]$, respectively, affords chelating tweezer type complexes **39** (Scheme 8, *i*). However, we found that the reaction of the low valent "$Pt(PPh_3)$" fragment with the *tert*-butylacetylide derivative yields $[Cp_2Ti(\mu\text{-}\kappa C^{\alpha}\text{:}\eta^2\text{-}C{\equiv}CBu^t)(\mu\text{-}\kappa^2 C^{\alpha}{-}C{\equiv}CBu^t)Pt(PPh_3)]$ (**40**, Scheme 8, *ii*), the formation of which can be formally considered as the result of the oxidative addition of a Ti^{IV}–C^{α} bond to the Pt^0 substrate, to give a complex with a formal Ti^{III}–Pt^{I} bond (Ti–Pt = 2.789 Å) [90]. The complex is stabilized by a rather unusual doubly alkynyl bridging system, with one $C{\equiv}CBu^t$ group κC^{α}-bonded to titanium and strongly η^2-bonded to platinum (2.054(13), 2.191(15) Å), while the other is asymmetrically κC^{α}-bonded to both metals (Pt–C^{α} 1.990(13) Å, Ti–C^{α} 2.435(14) Å). The complex is highly fluxional (even at −92 °C), involving a fast intramolecular μ-$C{\equiv}CBu^t$ migration between the metal centers. Curiously, treatment of the same precursor ($[Cp_2Ti(C{\equiv}CBu^t)_2]$) with the more acidic platinum(II) "*cis*-$Pt(R_f)_2$" fragment gives rise

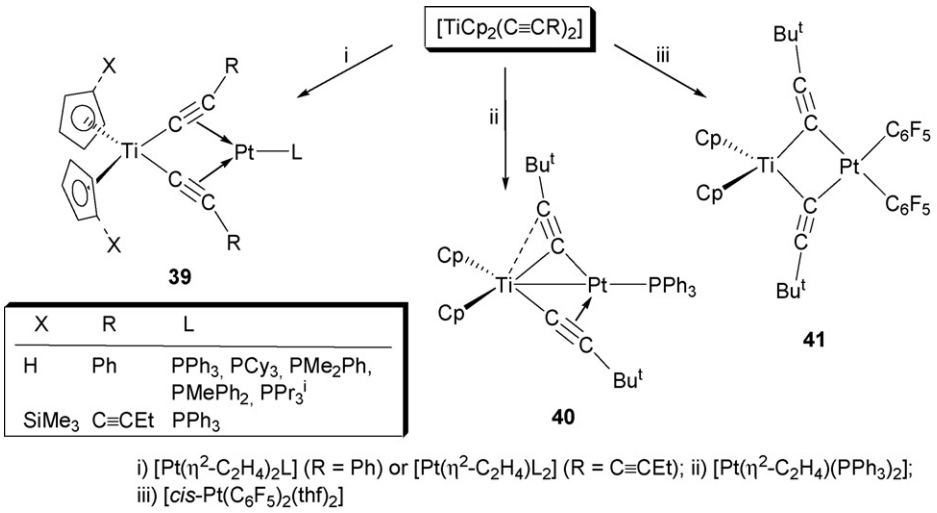

Scheme 8.

to complex **41** (Scheme 8, *iii*), which has been shown by X-ray to contain two asymmetric μ-κ$^2C^\alpha$-alkynyl ligands (Pt–C$^\alpha$ 2.014(11), 2.019(11) *vs.* Ti–C$^\alpha$ 2.257(10), 2.240(10) Å) and a very similar Ti–Pt distance of 2.831(2) Å [91]. All these systems (**39**–**41**) are good models for the reaction pathways of metal–metal cooperation in the C–C coupling alkynide processes. In fact, the reaction of similar bis(alkynyl)titanocenes [Ti(η^5-$C_5H_4SiMe_3$)$_2$(C≡CR^1)(C≡CR^2)] (R^1, R^2 = Fc, $SiMe_3$, Ph) with $PtCl_2$ produces [Ti(η^5-$C_5H_4SiMe_3$)$_2$Cl$_2$], Pt^0 and the corresponding butadiynes [92].

Monodentate bis(alkynyl)–dppm platinum(II) complexes have been successfully employed by Shaw and co-workers as precursors of alkynyl Pt–M^0 (M = W, Mo) species (**42**, Eq. (8)) [93–95]. The structure of the Pt^{II}–W^0 complex with R = Tol [93,94] shows the presence of one acetylide ligand acting as an asymmetrical κ$^2C^\alpha$ bridging group (Pt–C$^\alpha$ 2.094(9) Å; W–C$^\alpha$ 2.398(9) Å; M–C$^\alpha$–C$_\beta$ 136.8(8) and 138.4(8)°).

Chisholm et al. have reported the synthesis of the platinum–tungsten complexes **43** and **44** (Chart 7) by a simple deprotonation reaction of [*trans*-Pt(C≡CH)$_2$L$_2$] with the [$W_2(OBu^t)_6$] dimer [96,97]. In a similar manner to the reaction of organic 1-alkynes, facile oxidative addition of the bis-diynyl platinum(II) complex [*cis*-Pt(C≡C–C≡CH)$_2$(dppe)] to [Ru$_3$(μ-dppm)(CO)$_{10}$] takes place affording the 1,3-diyne-1,4-diyl/hydride $PtRu_3$ adduct **45** (Eq. (9)) [98].

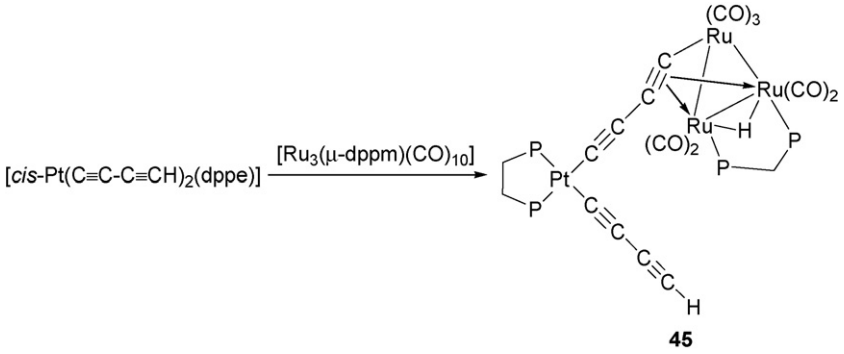

(9)

A series of monoplatinum containing ruthenium and osmium clusters have been reported. Most are formed by interaction of a low-valence platinum fragment with a M–C$^\alpha$(alkynyl) (M = Ru, Os) bond of the cluster core. Thus, trinuclear clusters [$PtRu_2$(μ-PPh_2)(μ$_3$-κ$^2C^\alpha$:κC$^\beta$–C≡C–C≡CR)(CO)$_6$L$_2$] (**46**, Chart 8), containing the diinyl fragment coordinated in a μ$_3$-κ$^2C^\alpha$:κC$^\beta$ fashion, are generated by treatment of [$Ru_2(CO)_6$(μ-PPh_2)(μ-κC$^\alpha$:η^2-C≡C–C≡CR)] with [Pt(η^2-C_2H_4)L$_2$] (L$_2$ = 2PPh$_3$, dppb) [99]. In a similar manner, reaction of the trinuclear ruthenium cluster [Ru$_3$(μ-H)(μ$_3$-C≡CBu^t)(CO)$_9$] with [Pt(cod)$_2$] causes the addition of a "Pt(cod)"

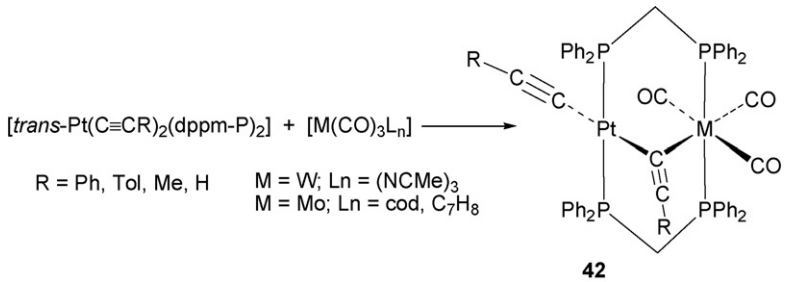

(8)

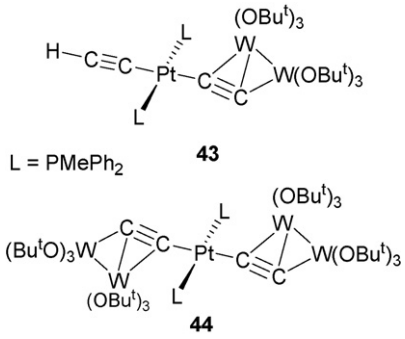

Chart 7.

unit, giving rise to a tetranuclear $PtRu_3$ cluster (**47**, Chart 8) having an overall "*out-of-plane*" spiked-triangular metal framework, and the alkynyl adopting an asymmetric μ_4-$\eta^2(\perp)$ coordination mode [100]. Displacement of cod ligand by diphosphines such as dppe, dppet, dppp, *S*,*S*-dppb affords related hydrido-alkynyl clusters $[PtRu_3(\mu\text{-H})(\mu_4\text{-C}{\equiv}CBu^t)(CO)_9(P\text{–}P)]$ (**47**, Chart 8) [100,101], which readily tautomerize in solution to the corresponding butterfly vinylidene clusters $[PtRu_3(\mu_4\text{-}\kappa^3C^\alpha{:}\eta^2\text{-C}{=}CHBu^t)(CO)_9(P\text{–}P)]$ (**48**, Chart 8), by a facile reversible skeletal rearrangement of the $PtRu_3$ metal core. Curiously, treatment of the *out-of-plane* spiked-triangular $PtRu_3$ cluster **47** (P–P = dppe) with $Ph_2PC{\equiv}CPPh_2$ causes rearrangement to a butterfly cluster $[PtRu_3(\mu\text{-}PPh_2)(\mu_4\text{-C}{\equiv}CBu^t)(CO)_7(dppe)]$ (**49**, Chart 8), with the alkynyl bridging a final rhomboidal metal core [102]. A structurally related platinum–triosmium cluster (**47**, Chart 8) has been prepared by reaction of $[Os_3Pt(\mu\text{-H})_2(CO)_{10}(PCy_3)]$ with LiC≡CPh, followed by protonation [103]. The two Ru–C^α bonds of two $[Ru_3(\mu\text{-H})(\mu_3\text{-}\eta^2\text{-C}{\equiv}CBu^t)(CO)_9]$ coordinate to a nacked Pt^0 to form the heptanuclear cluster $[Pt\{Ru_3(\mu\text{-H})(\mu_4\text{-}\eta^2\text{-C}{\equiv}CBu^t)(CO)_9\}_2]$ (**50**, Eq. (10)) (X-ray) [104]. Evidence for racemization of the chiral metal framework was found.

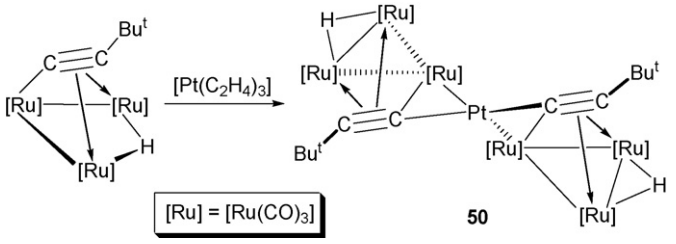

(10)

Interestingly, the reaction of $[cis\text{-}Pt(C{\equiv}CPh)_2(N\text{–}N)]$ with $[Os_3(CO)_{10}(NCMe)_2]$ evolves with alkynyl migration and opening of the Os_3 triangle, leading to unusual spiked-triangular clusters (**51**, Eq. (11)), having one alkynyl moiety coordinated in a μ_4-$\eta^2(||)$ bridging mode [105]. However, reactions of the related bis(acetylide)platinum(II) complex $[Pt(C{\equiv}CPh)_2(dppe)]$ with other clusters such as $[Ru_3(CO)_{12}]$ and $[Mn_2(CO)_9(NCMe)]$ affords mixed $PtRu_3$ and $PtMn_2$ clusters, in which head to head C^α–C^α coupling of the alkynyl groups takes place [106,107].

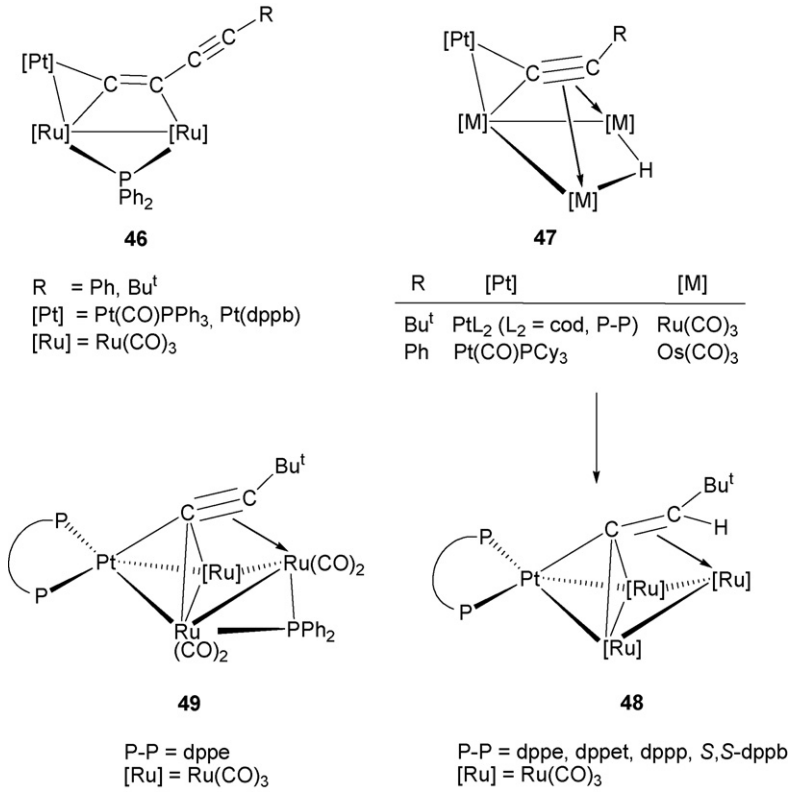

Chart 8.

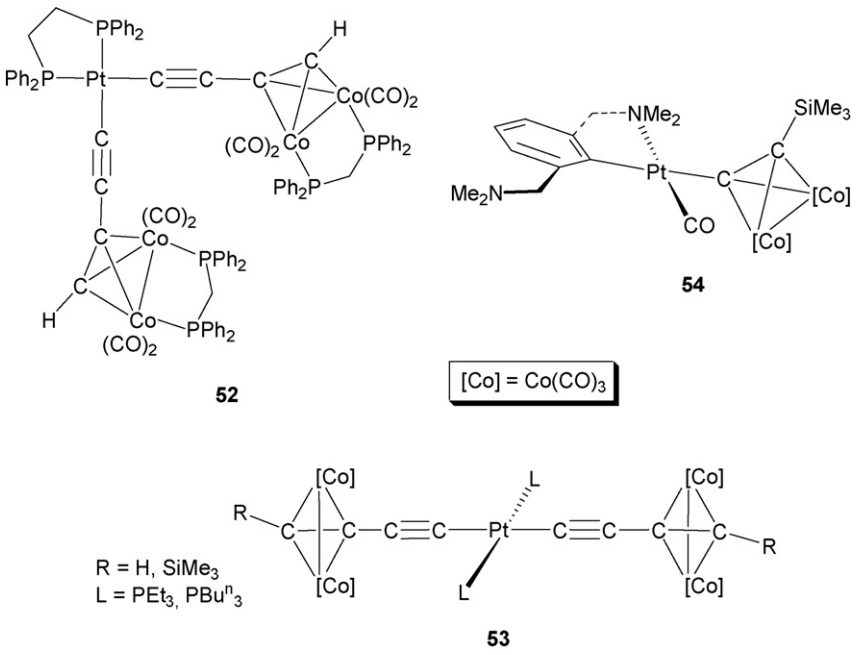

Chart 9.

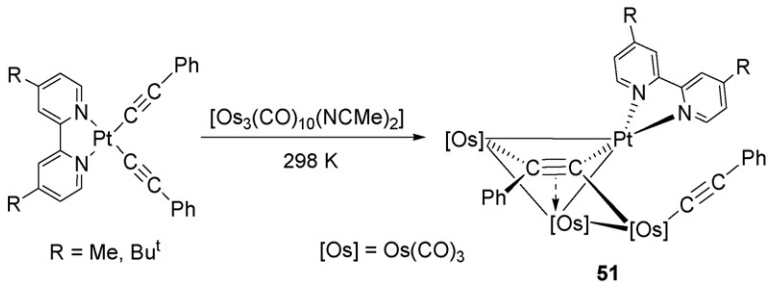

(11)

3.2. Heteronuclear platinum-group 9, 10 metal acetylide complexes

Several alkynyl platinum(II)-mono and bis(dicobalto-tetrahedrane) adducts have been reported (Chart 9). Reaction of neutral *cis*- [98] or *trans*- [108] bis(1,3-diyne-1-yl)platinum(II) complexes with 2 equiv. of $[Co_2(\mu\text{-dppm})(CO)_4]$ or $[Co_2(CO)_8]$, respectively, affords the corresponding 1:2 $Pt\{Co_2\}_2$ adducts (**52**, **53**, Chart 9). The structure for **52** was established by X-ray diffraction methods, confirming that the dicobalt "$Co_2(\mu\text{-dppm})(CO)_4$" units are attached to the external alkyne units. Similar reaction with $[Pt(N\wedge C\wedge N)(C{\equiv}CSiMe_3)]$ (N∧C∧N = 2,6-bis(dimethylamino)phenyl ligand) leads, *via* η^2-coordination to the alkynyl unit, to the heterotrimetallic complex **54** (Chart 9), in which CO has displaced one *o*-CH_2NMe_2 substituent to make the ligand C,N chelating bidentate [109].

Paramagnetic bimetallic and trimetallic platinum(II)-bis(η^2-alkyne)–cobalt(II) adducts **55** and **56** (Chart 10) were made by reaction of the appropriate mixed and homoleptic alkynyl platinates with $CoCl_2{\cdot}6H_2O$ in 1:1 and 1:2 stoichiometry [110]. X-ray analyses have shown that, while the binuclear anion **55** exhibits a tweezer-like double-alkynyl bridging system, with a planar PtC_4Co core and very long Pt–Co separation (3.446(3) Å), in the trinuclear adduct both dimetallacycles are bent (V-shaped, **C**, Chart 5), imposing shorter Pt···Co distances (3.077(3) Å). Bimetallic mixed platinum(II)–rhodium(I) or iridium(I) dppm/(μ-κC^{α}:η^2-C≡CR) A-frame complexes (**57**) have been prepared by Shaw et al. starting from appropriate alkynyl–bis(dppm)-platinum(II) complexes and $[Rh_2Cl_2(CO)_4]$ or $[Ir_2Cl_2(C_8H_{14})_4]$ (C_8H_{14} = cyclooctene) [111,112]. The crystal structures of $[(X)Pt(\mu\text{-dppm})_2(\mu\text{-}\kappa C^{\alpha}{:}\eta^2\text{-}C{\equiv}CMe)Rh(CO)](PF_6)$ (**57**, X = C≡CMe, Cl) were determined, confirming the μ-κC^{α}(Pt):η^2(Rh) bonding mode of the alkynyl group [111].

There are a few bimetallic derivatives stabilized by a hetero-bridged system of the type (μ-C≡CR)(μ-X). Stang and co-workers [113] reported the synthesis of Pt^{II}–M^{III} (M = Rh, Ir) complexes with

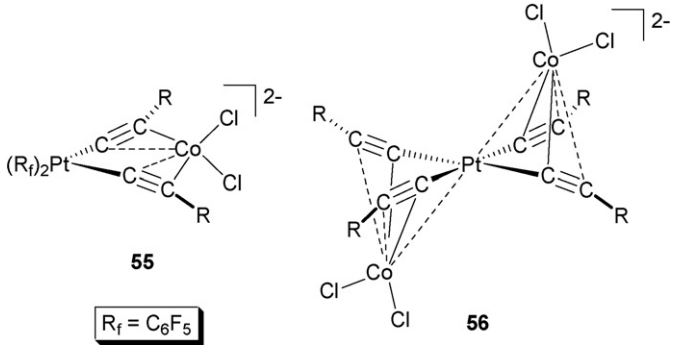

Chart 10.

a rare mixed (μ-H)(μ-C≡CPh) system (**58**), by direct C–H bond activation of a Pt^0 precomplexed η^2-alkyne with bis(triflate) d^6 species (Eq. (12)) [113]. The X-ray structure of the Pt–Rh derivative **58** confirms the oxidation of the platinum center, and formation of the phenylethynyl group, which is κC^{α}-bonded to Pt^{II} and η^2-bonded to the cationic Rh^{III} center. However, the reaction of the neutral alkynyl–halide complexes [MCp*(C≡CR)X(PEt_3)] (M = Rh, Ir) with the solvates [*cis*-M′(R_f)$_2$$S_2$] (M′ = Pt, Pd; S = thf) occurs with retention of the κC^{α}-M(Rh, Ir) coordination of the alkynyl ligand, yielding simple hetero-bridged (μ-X)(μ-κC^{α}(M):η^2(M′)) 1:1 M^{III}–M'^{II} adducts (**59**, Eq. (13), M = Rh, Ir; M′ = Pt, Pd), as confirmed by X-ray in several complexes [114].

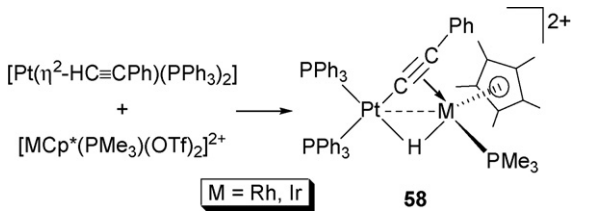

(12)

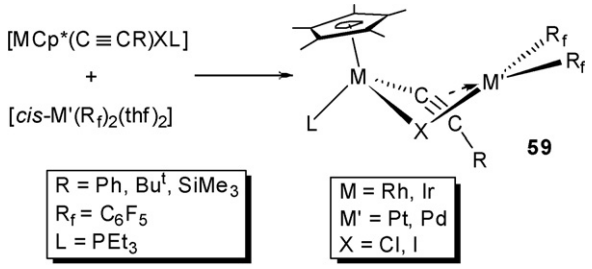

(13)

Our group has also shown that deprotonation of acidic coordinated ligands (PPh_2H, PPh_2OH) in alkynyl platinum compounds with acetylacetonate complexes [M(acac)L_2] (M = Rh, Ir) permits access to the hetero-bridged (μ-C≡CR)/(μ-PPh_2) Pt^{II}–Rh^{I} (**60**, **61**), and (μ-C≡CR)/(μ-PPh_2O) Pt^{II}–M (**62**, M = Rh^{I}, Ir^{I}) complexes shown in Scheme 9 [80]. All reactions take place with stereoretention, as confirmed by IR and NMR techniques, and the molecular structure of [*cis*,*cis*-(PPh_2H)(C≡CR)Pt(μ-κC^{α}:η^2-C≡CBu^t)(μ-PPh_2)Rh(CO)$_2$] (**61**).

The anionic mixed and homoleptic alkynyl platinates [*cis*-$Pt(R_f)_2(C{\equiv}CR)_2]^{2-}$ and $[Pt(C{\equiv}CR)_4]^{2-}$ (R = Ph, Bu^t, $SiMe_3$), respectively, are particularly fruitful as precursors, not only for the preparation of hetero Pt–d^6,d^8 (d^6 = Rh^{III}, Ir^{III}; d^8 = Rh^{I}, Ir^{I}, Pd^{II}) di- or trinuclear double-alkynyl bridging complexes, but also for the construction of high-nuclearity multimetallic systems (see Sections 3.3, 3.4 and 3.5). As shown in Schemes 10–15, heterometallic [Pt](μ-C≡CR)$_2$[M′] (M′ = Rh^{I}, Ir^{I}, Pd^{II}, Rh^{III}, Ir^{III}) complexes are accessible through simple displacement reactions of labile ligands (solvent, chloride) with a suitable source of M′. The course of these reactions is strongly influenced by the metal and substituents. Thus, the influence of the alkynyl substituent is usually decisive on the final stability of the double-alkynyl bridging heterometallic complexes, while the observed $\kappa C^{\alpha}/\eta^2$-alkynyl metal site preference depends on the electronic characteristic of the ML_n fragments. As shown in Scheme 10, a doubly alkynyl transfer process occurs when the homoleptic derivatives $[Pt(C{\equiv}CR)_4]^{2-}$ react with the solvento dicationic $[MCp^*(L)(acetone)_2]^{2+}$ (L = PEt_3, PPh_3), to give neutral chelating V-shaped doubly alkynyl bridging d^6(M)–Pt complexes **63**, in which the organometallic "*cis*-Pt(C≡CR)$_2$" unit is unusually stabilized by η^2-bis(alkyne) interactions, as confirmed by X-ray diffraction [115]. The terminal alkynyl ligands in complexes **63**

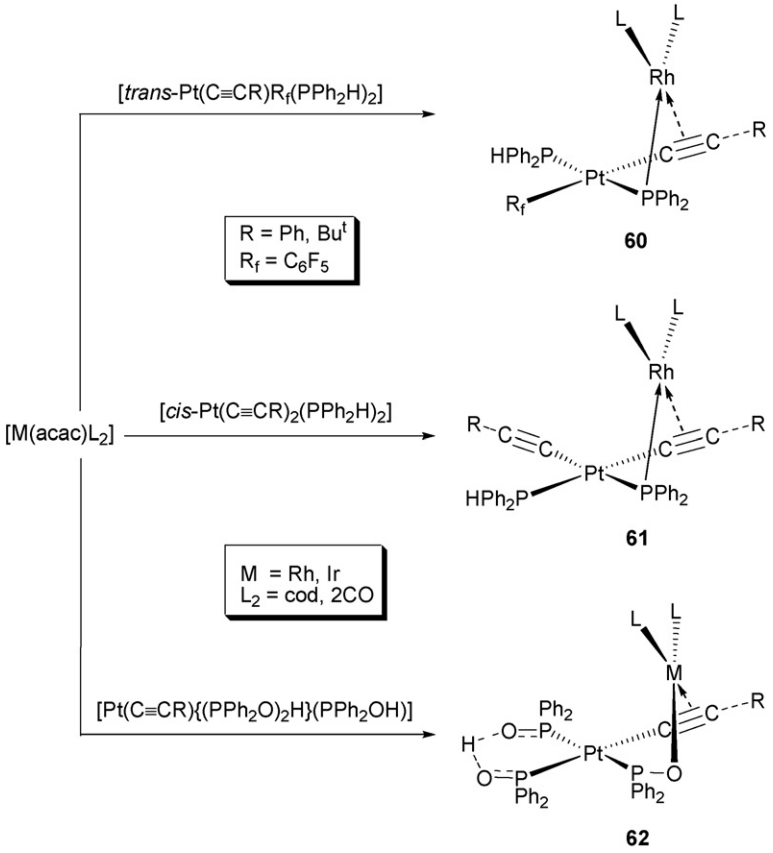

Scheme 9.

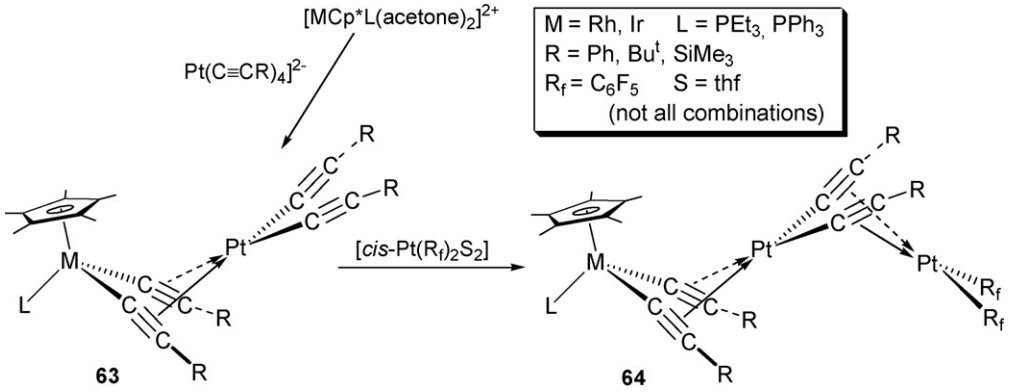

Scheme 10.

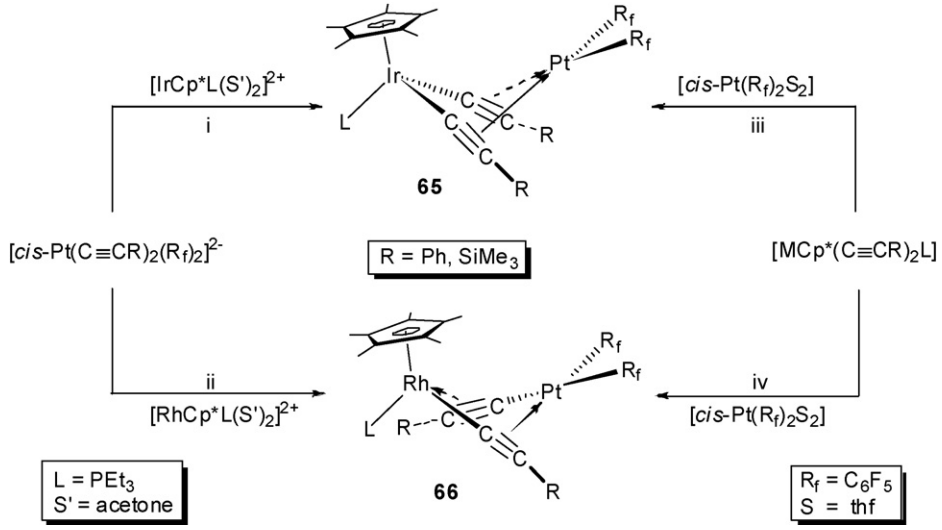

Scheme 11.

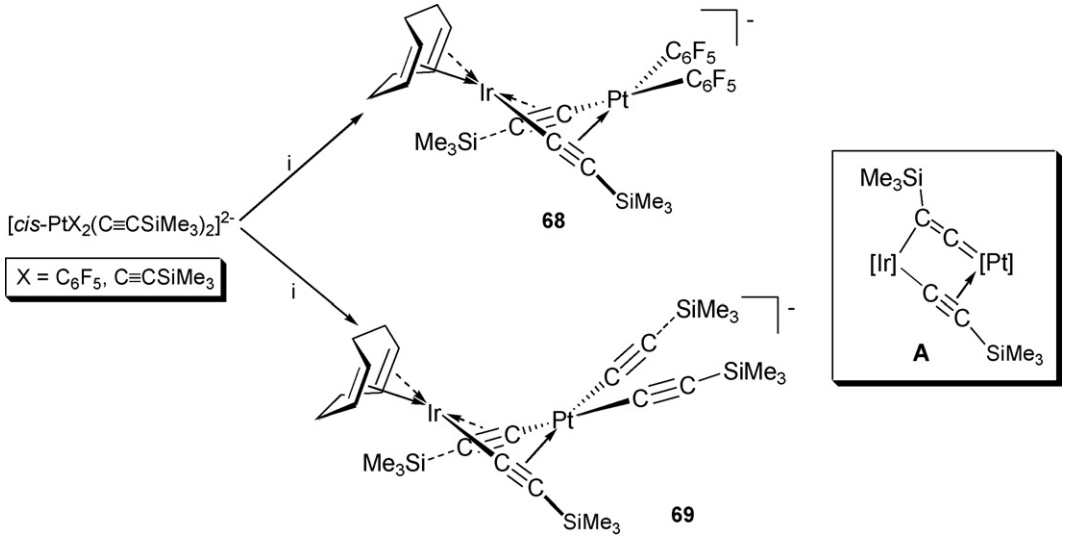

Scheme 12.

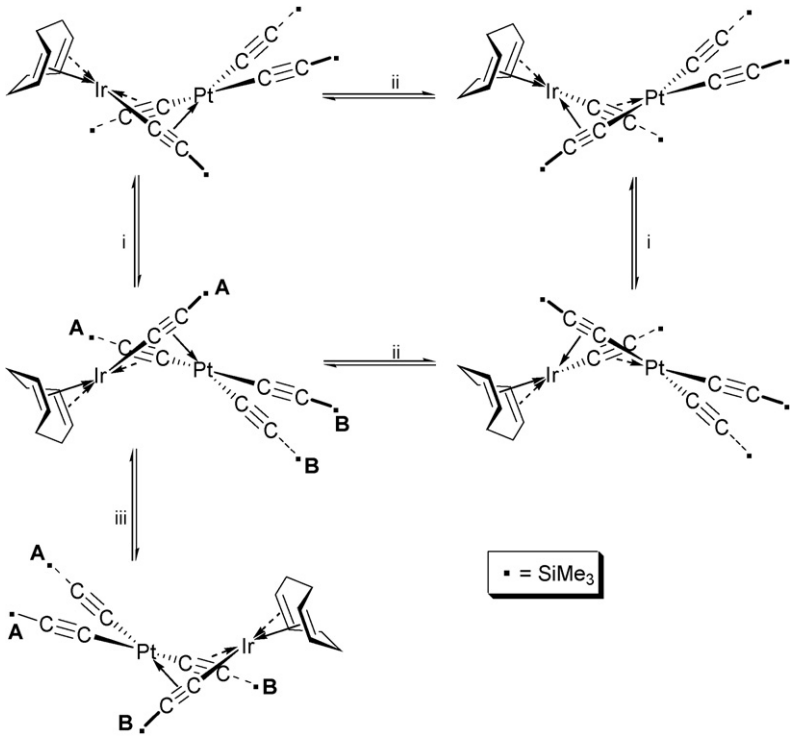

Scheme 13.

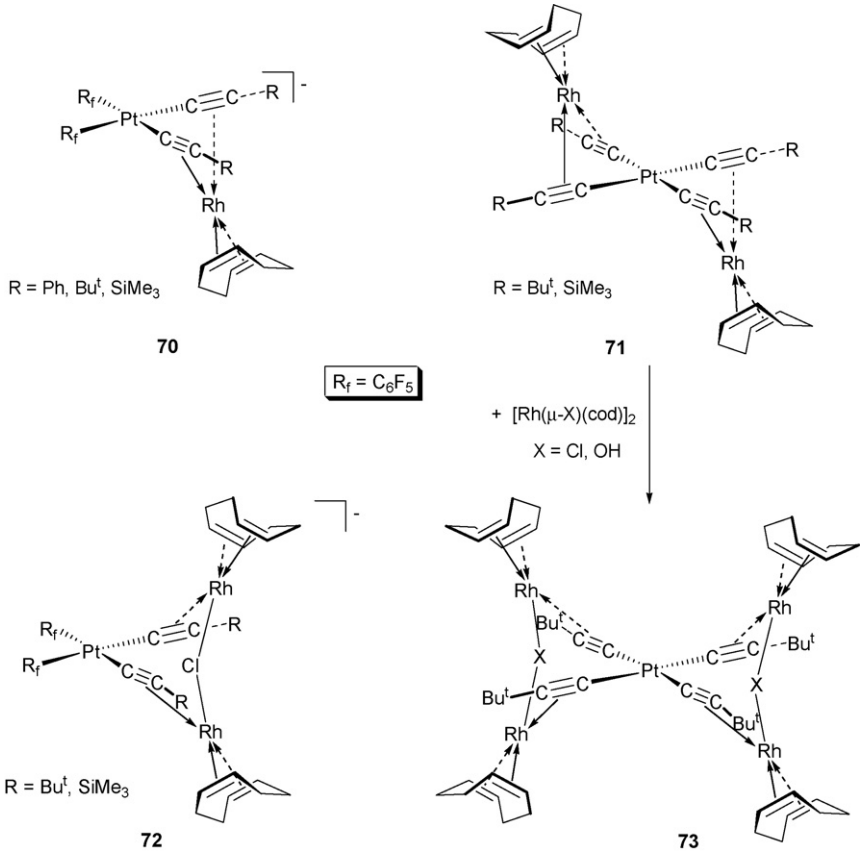

Scheme 14.

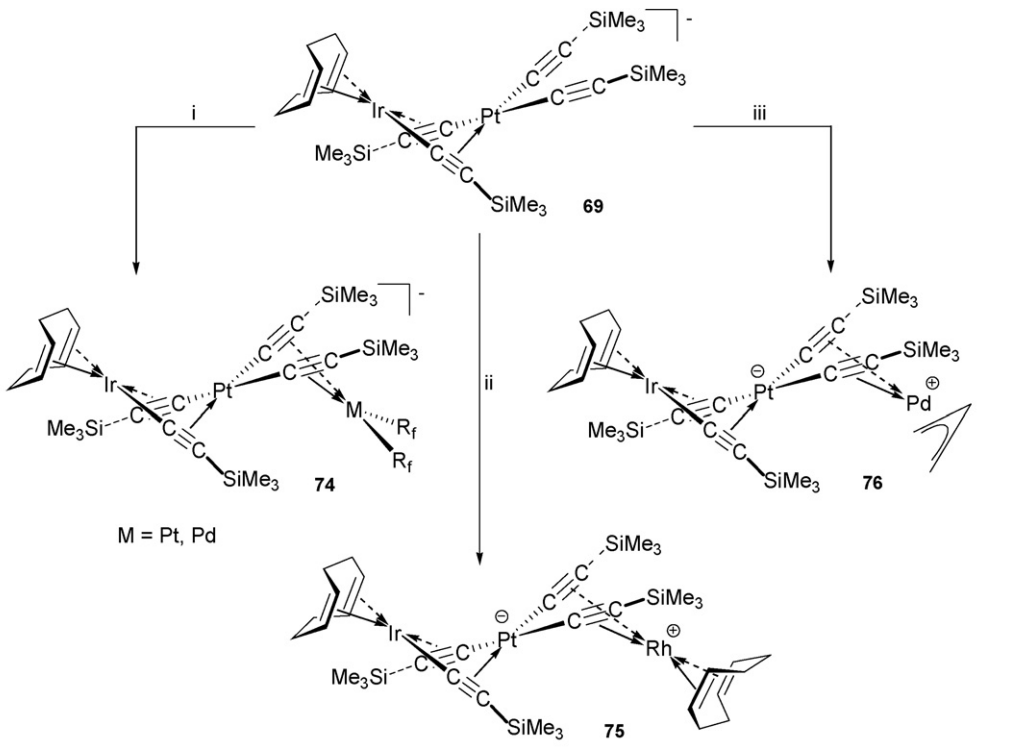

Scheme 15.

are also capable of displacing thf ligands on [*cis*-Pt(R_f)$_2$$S_2$] (S = thf) to give unusual bis(double-alkynide)bridged d^6(M)–Pt^{II}_2 trinuclear complexes **64**. The crystal structure of the $RhPt_2$ complex (**64**) with R = $SiMe_3$ confirms the presence of two chelating systems, which have their dative bonds pointing in the same direction [115].

Similar reactions of the solvento dicationic d^6 complexes with the mixed derivatives [*cis*-Pt(R_f)$_2$(C≡CR)$_2$]$^{2-}$ only afford stable heterometallic complexes with R = Ph and $SiMe_3$ (Scheme 11) [114]. In this case, the electrophilicity of the dicationic "IrCp*(PEt_3)$^{2+}$" fragment also causes the σ-migration of the two alkynyl groups, affording neutral fragments "IrCp*(κC^{α}-C≡CR)$_2$(PEt_3)" and "Pt(R_f)$_2$", which are held together by η^2-alkynyl–Pt bonding interactions (**65**, Scheme 11, *i*) [114]. In both complexes (**65**, R = Ph, $SiMe_3$), the platinum is located out of the 3-irida-1,4-diyne plane Ir(C≡C)$_2$, with the "Pt(R_f)$_2$" unit *endo* to the Cp* ring. However, the presence of two electro-withdrawing C_6F_5 groups enhances the electrophilicity of the Pt center, and the reactions with the related second-row rhodium dicationic unit [RhCp*(PEt_3)(acetone)$_2$]$^{2+}$ afford formally zwitterionic and highly fluxional σ/π {[Rh]$^+$–[Pt]$^-$} derivatives **66**, resulting from a simple alkynyl migration (Scheme 11, *ii*) [114]. These mixed d^6–d^8 complexes are alternatively obtained starting from neutral bis(alkynyl)-iridium (**65**, Scheme 11, *iii*) or rhodium (**66**, Scheme 11, *iv*) precursors [MCp*(C≡CR)$_2$(PEt_3)] and the solvate [*cis*-Pt(R_f)$_2$$S_2$], indicating that the observed thermodynamic site preference for κC^{α} (σ) coordination is mainly due to the electronic effect of the metal fragments. In the same line, the related reactions with the second-row unit "*cis*-Pd(R_f)$_2$" takes place with retention of the σ-coordination of the alkynyl groups yielding simple chelating V-shaped 1:1 adducts [(PEt_3)Cp*M(μ-κC^{α}:η^2-C≡CR)$_2$Pd(R_f)$_2$] (**67**, M = Ir, Rh) [114].

With the aim to get more insight into the driving force of these alkynyl transfer processes, we also examined the reactivity of the alkynyl platinates towards *low-valence* substrates of Rh and Ir^I. The course of these reactions (Schemes 12–15) is also influenced by the metal and substituents. Only the reactions with the iridium substrates [Ir(cod)S_x]$^+$ or [Ir(μ-Cl)(cod)]$_2$ evolve with monoalkynyl transference, but the final rectangular σ/π heterobimetallic complexes are only stable in the case of the trimethylsilyl derivatives **68** [116] and **69** [117] (Scheme 12). Both anions (**68** and **69**) show bent PtC_4Ir central cores, and asymmetrical η^2-metal-acetylenic linkages with M(Pt,Ir)–C_β bond distances slightly shorter (~0.10–0.12 Å) than the corresponding M–C^{α}, in agreement with a considerable vinylidene contribution (**A**, Scheme 12) to the bonding mode of the alkynyl groups. Both complexes **68** and **69** exhibit, even at low temperature, a very fast inversion of the central dimetallacycle Pt(C≡C)$_2$Ir (Scheme 13, *i*), followed by an additional κC^{α}:η^2 intramolecular exchange of both alkynyl ligands (Scheme 13, *ii*). Also, upon raising the temperature, a new dynamic process involving the exchange of the iridium unit between bridging and terminal alkynyl groups (Scheme 13, *iii*) is also observed for **69**.

By contrast, the reactions of [*cis*-Pt(R_f)$_2$(C≡CR)$_2$]$^{2-}$ and [Pt(C≡CR)$_4$]$^{2-}$ with the solvate [Rh(cod)(acetone)$_x$]$^+$ afford bi- and trinuclear formally zwitterionic complexes (**70** [116], **71** [118], Scheme 14), in which the alkynyls remain σ-bonded to Pt and are η^2-bonded to Rh^I; thus indicating a clear κC^{α}(σ)-site alkynyl preference of the third row Pt^{II} relative to the second-row metal Rh^I. The platinate precursors also act as bridging chelating bi- and tetradentate ligands towards Rh^I, as in complexes **72** and **73** (Scheme 14). Complexes **72** are generated by replacing one chloride ligand in the reaction of [*cis*-Pt(R_f)$_2$(C≡CR)$_2$]$^{2-}$ with [Rh(μ-Cl)(cod)]$_2$ [116], whereas subsequent reaction of the *tert*-butylacetylide derivative **71** with the dimers [Rh(μ-X)(cod)]$_2$ (X = Cl, OH) affords the pentanuclear $PtRh_4$ species **73** [118], the structures of which have been determined by X-ray [116,118].

The binuclear anionic system [(cod)Ir(μ-C≡C$SiMe_3$)$_2$ Pt(C≡C$SiMe_3$)$_2$]$^-$ (**69**, {Ir–Pt}$^-$), containing two terminal alkynyl ligands, also serve as a building block for assembly of

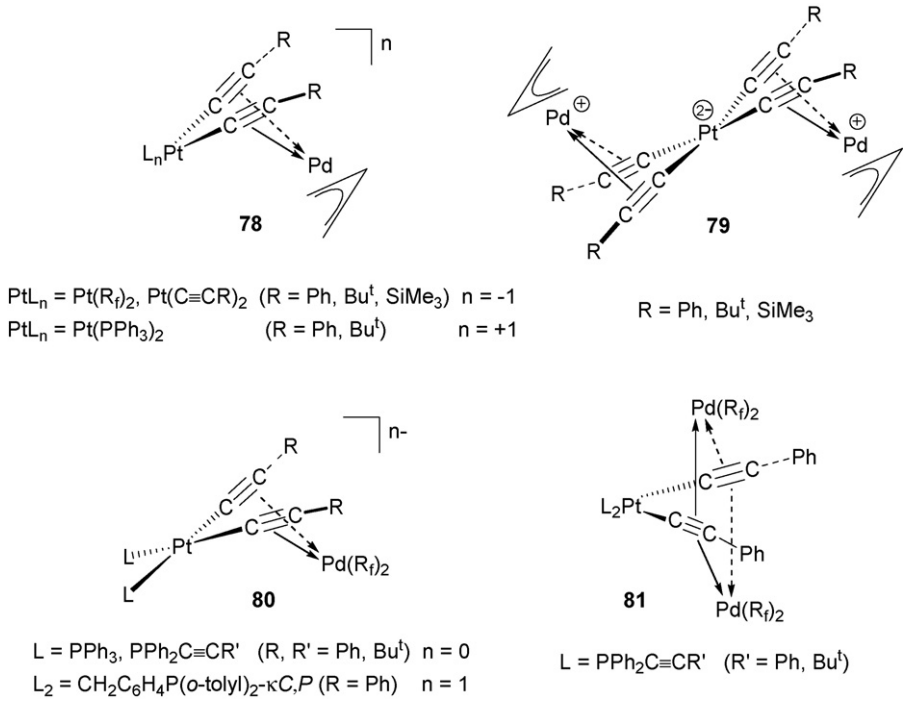

Chart 11.

trimetallic compounds. Simple complexation of both alkynyl fragments, not only to neutral [Pt(R$_f$)$_2$, Pd(R$_f$)$_2$] fragments, but also to cationic [Rh(cod), Pd(η^3-C$_3$H$_5$)] units occurs on reaction with appropriate metal sources (Scheme 15) [117]. The crystal structure of [(cod)Ir(μ-1κC^α:η^2-C≡CSiMe$_3$)(μ-2κC^α:η^2-C≡CSiMe$_3$)Pt(2κC^α:η^2-C≡CSiMe$_3$)$_2$Rh(cod)] **75** confirms the presence of two different bridging systems (σ/π and V-shaped) [117]. These results and the lack of reactivity of **69** {Ir–Pt}$^-$ towards the related "Ir(cod)$^+$" unit is consistent with a strong thermodynamic stability of Pt–alkynyl bond in this fragment, and a very low tendency of iridium to be stabilized by bis(η^2-alkyne) interactions. However, as shown in Eq. (14), the reaction between cyanide-bridged dianionic molecular squares Pt$_2$M$_2$ (M = Rh^I, Ir^I), containing terminal acetylide ligands, and 2 equiv. of [*cis*-Pt(R$_f$)$_2$S$_2$] affords the hexanuclear Pt$_4$M$_2$ complexes **77**, formed by a simultaneous σ-alkynyl migration from each platinum in the square (double Pt–C activation) to both platinum "Pt(R$_f$)$_2$" units, as confirmed by the crystal structure of the Pt$_4$Rh$_2$ complex [119]. In contrast to the precursor Pt$_2$Rh$_2$, where the molecular squares are not stacked, in the final Pt$_4$Rh$_2$ derivative **77** the squares are stacked in an eclipsed way along the *c*-axis, resulting in long channel-like cavities. The activation of the Pt–C(alkynyl) ligand is probably favoured by the higher negative charge on the platinum metal centers.

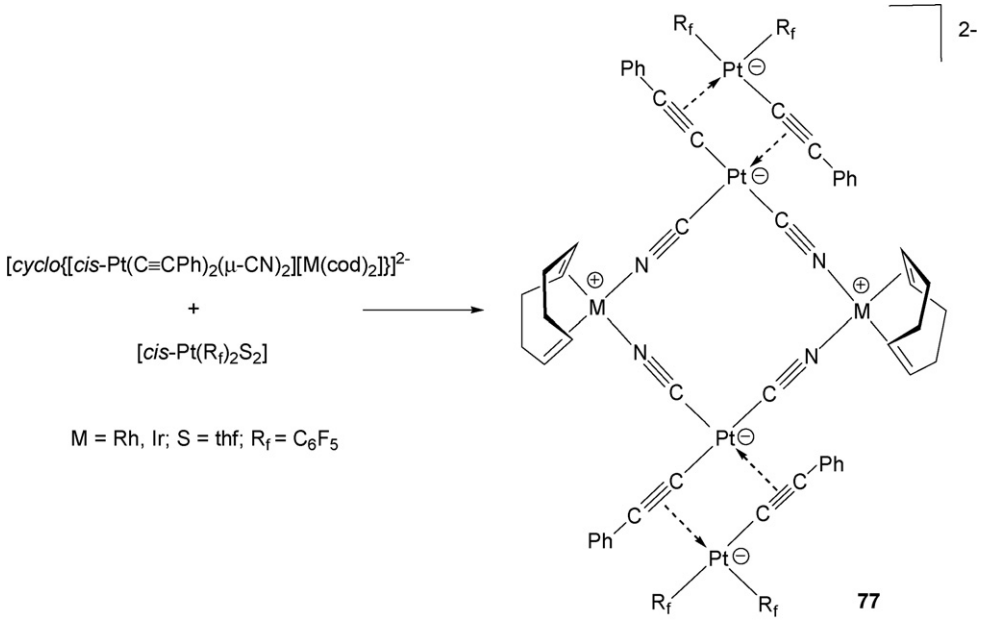

(14)

Several examples of alkynyl-bridged mixed platinum–palladium d^8–d^8 complexes prepared from reactions between alkynyl platinum precursors and cationic "$Pd(\eta^3\text{-}C_3H_5)^+$" [87,120] or neutral "*cis*-$Pd(R_f)_2$" [64,77,85] sources have been reported (Chart 11). In spite of the very electrophilic nature of the "$Pd(\eta^3\text{-}C_3H_5)^+$" unit, the reactions occur without alkynyl migration, even with anionic precursors [*cis*-$Pt(R_f)_2(C{\equiv}CR)_2]^{2-}$ and $[Pt(C{\equiv}CR)_4]^{2-}$, leading in those cases to final di- (**78**) or trinuclear (**79**) complexes (Chart 11), which are formally zwitterionic [87,120]. X-ray studies of [*cis*-$(R_f)_2Pt(\mu\text{-}\kappa C^\alpha{:}\eta^2\text{-}C{\equiv}CSiMe_3)_2Pd(\eta^3\text{-}C_3H_5)]^-$ and [*cis*-$(PPh_3)_2Pt(\mu\text{-}\kappa C^\alpha{:}\eta^2\text{-}C{\equiv}CBu^t)_2Pd(\eta^3\text{-}C_3H_5)]^+$ confirm that the naked palladium center is sandwiched between both acetylenic fragments and the allylic unit [87,120]. A similar behaviour was found in related reactions of neutral [*cis*-$Pt(C{\equiv}CR)_2L_2$] (L = phosphine) or anionic $[Pt(C{\wedge}P)(C{\equiv}CPh)_2]^-$ with the neutral unit "*cis*-$Pd(R_f)_2$", affording chelating V-shaped binuclear complexes **80** (Chart 11) [64,85]. By using 2 equiv. of [*cis*-$Pd(R_f)_2(thf)_2$], mixed triangular $PtPd_2$ derivatives **81** are obtained (Chart 11, compounds related to complexes **13B** in Chart 3 and **30** in Scheme 6), but these derivatives decompose in solution (~12 h, depositing Pd), leading to the corresponding binuclear derivatives **80** and C_6F_5–C_6F_5 [64]. Only the reaction of the dianionic [*cis*-$Pt(R_f)_2(C{\equiv}CBu^t)_2]^{2-}$ and [*cis*-$Pd(R_f)_2S_2$] (S = thf) evolves with alkynyl transfer, and final formation of a rectangular σ,π double-alkynyl bridging system (**82B**, Eq. (15)). Control of this reaction at low temperature indicates the initial formation of the expected chelating V-shaped adduct (**82A**), which upon standing at room temperature isomerizes to the final σ,π complex **82B** [77]. The stronger tendency of platinum to be $\kappa C^\alpha(\sigma)$-bonded to the alkynyl group is consistent with the known lower stability of palladium alkynyl complexes. In the same line, alkynyl ligand transfer from mononuclear palladium complexes to iodo-aryl platinum complexes has been observed by Osakada et al. [10,121]. The intermolecular transfer, which is promoted with or without CuI catalyst, has been suggested to occur via a bimetallic state with alkynyl bridging between Pt and Pd centers.

The synthesis of these complexes has followed two main routes: (a) reaction of alkynylplatinum(II) complexes with diverse M^I (M = Cu, Ag, Au) sources or (b) treatment of platinum derivatives containing weakly bonded ligands (such as halide, SMe_2, tht, thf, etc.) with group-11 metal acetylides (in some occasions prepared *in situ* from HC≡CR/amine/CuI systems). In agreement with the strength of the Pt–C≡C bonds, both spectroscopic and structural studies have demonstrated that, in the final heteropolynuclear complexes, the alkynyl ligand is always κC^α bonded to the platinum and η^2-coordinated (symmetrical or asymmetrical, half way between η^2 and κC^α) to the heterometal. Notwithstanding, as shown below, the stability and properties of related platinum alkynyl metal complexes depend on the alkynyl substituents, coligands and the heterometal and, in some instances, alkynyl transfer process from platinum to the heterometal without retention of the initial nuclearity has been observed. Although some reactions between Pt^0 substrates and [M(C≡CR)] have been examined, the final systems only show terminal alkynyl ligands [123,124]. In contrast, numerous heteropolymetallic Pt^{II}-M (group-11 metal) complexes having square-planar platinum frameworks with one, two (*trans* or *cis*), three or four alkynyl groups have been reported.

(i) *Complexes based on monoalkynylplatinum frameworks* are rare. Thus, treatment of the orthometalated complex [Pt]C≡$CSiMe_3$ ([Pt{2,6-$(Me_2NCH_2)_2$–C_6H_3}]$^+$) with $[Cu(NCMe)_4]^+$ or Ag^+ leads to heterotrinuclear cationic complexes **83** [109] (Chart 12). The bis η^2-metallaalkyne linear coordination has been confirmed in the Pt_2Cu derivative.

Our group found that the reaction of [$Au(C{\equiv}CBu^t)(PPh_3)$] with the solvate [*cis*-$Pt(R_f)_2(CO)(thf)$] takes place with alkynyl migration from gold to platinum, giving rise to the bimetallic zwitterionic Pt–Au derivative **84** [70]. Puddephatt et al. reported that the interaction of [*trans*-$PtCl_2(SMe_2)_2$] with 1 equiv. of $[Au(C{\equiv}CBu^t)]_n$ affords unstable species **85**, in which the AuCl unit is proposedly

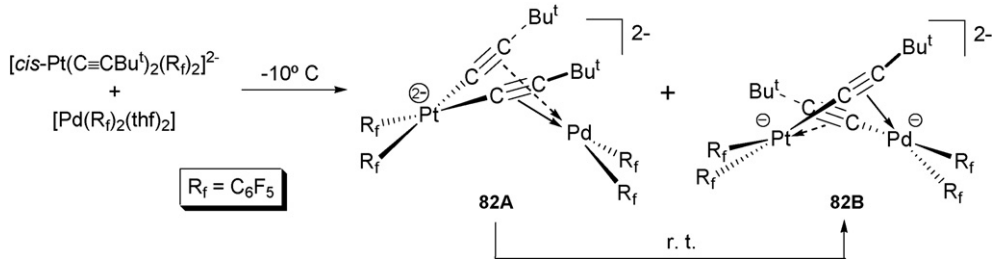

(15)

linked by the alkynylplatinum (Eq. (16)). Further treatment with dppm afforded complex **86**, in which the *tert*-butylethynyl group is displaying a semibridging coordination mode with a rather long Au–C^α distance [2.70(1) Å] [125].

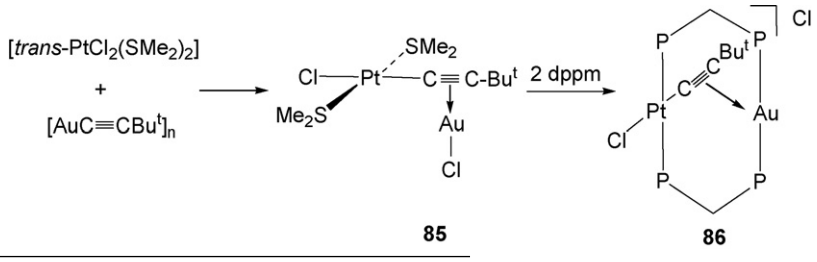

(16)

3.3. Heteronuclear platinum-group 11 (Cu, Ag, Au) metal acetylide complexes

Many alkynyl containing platinum complexes with coinage metals have been reported and several extensive reviews have discussed their chemistry in detail [5,6,9,47,122]. Therefore, our intention is to comment briefly on some relevant previous results and to describe recent developments to illustrate not only the flexibility of the alkynyl ligands but also the role of the metallophylic interactions [Pt···Pt, Pt···M and M···M (M = Cu, Ag, Au)] in the final structures and properties of the complexes.

(ii) *Complexes based on trans-configured dialkynylplatinum frameworks*. In a similar way to diynes, 3-platinapenta-1,4-diynes [*trans*-$Pt(C{\equiv}CR)_2L_2$] (L = PMe_2Ph, PPh_3; R = Ph, Bu^t) react with copper halides CuX (X = Cl, Br) [126–128] or AgOTf (OTf = OSO_2CF_3)

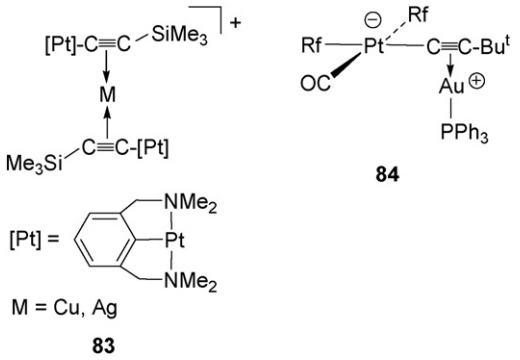

Chart 12.

[129] to produce polymeric neutral structures **87** or **88** (Chart 13). In [*trans*-$PtL_2(\mu\text{-}\kappa C^{\alpha}:\eta^2\text{-}C{\equiv}CR)_2\{Cu(\mu\text{-}Cl)_2Cu\}]_n$ (L = PMe_2Ph, PPh_3; R = Ph, Bu^t), the *trans* platinum units are linked by 4-membered $Cu_2(\mu\text{-}X)_2$ cycles at which the C≡CR units are η^2-coordinated to the Cu^I. The X-ray of **88** reveals the presence of an extended zig-zag backbone constructed by [*trans*-$Pt(PPh_3)_2(C{\equiv}CPh)_2$] fragments and binuclear $Ag_2(\mu\text{-}OTf)_2$ units connected through symmetrical η^2-silver linkages (Ag–C_α, C_β = 2.324 Å) [129]. In contrast, treatment of the same complex with $[Cu(NCMe)_4]NO_3$ generates the discrete trinuclear complex **89** (Chart 13), as has been confirmed by X-ray [127].

Trinuclear dicationic complexes PtM_2 (**90**–**93**) (Scheme 16) are accessible by starting from dialkynyl complexes containing two *trans* 2-diphenylphosphinopyridine (dppy) [130] or large bite 2-N(diphenylphosphinomethyl-N-benzyl)aminopyridine [131] P–N ligands and $[M(NCMe)_4]^+$. The crystal structure of **91** (M = Cu) confirms the tetrahedral environment of copper ion and that the Cu···Pt···Cu unit is held [129] together by two bridging dppy and $\mu\text{-}\kappa C^{\alpha}:\eta^2$-C≡CPh ligands. Crystallization of the unsolvated $PtCu_2$ derivative **92**, containing the large bite PN ligand, in CH_2Cl_2/MeOH or CH_2Cl_2/NCMe leads to the tricoordinated solvated complexes **93** (L′ = H_2O, NCMe) as has been confirmed by X-ray [131]. Interestingly, the unsolvated **92** can be recovered by heating or under reduced pressure. These complexes display interesting long-lived dual (**92**, **93**) or multiple (**90**, **91**) emissions, which have been ascribed to intraligand phosphorescence of the bridging P–N groups mixed with some ^{3}MLCT and Pt···M bonding interactions, respectively.

Chen et al. have recently reported [47,132] not only similar trinuclear dicationic complexes PtM_2 **94**, but also monocationic Pt–M (M = Cu, Ag) **95** and a very unusual tricationic Pt_2Ag_3 **96**, generated by the reactions of homoleptic $[Pt(C{\equiv}CR)_4]^{2-}$ with $[M_2(\mu\text{-dppm})_2(NCMe)_2]^{2+}$ (Chart 14).

It appears that the solvent and solution concentrations play a major role in determining the observed nuclearity. X-ray structures of the trinuclear $PtCu_2$ derivatives **94** show quasi-linear trinuclear arrays, symmetrical $\mu\text{-}\kappa C^{\alpha}:\eta^2$ and relatively long Pt···Cu distances (>3.4 Å). By contrast, the bimetallic **95** complexes exhibit a $\mu\text{-}\kappa C^{\alpha}:C^{\alpha}$ bridging acetylide and short intramolecular Pt···M distances (2.7–3.00 Å). The Pt_2Ag_3 complex **96** is composed of two cationic PtAg units, having a short contact (3.00 Å), associated with another Ag^I center by symmetrical η^2-coordination (one from each unit) [132]. Complexes **94**–**96** emit strongly in the solid state (298 and 77 K) from spin forbidden triplet states with maxima progressively red-shifted with the electron-donating ability of the alkynyl substituents ($Bu^t > C_6H_4OCH_3 > Tol > Ph$ and $SiMe_3 > Ph$) implying that the emission has a substantial ligand-to-cluster charge transfer (RC≡C → Pt–M; LMMCT) in view also of the Pt···M interactions [47]. Surprisingly, the related reaction of $[Pt(C{\equiv}CR)_4]^{2-}$ (R = Ph, Tol) with $[Ag_2(\mu\text{-dppa})_2(NCMe)_2]^{2+}$ (1:1, molar ratio) containing the facile deprotonating bis(diphenylphosphinoamine) ligand, evolves with additional deprotonation, affording the unusual hexanuclear neutral Pt_2Ag_4 cluster **97** (Chart 14) in which a dianionic face-to-face diplatinum entity $[Pt_2(C{\equiv}CR)_4(\mu\text{-}PPh_2NPPh_2)_2]^{2-}$ is connected to two cationic $[Ag_2(\mu\text{-}PPh_2NPPh_2)]^+$ units [47,133]. The presence of very short Pt···Pt (3.15 Å, R = Ph; 3.11 Å, R = Tol), Pt···Ag (2.90–2.94 Å) and Ag···Ag (3.18–3.33 Å) indicates relatively strong intermetallic contacts. They show strong phosphorescence (solid, solutions) slightly blue-shifted in the tolylacetylide, being therefore tentatively ascribed to cluster-to-acetylide $^3[Pt_2Ag_4 \rightarrow C{\equiv}CR]$ [134] ligand transfer modified by the short intermetallic contacts [47].

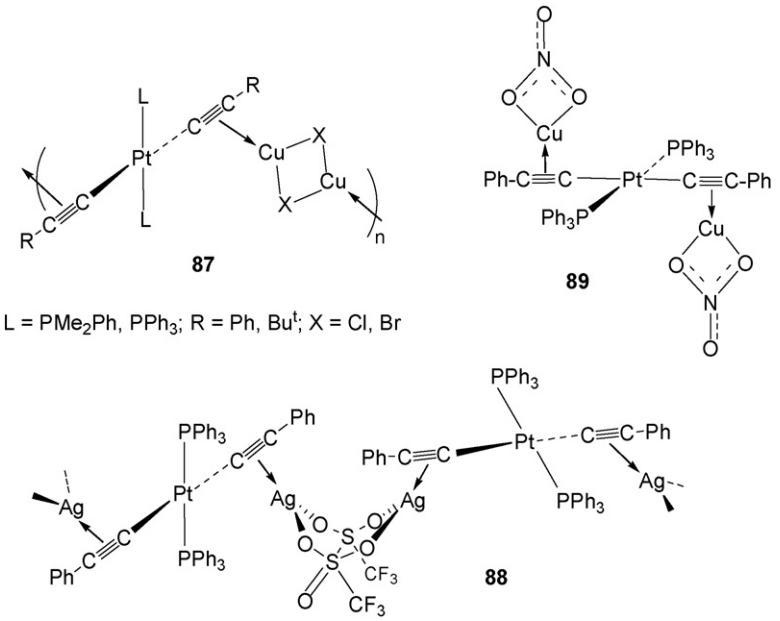

Chart 13.

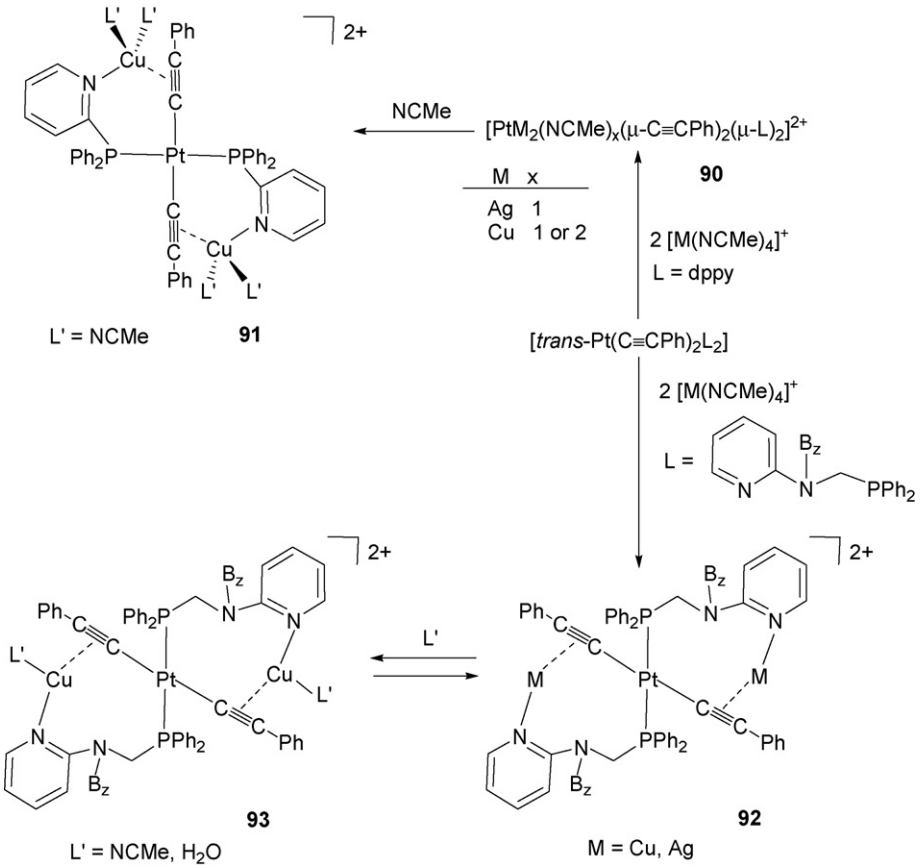

Scheme 16.

Yam et al. have reported a different type of face-to-face tetranuclear dicationic Pt_2M_2 complexes originated by encapsulation of $[M(NCMe)]^+$ units (M = Cu, Ag) **98** (Chart 15) between two adjacent acetylide ligands in the *trans-trans*-tetraalkynylplatinum precursor [134,135]. The presence of the heterometal push the Pt···Pt atoms in closer proximity [3.0124(9) Å, M = Cu; 3.0637(9) Å, M = Ag] in relation to the precursor [3.437(1) Å] [134]. In solid and glass state (77 K), these complexes exhibit intraligand phosphorescence and a low energy structured band, red-shifted (solid 77 K, 634 nm Pt_2Cu_2; 620 nm Pt_2Ag_2) in relation to the precursor (Pt_2, 607 nm), attributed to ^{3}MMLCT [$d\sigma^* \rightarrow p(\sigma)/\pi^*(C{\equiv}CPh)$], where the $d\sigma^*$ and $p(\sigma)$ are the antibonding (d_z2–d_z2) and bonding [p_z(Pt)–p_z(Pt)] combinations, respectively, of the Pt···Pt interaction. The slightly higher emission of the Pt_2Ag_2 complexes in relation to the copper one has been ascribed to the weaker Lewis acidity of Ag^I as well as its larger size, which raises the π^*(C≡CPh) orbital energy and lowers the $d\sigma^*$ orbital increasing the HOMO–LUMO gap [57,135].

(iii) *Systems based on cis-configured dialkynylplatinum complexes.* As has been shown in Section 2, a 3-platina-1,4-butadyine fragment having a mutually *cis* disposition of the alkynyl moieties *cis*-[Pt](C≡CR)$_2$ is a versatile framework upon which to construct polymetallic complexes. Its reactivity towards diverse group-11 transition metal sources affords a wide range of heteropolymetallic depending on the charge of the platinum fragment, the stoichiometry, the alkynyl substituents and also of the auxiliary ligands. Some aspects of this chemistry have been reviewed previously by Lang et al. [9,122] and our group [6].

The proximity of both alkynyl fragments in neutral [Pt](C≡CR)$_2$, [Pt] = Pt(N–N) (N–N = diimine) [136–139], PtL_2 (L = PMe_2Ph, ½ dppe; PBu_3) [98,140,141] provides access to a wide range of heterobimetallic complexes **99** (Eq. (17)) in which the 3-platina-1,4-butadiyne acts as a tweezer or chelating ligand to MX (M = Cu, Ag; X = inorganic or organic ligand) [122].

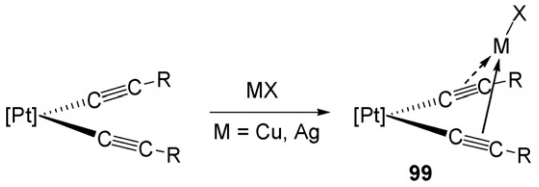

(17)

As shown in Eq. (17), in the final complexes the tricoordinated heterometal (Cu^I, Ag^I) [136,137,140,141] is η^2-bonded to both C≡C triple bonds and located out of the platinadiyne fragment, forming an V-shaped (Chart 5, **C**) doubly alkynyl bridging system or "nonplanar" tweezer molecule [9], as confirmed in selected X-ray studies [136,137,140,141]. In these Pt–M systems (M = Cu, Ag), the observed η^2-M–C_α,C_β bond distances are shorter in the Pt–Cu derivatives and the corresponding ν(C≡C) absorptions occurs also at lower frequencies for the platinum–copper species, thus indicating that the η^2-alkyne interactions are stronger with Cu^I, probably due to stronger π-back bonding [$d^{10} \rightarrow \pi^*$(C≡CR)] [140]. Some complexes having the CuX (X = Cl, I) η^2-coordinated to both acetylides are so stable that they are generated serendipitiously (or as secondary species) in reactions of dichloride platinum precursors with terminal acetylenes catalyzed by CuX [138,140,141].

By contrast, cationic heterobimetallic adducts having more acidic fragments such as ML^+ units are less stable. Thus, complex [(4,4′-Me_2bipy)Pt(μ-κC^α:η^2-C≡CPh)$_2$AgPPh$_3$]BF_4 **100** is stable in the solid state, but in solution (CH_2Cl_2) evolves with alkynylation of the silver center giving rise to [Pt(C≡CPh)(4,4′-Me_2bipy)(PPh_3)]BF_4 along with the polymeric [Ag(C≡CPh)]$_n$ [142]. Similarly, the pentametallic derivative [(O_3ClO)Ag(μ-1,2,3,4-bipym)Pt(μ-κC^α:η^2-C≡CFc)$_2$Ag($OClO_3$)] **101** (bipym = 2,2′-

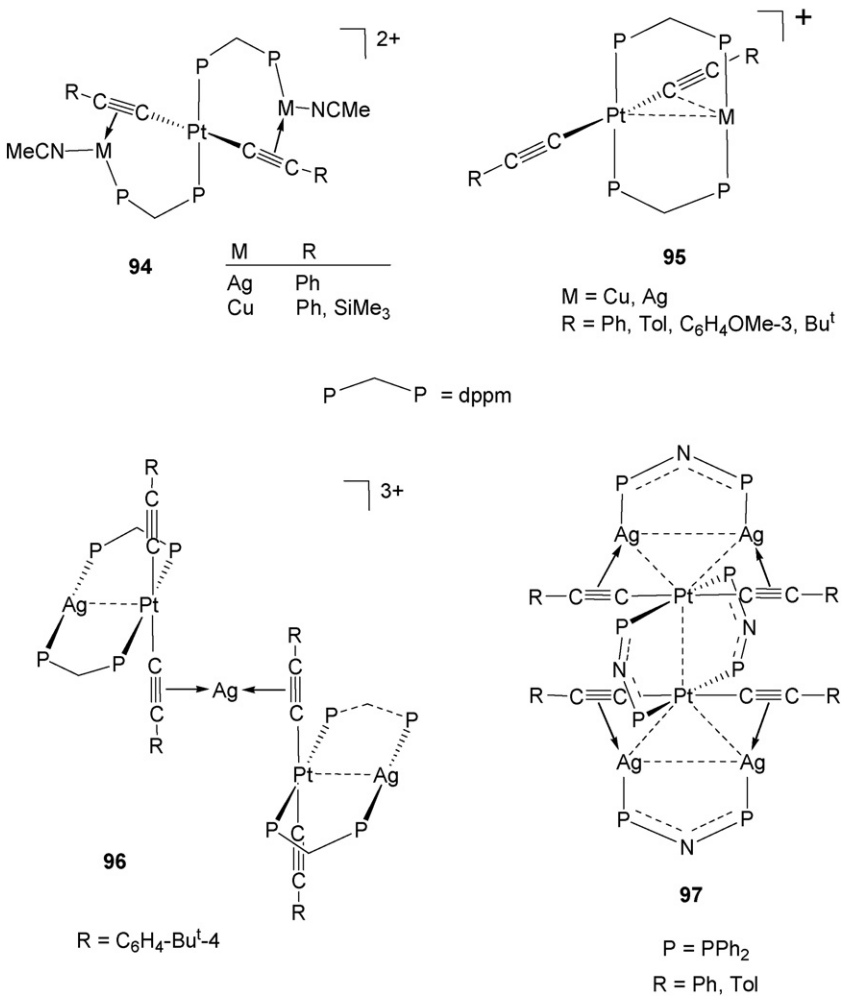

Chart 14.

bipyrimidine, Fc = ferrocenyl) decomposes in acetonitrile through a redox reaction to give Fc–C≡C–C≡C–Fc and elemental silver [143]. An interesting type of trinuclear cationic $[\{[Pt](\mu\text{-}C{\equiv}CR)_2\}_2M]^+$ complex **102** is easily generated, upon standing in solution with 1,1 adducts having phosphorus donors as auxiliary ligands at platinum (Scheme 17). X-ray diffraction studies reveal that in these complexes the M^I is tetrahedrically η^2-coordinated to the alkynyl units of two nearly orthogonal platinum fragments [141,144,145]. As expected, this type of complexes are straightforward produced when the reactions between *cis*-dialkynyl platinum precursors and the M^+ source are performed using a 2:1 molar ratio [145–147]. In the case of dialkynyldiimine platinum substrates, Lang et al. have found a third route based in two successive steps, which are shown in Scheme 18. Curiously, the formation of the final complexes takes place through isomeric intermediates, which are structurally different for copper than for silver ions.

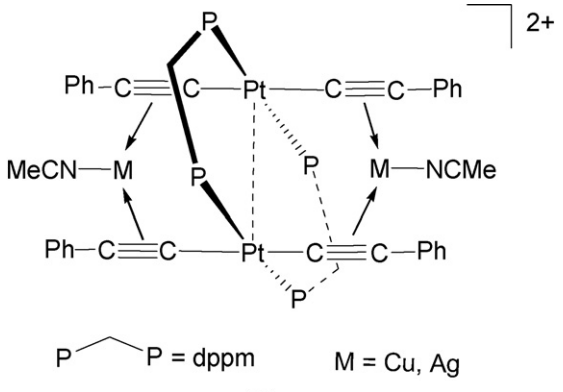

Chart 15.

Thus, displacement of the acetonitrile ligand in the Pt–Cu derivative **103** by the dialkynyl precursor [Pt(4,4′-Me_2bipy)(C≡CPh)$_2$] initially gives the trinuclear dicoordinate bis(alkyne) Cu^I (14 valence electron) **104**, in which the platinum fragments are parallel and only one of each of the C≡CPh units is acting as bridging ligand (X-ray) [146]. On stirring in solution **104** evolves to final 18 e^- tetrahedrically Cu^I coordinated complex **105Cu**. By contrast, in the case of the platinum–silver derivatives type **106**, and probably due to the stronger metallophilic Pt···Ag bonding interactions, a different type of intermediate **107** is obtained. The molecular structure of the $[\{Pt(bipy)(\mu\text{-}C{\equiv}CPh)_2\}_2Ag]BF_4$ reveals that the Ag^+ is sandwiched between the platinum fragments, being preferentially bonded to the Pt–C_α bonds [Pt–Ag = 2.8965(3) Å; Ag–C_α = 2.447(7), 2.548(7) Å], giving rise to a nearly planar AgC_4 environment [147]. This intermediate slowly isomerizes (7 days) to form again the thermodynamically more stable species **105Ag** (X-ray) [122]. Spectroscopically, the stronger interaction of Ag^+ with the C_β carbon in isomer **105Ag** is reflected in the displacement of the ν(C≡C) vibrations to lower frequencies (*i.e.* 2087, 2074 cm^{-1} *vs.* 2116, 2097 cm^{-1} for

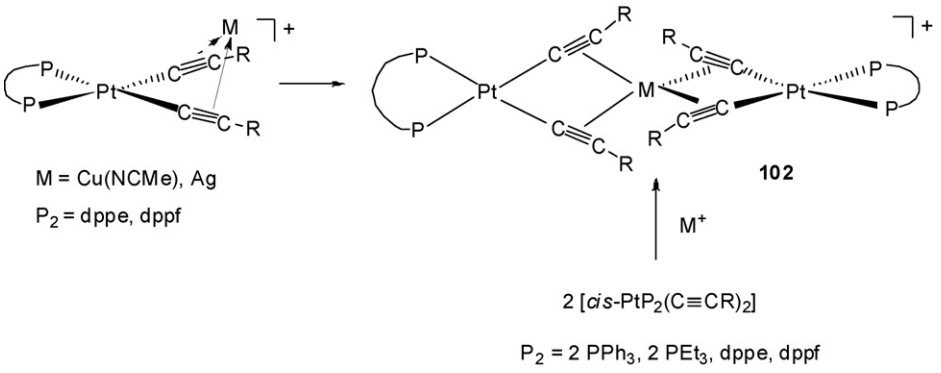

Scheme 17.

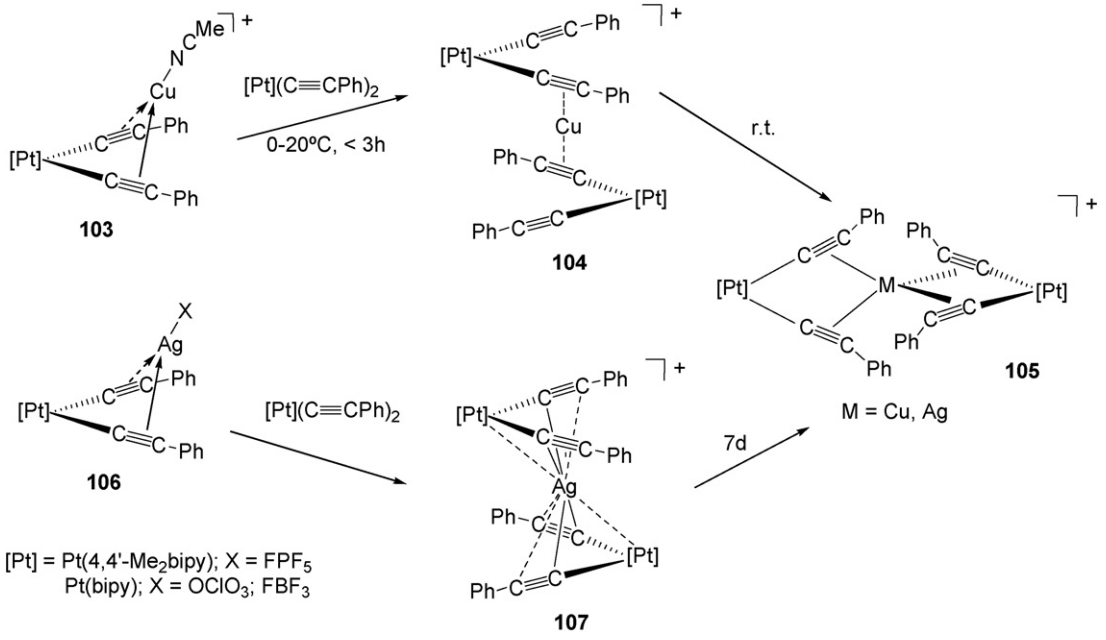

Scheme 18.

[{Pt(bipy)(C≡CPh)$_2$}$_2$Ag]BF$_4$ **107**). The tendency of Cu^I to linear dicoordination is also reflected in the ease formation of a tetranuclear dicationic Pt_2Cu_2 complex **108** by prolonged stirring of the binuclear derivative [Pt(bipy)(μ-C≡CPh)$_2$Cu(PPh$_3$)]BF$_4$ generated in solution [146] (Chart 16).

In this complex (**108**), the 3-platina-1,4-diyne fragments behave as a bidentate bridging ligand to two dicoordinate Cu^I ions. Interestingly, Forniés and co-workers have demonstrated that this type of tetranuclear Pt_2M_2 complex, having

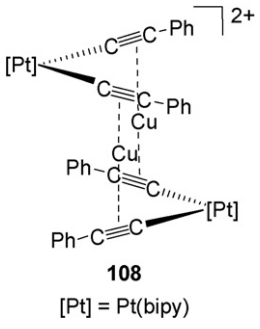

Chart 16.

two dialkynyl platinum fragments connected by M$^+$ ions, are always generated by starting from anionic platinate building blocks (**109**–**111**, Scheme 19) [85,148,149]. In these systems, weakly donor groups such perchlorate, triflate or acetonitrile are easily displaced from the electrophilic M^I ions by the platina-alkyne unit. The dianionic Pt_2M_2 complexes **109** are even formed by depolymerization of AgCl and CuCl and further displacement of chloride ligand, indicating that the η^2-alkyne fragments have a higher coordinating ability towards M^I than Cl$^-$ ion. X-ray diffraction studies of [Pt$_2$Ag$_2$(R$_f$)$_4$(C≡CPh)$_4$]$^{2-}$ (**109**) [148], [PtAg$_2${(PPh$_2$O)$_2$H}$_2$(C≡CPh)$_4$] (**110**) [149] and [Pt$_2$Cu$_2$(C∧P)$_2$(C≡CPh)$_4$] (**111**) [85] reveal that, while in the anion the platinum fragments are parallel and disposed in an *anti* fashion, in the neutral complexes they are staggered with the platinum planes forming dihedral angles of ≈136° and ≈124°, respectively. The Pt···Cu separations [2.9436(6)–3.1793(5) Å] are close to the van der Waals limit (3.15 Å), but the Pt···Ag (3.10 Å) and Ag···Ag [2.939(1) Å] are shorter than the corresponding van der Waals radii (3.47 and 3.44 Å, respectively), suggesting that the metallophilic bonding interactions are stronger in the latter. Similar tetranuclear trimetallic complexes **112** [d^{6}MPt] (d^6 = Rh^{III}, Ir^{III}) [150] have also been synthesized by reaction of bimetallic chloride bridged [(PEt$_3$)Cp*M′(μ-Cl)$_2$Pt(R$_f$)$_2$] (M′ = Rh, Ir) with the alkynylating polymeric species [M(C≡CPh)]$_x$ (M = Cu, Ag), being

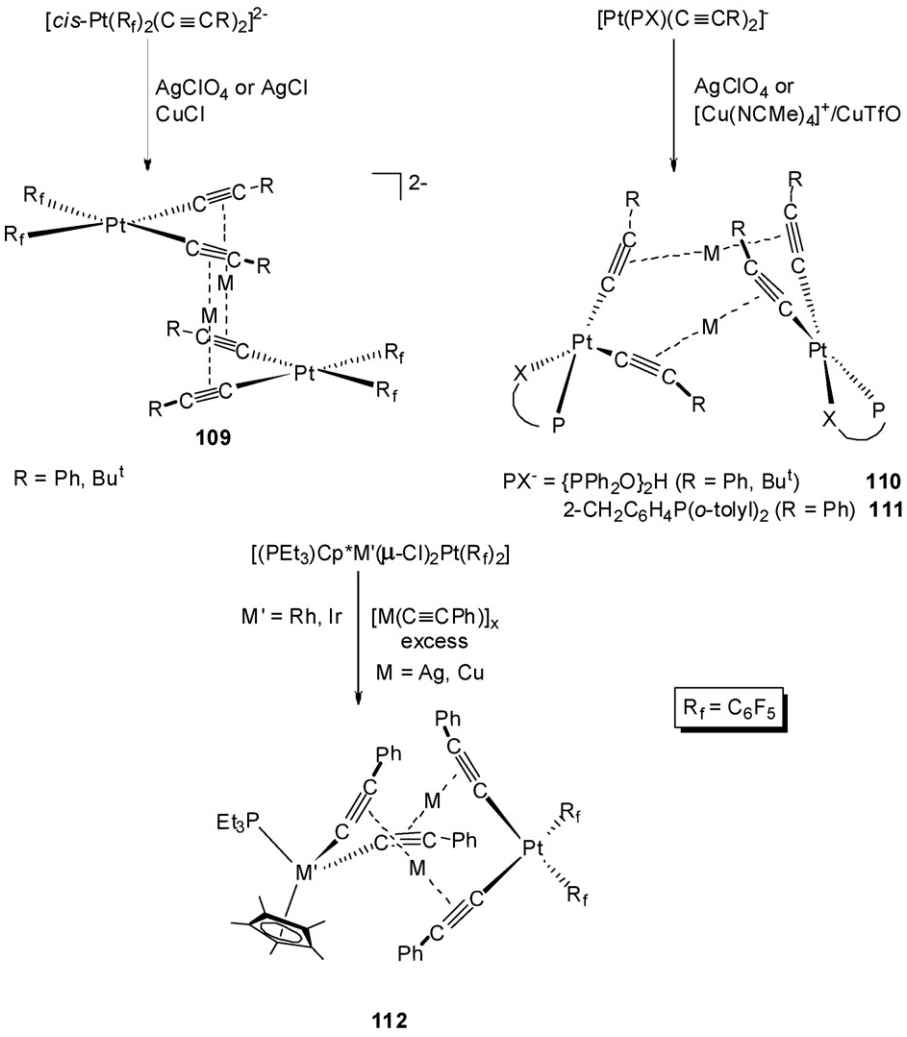

Scheme 19.

structurally characterized in the case of the $RhCu_2Pt$ derivative. As in previous Pt–M (M = Cu, Ag) systems, structural and spectroscopic data in complexes **109**–**112** indicate that the η^2-alkyne–metal interaction is stronger in copper than in silver complexes. Complexes $[Pt_2M_2\{(PPh_2O)_2H\}_2(C{\equiv}CR)_4]$ **110** are emissive in frozen CH_2Cl_2 solutions, shifted to lower energy along the series Cu, Ph > Ag, Ph > Cu, Bu^t > Ag, Bu^t, suggesting the involvement of the $\pi^*(C{\equiv}CR)$ and d^{10} metal orbitals on the lowest excited state [149].

As expected, treatment of the tetranuclear Pt_2Ag_2 anionic complexes **109Ag** with stronger donor phosphine ligands (PPh_3, PEt_3 or dppe) results in the formation of dynamic chelating type dinuclear **113** and tetranuclear **114** (Scheme 20) anionic derivatives, in which the alkynyl groups exhibit a rather asymmetric bonding mode halfway between μ-η^2 and μ-κC^{α} [Ag–C_{α} 2.307(7)–2.438(7) *vs.* Ag–C_{β} 2.545(7)–2.843(8) Å] [151].

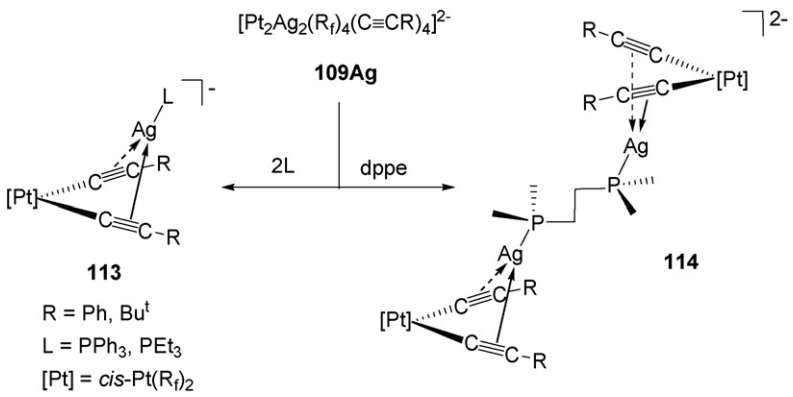

Scheme 20.

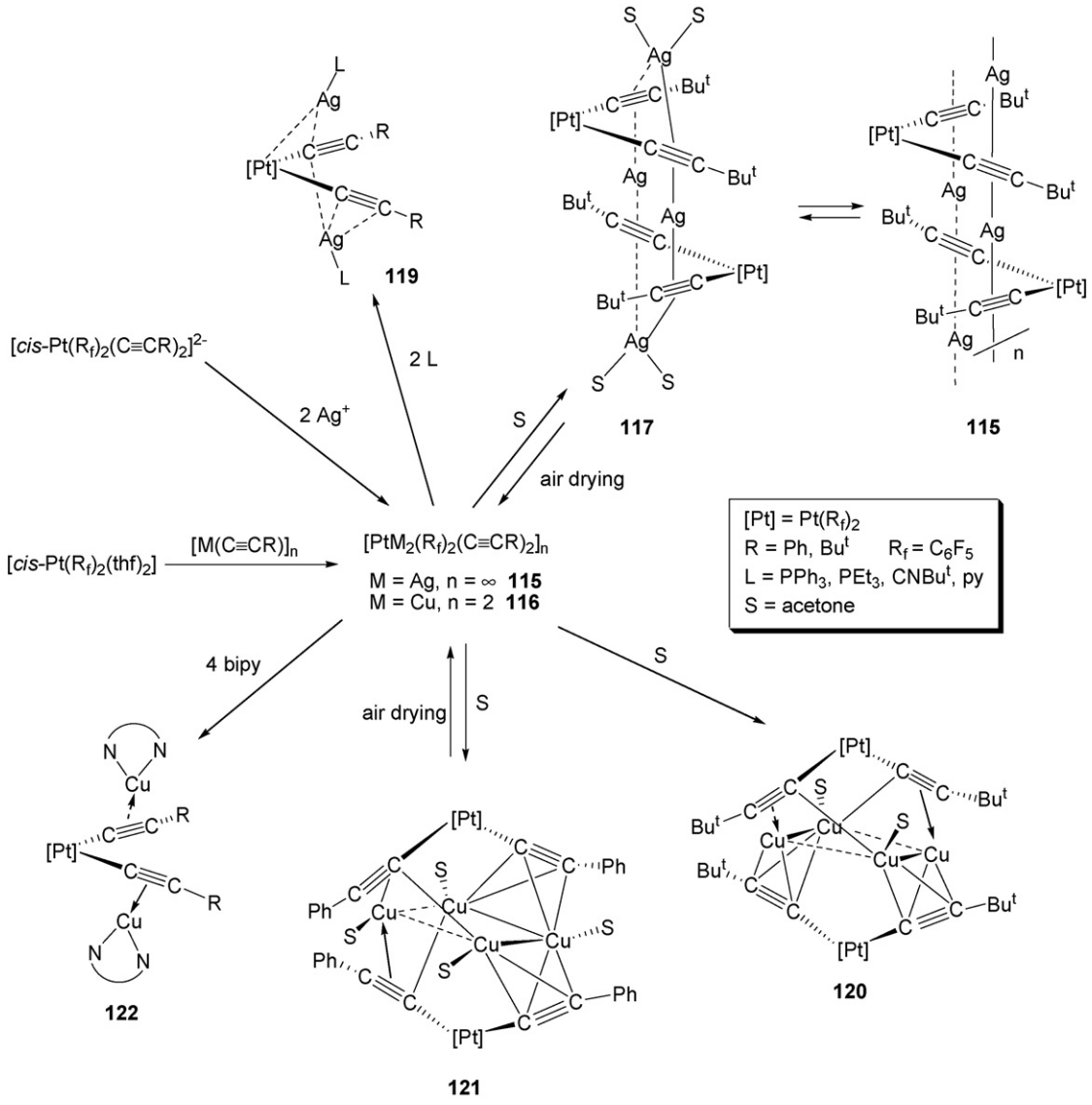

Scheme 21.

The dianionic fragments $[cis\text{-}Pt(R_f)_2(C{\equiv}CR)_2]^{2-}$ are excellent synthons of higher nuclearity species in which the dialkynylplatinate unit acts as tetradentate μ_3 or μ_4 bridging ligand. As shown in Scheme 21, treatment of this precursor with 2 equiv. of $AgClO_4$ gives insoluble and deeply yellow species of stoichiometry $[PtAg_2(R_f)_2(C{\equiv}CR)_2]$ **115** [152]. These species and the related platinum–copper systems (**116**) are alternatively obtained by a double-alkynylation reaction of the solvate $[cis\text{-}Pt(R_f)_2(thf)_2]$ with the corresponding polymeric $[M(C{\equiv}CR)]_n$ (M = Ag, Cu; R = Bu^t, Ph) [153]. Interestingly, the yellow Pt–Ag/Bu^t derivative dissolves reversibly in acetone affording the colourless hexanuclear adduct $[Pt_2Ag_4(R_f)_4(C{\equiv}CBu^t)_8(acetone)_4]$ **117** (Scheme 21), which displays two bridging Ag centers exclusively bonded to alkynyl groups and two terminal ones, which are also stabilized by two weakly bonded acetone molecules. As a consequence, the 3-platina-1,4-diyne fragments behaves as tridentate bridging ligands and the alkynyl groups adopt an asymmetric μ_3-η^2 bonding mode [152]. Related hexanuclear complexes $[Pt_2Ag_4(R_f)_4(C{\equiv}CR)_4L_2]$ (L = PPh_3, PEt_3, $CNBu^t$, py) **118** are obtained by reaction of the polymeric $[Pt(R_f)_2(C{\equiv}CR)_2Ag_2]_n$ with the corresponding L in adequate molar ratio (Ag:L 2:1), as has been confirmed by X-ray [154]. In contrast, total depolymerization takes place when a higher proportion of L is used yielding trinuclear $[PtAg_2(R_f)_2(C{\equiv}CR)_2L_2]$ derivatives **119** (Scheme 21) [154,155]. The structure of the complex with L = PPh_3 and R = Ph shows that while one of the $AgPPh_3$ units is asymmetrically bonded to both alkynyl groups, the second is essentially bonded to one of the Pt–C_α bonds [Pt–Ag 2.812(2) Å; Ag–C_α 2.29(2) Å]. As a result, one C≡CPh acts as a μ-η^2 and the other bridges the three metals in a predominantly μ_3-κC^α manner [155].

The related platinum–copper derivatives **116** interact with acetone giving rise to structurally different derivatives **120** and **121**. X-ray diffraction studies of **120** and **121** shows the presence of a nearly planar tetranuclear Cu_4 unit with two short Cu···Cu distances (≈2.6 Å) and two longer ones (>2.8 Å), which is bicapped by two orthogonal dialkynylplatinate fragments acting in these systems as bridging tetradentate ligands [153]. The structures of **117**, **119**–**121** suggest that the unsolvated **115** and **116** species presumably have a different structure. For the Pt–silver species **115**, a polymeric structure of the type shown in Scheme 21 is suggested, which can be partially or totally depolymerized with acetone or donor ligands. By contrast, the unsolvated platinum–copper **116** presumably has a dimer structure similar to those of **120** and **121** based on a tetranuclear Cu_4 unit, probably with very short Cu···Cu contacts, capped with both dialkynyl fragments through η^2···Cu

alkyne bonds. In donor solvents such as acetone, interaction of the solvent with the copper atoms probably causes a weakening of Cu···alkyne and/or Cu···Cu interactions. These latter clearly disappear on treatment with bipy leading to trinuclear derivatives **122**, in which the 3-platina,1-4-diyne fragment acts as bidentate bridging ligand to two separated (Cu···Cu ≈ 4.3 Å) tricoordinated Cu^I ions [153]. The presence of very short metal···metal contacts seems to be responsible of the emissive behaviour of these clusters. A comparison of the photoluminescence spectra of the platinum–copper derivatives (**116**, **120**) with those of the related platinum–silver species (**115**) and the mononuclear [*cis*-$Pt(R_f)_2(C{\equiv}CR)_2]^{2-}$ suggest the presence of emitting states bearing a large cluster-to-ligand charge transfer (CLCT) [153].

As shown in Scheme 22, double deprotonation of bis(3,5-dimethylpyrazole)bis(phenylethynyl)platinum(II) in the presence of adequate M^I (M = Cu, Ag, Au) sources affords discrete hexanuclear clusters [$Pt_2M_4(\mu$-C≡CPh$)_4(\mu$-dmpz$)_4$] **123** and **124** (X-ray) [156]. However, while in the Pt_2Cu_4 derivative **123**, all copper centers have similar local geometry being linearly coordinated to a nitrogen and η^2 to one alkynyl fragment, in the Pt_2M_4 (M = Ag, Au) derivatives **124**, the silver and gold atoms present three different linear environments. Two of the atoms show similar mixed coordination to the Cu in complex **123**, while the other two are linked to two nitrogen and two η^2-alkynyl units, respectively.

These clusters exhibit a characteristic low energy absorption, red-shifted in Pt_2Cu_4 **123** (346 nm) in relation to Pt_2Ag_4 and Pt_2Au_4 **124** (≈330 nm), assigned as an admixture of ^{1}MLCT [Pt/π(C≡CPh) → π*(C≡CPh)] and ^{1}LM′CT (ligand or platina–ligand-M′ charge transfer) [Pt–C≡CPh → M′(d^{10})] perturbed by the presence of Pt···M (d^{10}) bonding interactions. The transition may be viewed as an ^{1}MLM′CT with intraligand C≡CPh character. As illustrated in Fig. 2, these clusters exhibit bright luminescence in fluid solution upon excitation in the low energy absorption, which follow the energy order Ag > Au > Cu. The emission is associated with the η^2-platina-alkyne entities and ascribed to the ^{3}MLM′CT [Pt(*d*)/π(C≡CPh) → Pt(p_z)M′(*sp*)/π*(C≡CPh)] modified by Pt···M′

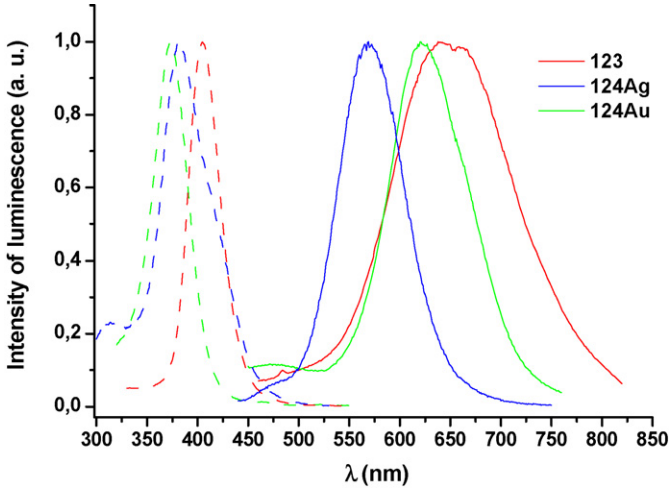

Fig. 2. Normalized excitation and emission spectra of **123**, **124Ag** and **124Au** in fluid CH_2Cl_2 solution (10^{-3} M) at 298 K: **123** (λ_{ex} 420, λ_{em} 640); **124Ag** (λ_{ex} 420, λ_{em} 560); **124Au** (λ_{ex} 370, λ_{em} 620).

(d^{10}) interactions. The emission may be viewed as a ^{3}MLM′CT with intraligand character. In rigid media (glass, solid) an additional high energy occurs, clearly structured in the Pt_2Au_4 derivative, which is attributed to emissive states derived from ^{3}LM′CT transitions [π(dmpz) → M′(d^{10})] [156].

A very unusual Pt_2Cu_6 heteropolynuclear alkynyl cluster [Pt_2Cu_6(bzq$)_2$(C≡C–C_5H_4N-2$)_6I_2$] **125** is generated by treatment of [Pt(bzq)(μ-Cl)$]_2$ with 2-ethynylpyridine (HC≡C–C_5H_4N-2) and CuI in presence of NEt_3 [157]. The formation of this cluster is of interest because this is the first copper cluster formed following the Sonogashira protocol. An X-ray diffraction study reveals that this cluster is formed by an hexanuclear dicationic central copper core [Cu_6(C≡C–C_5H_4N-2$)_2I_2]^{2+}$ with an open book shape [Cu···Cu distances = 2.5185(11), 2.5338(10) Å; 2.8189(11)–3.0327(11) Å],

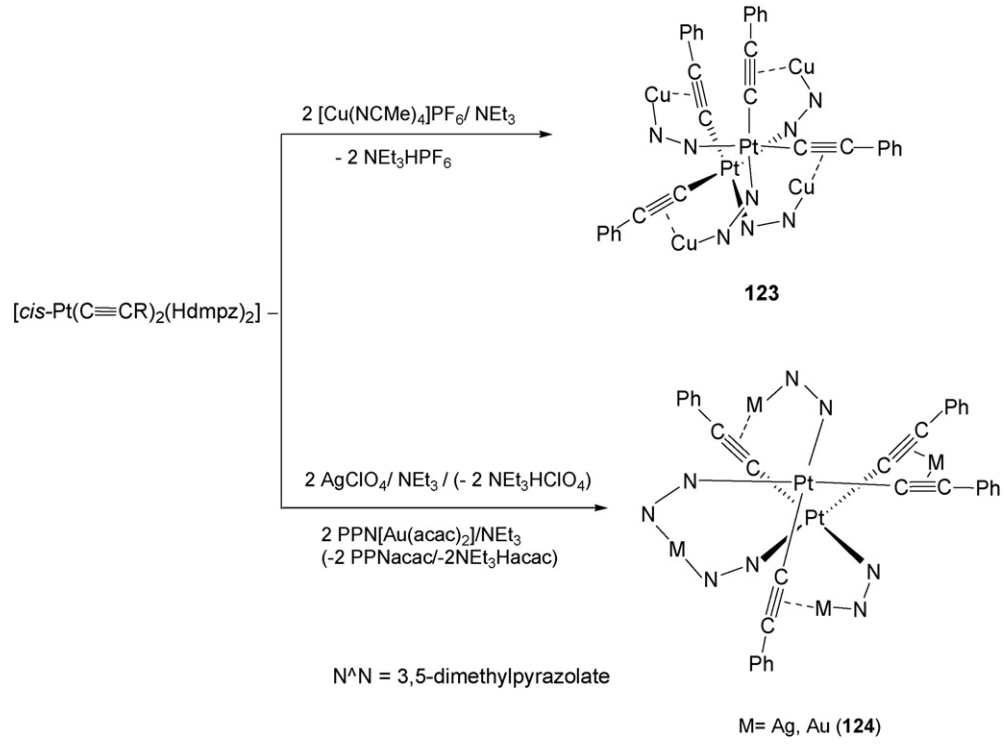

Scheme 22.

enveloped by two monoanionic benzoquinolinate dialkynylplatinate(II) $[Pt(bzq)(C{\equiv}C{-}C_5H_4N\text{-}2)_2]^-$ fragments (Fig. 3). As a result, three types of copper environments and three different coordination modes for the alkynyl entities are found (μ-PtκC^{α}:CuκN, μ_3-PtκC^{α}:Cuη^2:CuκN and μ_4-Cu$_3\kappa C^{\alpha}$:CuκN modes). The low energy emission observed in the solid state (638 nm, τ = 10.9 μs, 298 K; 660 nm, τ = 18.9 μs, 77 K) and in CH_2Cl_2 glass at 77 K (615 nm, τ = 59 μs) is related to the short Cu···Cu interactions in the Cu_6 core and suggested to have substantial ligand-to-metal charge transfer ^{3}LM′CT [2-pyridylethynyl → Cu$_n$] character, probably mixed with a Cu^I-centered d/sp character. The additional high energy emission seen in glass state (540 nm) and in fluid solution (560 nm) originates from intraligand $^3\pi\pi^*$ excited states of the 2-pyridylethynyl ligands associated with the platinum fragments perturbed by coordination (η or κN) to the copper. Notwithstanding, the unambiguous assignment of the luminescence observed is not easy, due to the complex architecture of the cluster.

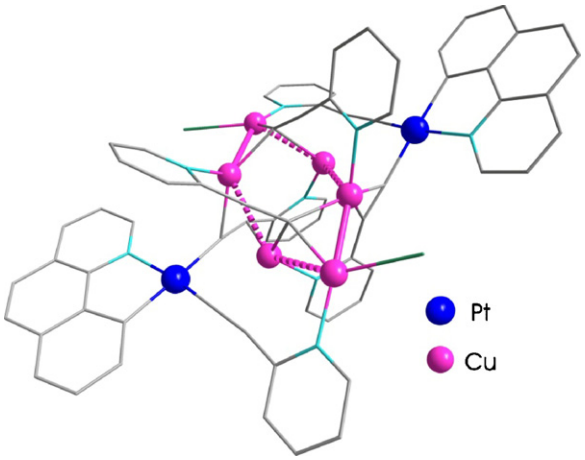

Fig. 3. Simplified view of $[Pt_2Cu_6(bzq)_2(C{\equiv}C{-}C_5H_4N\text{-}2)_6I_2]$ **125** (Ref. [157]).

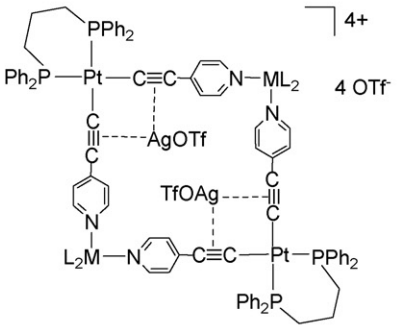

126

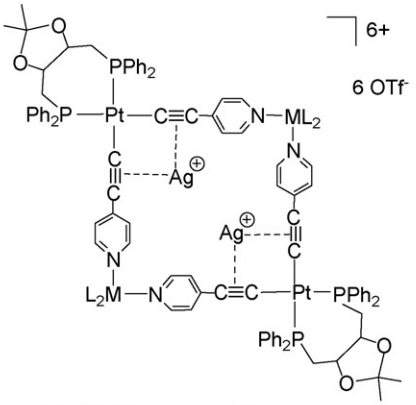

127

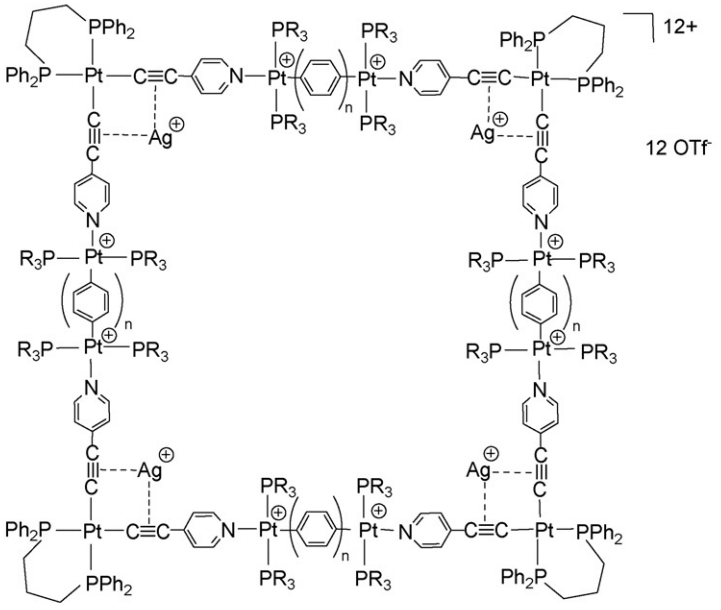

128

Chart 17.

Stang and co-workers [158–161] and others [98] have elegantly used square-planar macrocyclic Pt_8, Pt_4 and Pt_2Pd_2 complexes, having $C{\equiv}C{-}C_6H_4N\text{-}4^-$, $C{\equiv}C{-}C{\equiv}C^{2-}$ and PtL_2 units as linkers and suitable dialkynyl platinum(II) units at two or at the four corners, as host for acidic Ag^I (and also Cu^I) [98] guests. The resulting 1:2 or 1:4 bis η^2-complexed adducts **126**–**128** (Chart 17) have been adequately characterized by analytical, spectroscopic and physical means.

The 1:2 host–guest assemblies based on 4-ethynylpyridyl linkers **126** [162] and **127** [161] (chiral molecular squares) have sufficient space to accommodate neutral aromatic guests giving rise to stable inclusion complexes such as those shown in Eq. (18) (**129**).

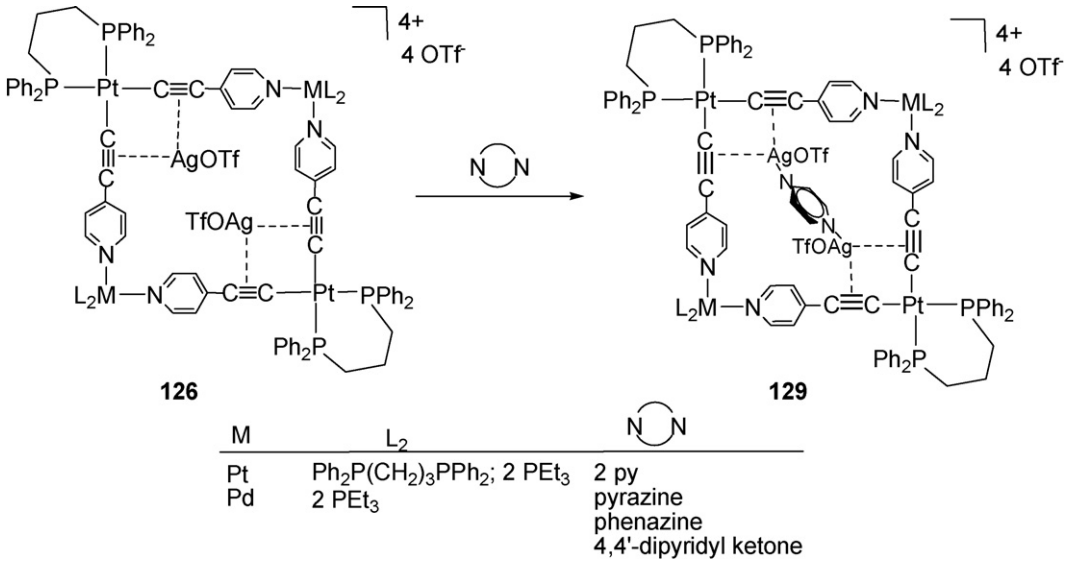

(18)

The X-ray structure of the host–guest complex [*cyclo*-bis{(dppp)Pt(C≡C–$C_6H_4N)_2$Pt($PEt_3)_2$}Ag_2(μ-phenazine)](OTf)$_6$ **129phenazine** reveals that the guest phenazine is oriented nearly orthogonal to the square Pt_4 and is bonded by the N atoms to the η^2 complexed Ag ions, which adopt a pseudo*trans* arrangement with respect to the Pt_4 plane [162]. In the case of the chiral tetranuclear macrocycles precursors, circular dichroism is a valuable tool for detecting either the formation of 1:2 adducts **127** and the additional inclusion of neutral aromatic guests **129** [161]. In this way, smaller mono and bimetallic diasteromerically pure novel platinum macrocycles based on interesting alkynyl ligands containing two or four β-lactams fragments have also been recently employed to form 1:1 (**130a**, **b**) and 1:2 (**131**) (Chart 18) host/AgTfO guest complexes [163] in a tweezer fahion.

(iv) *Systems based on tris and tetraalkynyl platinate fragments*: Sonogashira reported the unusual paramagnetic trimetallic hexanuclear green cluster **132**, generated by treatment of [$(C_5H_4)_2$Fe{PtCl(cod)}$_2$] with excess of [Cu(C≡CPh)]$_n$, prepared *in situ* (Eq. (19)). The presence of Fe^{III} was detected by ESR and the molecular structure was confirmed by X-ray [164].

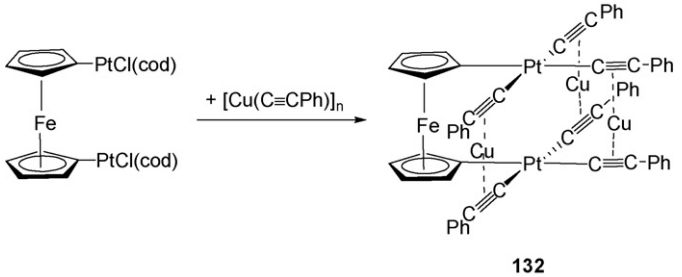

(19)

Diverse heteropolynuclear complexes depending on the nature of the M^I source, the stoichiometry and also the alkynyl substituent have been isolated [6] using homoleptic $[Pt(C{\equiv}CR)_4]^{2-}$ [165,166] as building blocks, some of which exhibit rich luminescence properties. Thus, simple trinuclear 1:2 adducts $(NBu_4)_2$[{Pt(μ-$\kappa C^{\alpha}{:}\eta^2 C{\equiv}CR)_4$}$(MX)_2$] **133** (R = Ph, Bu^t; M = Ag, Cu; X = Cl, Br) [166], having the dianionic platinum fragment acting as tetradentate bridging ligand of two neutral MX units, are isolated by reaction of $(NBu_4)_2$[Pt(C≡CR)$_4$] with MX (molar ratio 1:2 for R = Ph or 1:8 for R = Bu^t) (Scheme 23). NMR studies in solution indicate that *tert*-butylacetylide derivatives eliminate in a reversible way

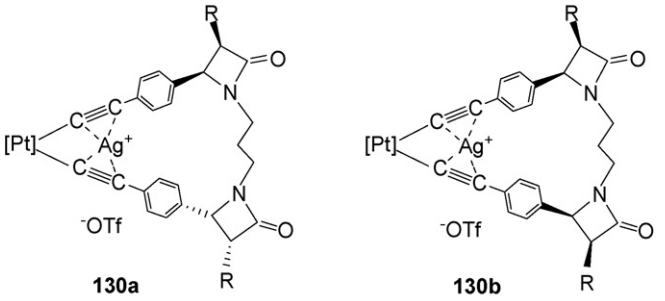

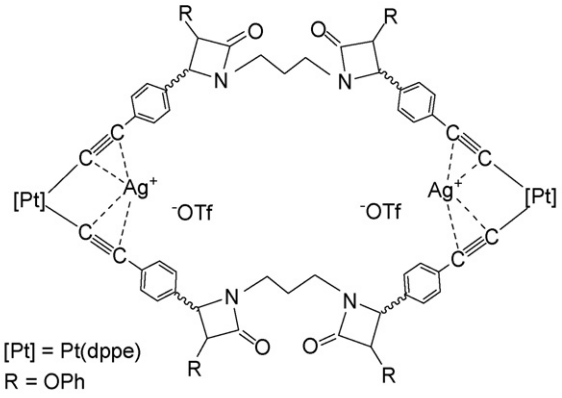

Chart 18.

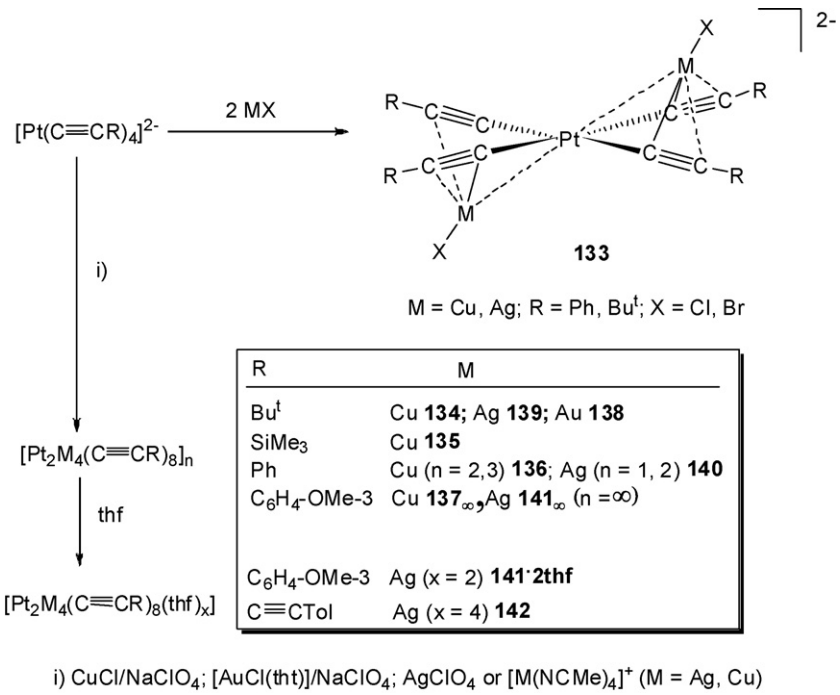

Scheme 23.

NBu_4X leading to higher nuclearity species [167], some of this chemistry has been reviewed [6]. In fact, in the presence of $NaClO_4$ as an abstractor of chloride, the reactions with CuCl evolves with formation of hexanuclear $[Pt_2Cu_4(C{\equiv}CR)_8]$ **134**–**137** complexes. The related platinum–gold cluster $[Pt_2Au_4(C{\equiv}CBu^t)_8]$ **138** is also accessible by this route [165] (Scheme 23), while the corresponding platinum–silver systems $[Pt_2Ag_4(C{\equiv}CR)_8]$ **139**–**142** are usually generated employing $AgClO_4$ [165,168]. Similar synthetic strategy but using $[M(NCMe)_4]^+$ as M^I source has been reported by Yam et al. [169,170].

X-ray diffraction studies (M = Ag, Cu; R = Bu^t) and properties of the bulky (R = Bu^t, $SiMe_3$) derivatives **134**, **139** indicate the formation of discrete octahedral Pt_2M_4 cores in which two staggered (C_α–Pt–Pt–C_α = 37.13° and 32.84°, M = Ag; 36.7°, M = Cu) platinate units are connected by dicoordinated M^I ions (Fig. 4) [165,171]. The M^I-alkyne bond distances are slightly asymmetric and shorter in the Pt_2Cu_4 derivative (M-C_α,$C_\beta \approx$ 2.25 and 2.43 Å for M = Ag *vs.* ≈2.00, 2.15 Å for M = Cu) and, as a result, the Pt···Pt separation within the core is shorter in the latter (3.706 Å in Pt_2Cu_4 *vs.* 4.18 Å in Pt_2Ag_4). In both complexes, the observed Pt···M distances [3.025–3.170 Å, M = Ag; 2.9615(7)–3.0668(7) Å, M = Cu] are shorter than the corresponding van der Waals limits (Pt···Ag 3.47 Å, Pt···Cu 3.15 Å), indicative of the presence of some weak metallic interactions, which seem to be stronger in the platinum–silver derivative. The ν(C≡C) vibration occurs at lower frequencies in the Pt_2Au_4 derivative **138** (1995 cm^{-1}) than in the copper and silver clusters (2017, **134** and 2043 cm^{-1} **139**, respectively) pointing to stronger alkyne–metal bonding [165]. This result is in line with recent experimental observations and DFT calculations on monomeric coinage internal alkyne adducts $[N\{(C_3F_7)C(Dipp)N\}_2]M(EtC{\equiv}CEt)$ (Dipp = 2,6-diisopropylphenyl), which show that the gold(I) forms the strongest bond with the alkyne, while the silver(I) forms the weakest bond [172].

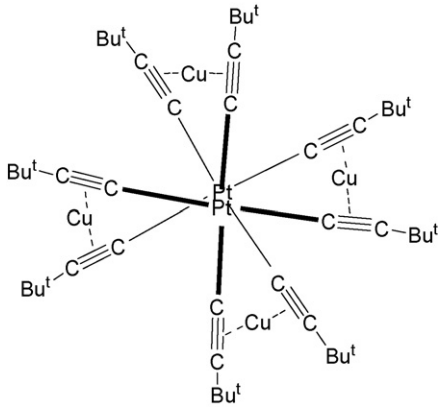

Fig. 4. Schematic view of $[Pt_2Cu_4(C{\equiv}CBu^t)_8]$ **134**, showing the staggered platinate units connected by dicoordinated Cu^I ions.

These discrete clusters exhibit intense long-lived room temperature luminescence in the solid state, whose energy depends strongly on the nature of the heterometal (green 476 nm $[Pt_2Ag_4(C{\equiv}CBu^t)_8]$ **139**, orange 570 nm $[Pt_2Cu_4(C{\equiv}CBu^t)_8]$ **134**, orange-red 650 nm $[Pt_2Au_4(C{\equiv}CBu^t)_8]$ **138**) and the nature of the alkynyl substituent (595 nm $[Pt_2Cu_4(C{\equiv}CSiMe_3)_8]$ **135**) [169,173,174]. On the basis of qualitative EHMO calculations carried out on $[Pt_2Ag_4(C{\equiv}CBu^t)_8]$ [174] [HOMO Pt(*d*) 54%/π(C≡C); LUMO Pt(p_z) 20%/Ag(*sp*) 24%/≡C_β 56%], the emission has been assigned to a platina–ligand-heterometal charge transfer excited state ^{3}MLM′CT mixed with intraligand character, probably modified by Pt···M and M···M interactions.

In the arylethynyl derivatives (M = Cu **136**, **137**; Ag **140**, **141**, Scheme 24) the presence of axial Pt···Pt bonding, due to overlap of the predominantly d_z2 orbitals between clusters (see Scheme 24 for R = Ph), or weak noncovalent metal solvent [Pt···$HCCl_3$ or Ag···O(thf)] bonding interactions play a remarkable role in the structures and optical properties. The factors influencing the interaction between adjacent clusters are not clear. It was favoured in non-donor solvents (CH_2Cl_2, $CHCl_3$) and is particularly enhanced in platinum–copper derivatives (**136**, **137**), presumably by the stronger η^2-alkynyl–Cu bond, as revealed by lower ν(C≡C). It was suggested that the η^2-alkynyl–M′ (M′ = d^{10}) bonding within the cluster enhances the strength of the [d(Pt) → π^*]Pt→C ≡ CR back

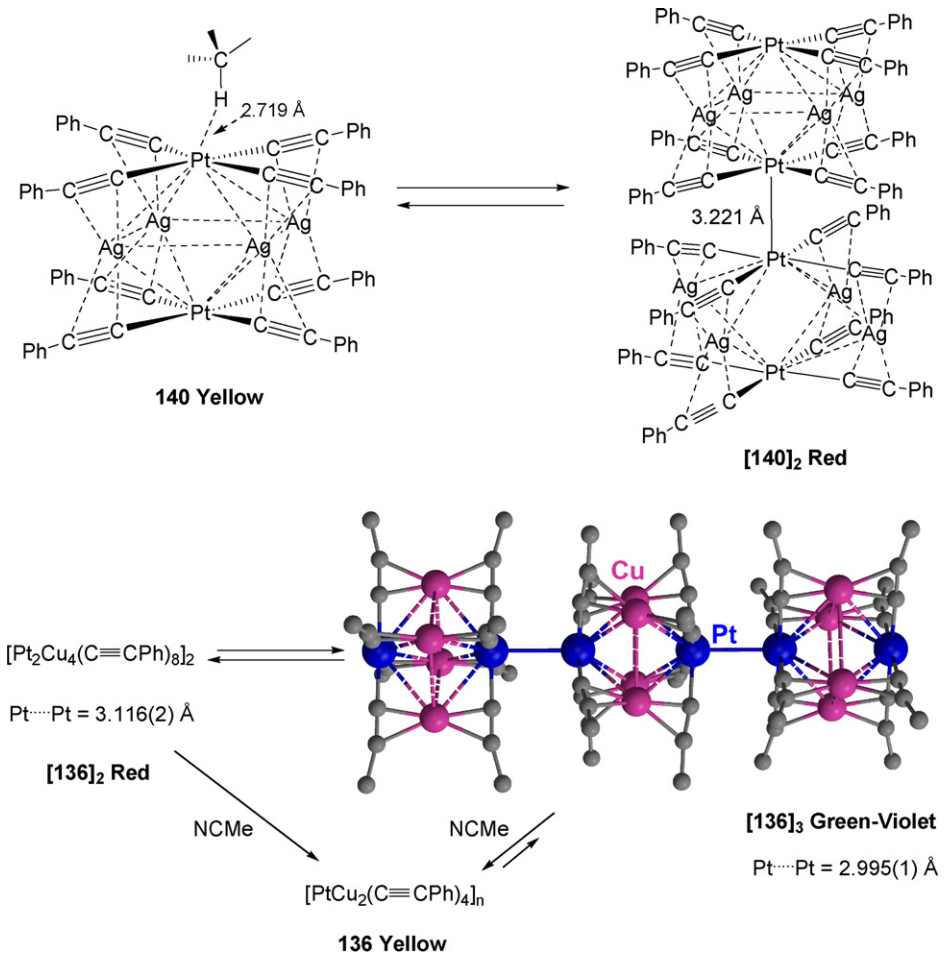

Scheme 24.

bonding component, decreasing the electron density at Pt centers, thus favouring the formation of Pt–Pt bonds and the appearance of low energy absorption and emission [168,175]. Our group and Yam et al. examined the rich polymorphism and interesting properties exhibited by the phenylethynyl derivatives [168,169,175]. Thus, we found that $[Pt_2Ag_4(C{\equiv}CPh)_8]$ **140** cocrystallizes, even from very concentrated solution in chloroform or CH_2Cl_2/*n*-hexane, as a mixture of red and yellow crystals (Scheme 24) [168]. X-ray diffraction studies confirm that in the red crystals ($[\mathbf{140}]_2$ red) two eclipsed clusters are linked (staggered) by a Pt···Pt bonding interaction of 3.221 Å, whereas in the yellow ones (**140** yellow) an extended chain of discrete monomers was found, separated by $HCCl_3$ molecules due to short Pt···$HCCl_3$ contacts. For the related $[Pt_2Cu_4(C{\equiv}CPh)_8]$ **136** derivative (Scheme 24) violet-green crystals with metallic reflectance appear using concentrated solutions ($[\mathbf{136}]_3$ violet), which were formed by discrete trimers connected by two unsupported and very short Pt···Pt bonds of 2.995(1) Å [175]. From diluted solutions trimers and red crystals (dimers, $[\mathbf{136}]_2$ red) with a longer Pt···Pt separation of 3.116(2) Å were separated. In the dimer, one cluster is staggered while the other is eclipsed. However, in the trimer it was found that the two external are eclipsed, whereas the central is staggered, suggesting a remarkable flexibility of the tetraalkynylplatinate entities. To minimize steric repulsions, the platinum fragments involved in the Pt···Pt bonding are always twisted (≈40–45°). A very insoluble third yellow form (**136** yellow) was found upon treatment of the red and green-violet crystals with acetonitrile [175]. Its optical properties and the fact that it reverts under prolongated pressure to the soluble green-violet trimer suggests it to be not a simple monomer but a different polymeric species $\{PtCu_2(C{\equiv}CPh)_4\}_n$.

The *meta*-methoxy derivatives $[Pt_2M_4(C{\equiv}CC_6H_4OMe\text{-}3)_8]_\infty$ are obtained (CH_2Cl_2/*n*-hexane) as garnet (M = Ag $[\mathbf{141}]_\infty$) or very dark garnet nearly black (M = Cu $[\mathbf{137}]_\infty$) solids (Scheme 23). The crystal structure of the silver derivative $[Pt_2Ag_4(C{\equiv}CC_6H_4OMe\text{-}3)_8]_\infty$ $[\mathbf{141}]_\infty$ reveals, in this case, the formation of an unprecendent infinite stacked chain of clusters linked by short Pt···Pt bonds [3.1458(8) Å] and, again rotated (43.8°) along the chain (Fig. 5) [168]. The presence of extended C–H···O(OMe) contacts between alternate clusters clearly contributes to the stability of the chain and probably also to the axial Pt···Pt bonds. The solvent play an important role in the final structure of the platinum silver derivative, which forms a yellow monomer unsolvated form in acetone (**141**) and a discrete 1:2 adduct in tetrahydrofurane [**141**·**2thf**]. The crystal structure of [**141**·**2thf**] reveals that two molecules of thf are contacting in a bridging fashion to each two Ag ions (Fig. 5d). The structure of a rather similar adduct $[Pt_2Ag_4(C{\equiv}C\text{–}C{\equiv}CTol)_8(thf)_4]$ **142**, generated from $[Pt(C{\equiv}C\text{–}C{\equiv}CTol)_4]^{2-}$ and $[Ag(NCMe)_4]^+$ in thf has been reported [170]. As a result of these contacts (Ag–O), the interaction with the alkynyl fragments decrease slightly, shifting the ν(C≡C) to higher energies ([**141**·**2thf**] ν(C≡C) 2039 cm^{-1} *vs.* $[\mathbf{141}]_\infty$ 2029 cm^{-1}, **141** 2033 cm^{-1}). In the same line, the intense green-yellow luminescence of the unsolvated monomer **141**, both in the solid state (550 nm, solid) and in solution (570 nm CH_2Cl_2, $\phi = 0.39$), is remarkably blue-shifted and considerably less intense for the solvate [**141**·**2thf**] (537 nm solid, 557 nm thf, $\phi = 0.019$) (see Fig. 6).

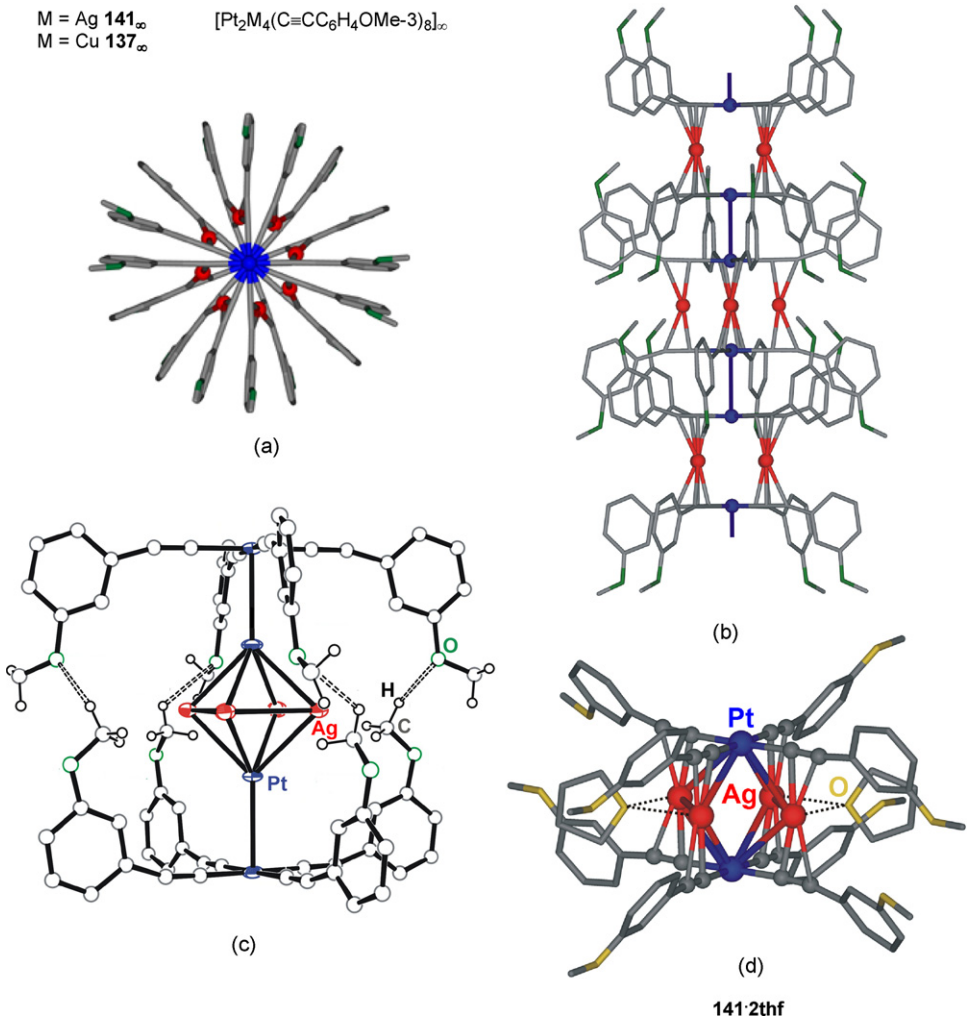

Fig. 5. Schematic view of three units of the extended structure of $[Pt_2Ag_4(C{\equiv}CC_6H_4OMe\text{-}3)_8]_\infty$ $[\mathbf{141}]_\infty$ along the *a* (a) and *b* (b) axes. (c) Illustration of the hydrogen C–H···O(Me) bonds. (d) Schematic view of the structure of $[PtAg_2(C{\equiv}CC_6H_4OMe\text{-}3)_4]\cdot 2thf$ (Ref. [168]).

The presence of better π*(C≡Caryl) accepting orbitals (aryl = Ph, C_6H_4-OMe-3), which lowers the energy of the LUMO is the primary reason why these discrete clusters and also the yellow form of $[Pt_2Ag_4(C{\equiv}CPh)_8]$ [**140**, 545 nm (298 K) solid] emit at lower energies than the related *tert*-butylacetylide $[Pt_2Ag_4(C{\equiv}CBu^t)_8]$

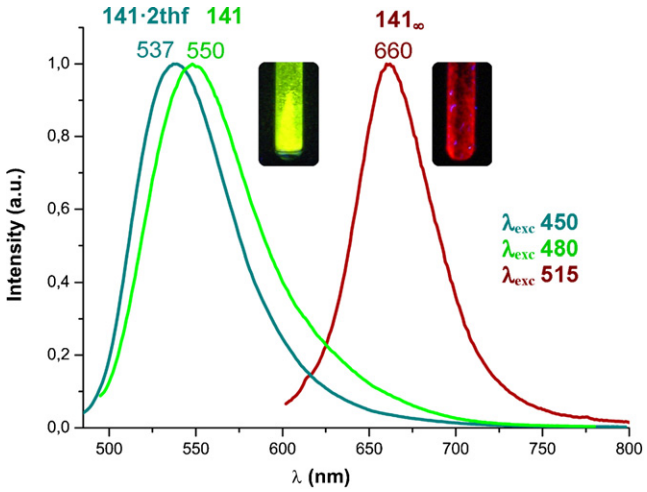

Fig. 6. Normalized emission spectra of $[Pt_2Ag_4(C{\equiv}CC_6H_4OMe\text{-}3)_8]_\infty$ ($[\mathbf{141}]_\infty$), **141** and [**141**·**2thf**] in the solid state at 298 K.

139 (476 nm). The axial Pt···Pt interaction between clusters in the dimers $[Pt_2M_4(C{\equiv}CPh)_8]_2$ (M = Ag [**140**]$_2$, Cu [**136**]$_2$), trimer $[Pt_2Cu_4(C{\equiv}CPh)_8]_3$ [**136**]$_3$ and chains [**141**]$_\infty$, [**137**]$_\infty$ (Table 1) is reflected in the solid state as a broad absorption at low energy (*i.e.* 621 nm [**136**]$_3$; 633 nm [**141**]$_\infty$; 680 nm [**137**]$_\infty$), which disappears in diluted solutions, and mainly in the photoluminescence behaviour (Table 1). The trimer derivative $[Pt_2Cu_4(C{\equiv}CPh)_8]_3$, [**136**]$_3$ (violet-green), having a very short Pt···Pt distance [2.995(1) Å], and the platinum–copper extended chain $[Pt_2Cu_4(C{\equiv}CC_6H_4OMe\text{-}3)_8]_\infty$ [**137**]$_\infty$ (nearly black) exhibit a near-infrared luminescence (Table 1), which is more intense and shifted to higher energies in the corresponding dimers $[Pt_2M_4(C{\equiv}CPh)_8]_2$ [M = Ag [**140**]$_2$, Cu [**136**]$_2$] and in the related stacked platinum–silver chain [**141**]$_\infty$ (660–700 nm), in which the Pt···Pt separations are larger (see Fig. 6 for [**141**]$_\infty$). These emissions, as in other stacked chain Pt···Pt systems, are associated with the axial Pt···Pt bonding being ascribed to phosphorescence from metal–metal-to-ligand charge transfer (^{3}MMLCT) [176] or an admixture of metal–metal (Pt–Pt) centered $^3(d\sigma^*p_z\sigma)$ and ^{3}MMLCT excited states. In agreement with this assignment, upon cooling at 77 K, the emission maxima always shift to lower energies, a feature related to a presumably slight contraction of the Pt···Pt separation, which rises the energy of the dσ* HOMO [176]. In frozen solution (77 K), the tendency to stack increases in the platinum–copper derivatives *vs.* the platinum–silver ones and is stronger in the 3-methoxyphenylethynyl derivatives [168].

Table 1
Photophysical data of the stacked $[Pt_2M_4(C{\equiv}CR)_8]_n$ in the solid state.

	d (Pt–Pt)/Å	λ_{em}/nm (298 K)	λ_{em}/nm (77 K)	τ (μs)
$[Pt_2Ag_4(C{\equiv}CPh)_8]_2$ [**140**]$_2$ red	3.221(2)	659/662[a]	688	Not measured
$[Pt_2Cu_4(C{\equiv}CPh)_8]_2$ [**136**]$_2$ red	3.116(2)	700/715[a]	720	0.48 ± 0,5 (298 K)
$[Pt_2Cu_4(C{\equiv}CPh)_8]_3$ [**136**]$_3$ green-violet	2.995(1)	806[a]		0.5
$[Pt_2Ag_4(C{\equiv}CC_6H_4OMe\text{-}3)_8]_\infty$ [**141**]$_\infty$ Garnet	3.1458(8)	660	707	0.15 (298 K) 10.1 (77 K)
$[Pt_2Cu_4(C{\equiv}CC_6H_4OMe\text{-}3)_8]_\infty$ [**137**]$_\infty$ nearly black	–	783sh, 803	823	9.0 (298 K) 8.3 (77 K)

[a] KBr pellets.

The discrete cluster $[Pt_2Ag_4(C{\equiv}CBu^t)_8]$ **139** is an adequate synthon for higher nuclearity species (Scheme 25). Thus, treatment of this cluster with $AgClO_4$ (1:4 molar ratio) affords yellow crystals of the novel polymeric complex **143** based on 10-nuclear backbones $[Pt_2Ag_8(C{\equiv}CBu^t)_8(acetone)_2(OClO_3)_2]^{2+}$ connected through bridging perchlorate groups (X-ray) [173]. The interaction of the external silver ions with acetone and perchlorate groups (terminal and bridging) is weak, being easily displaced by 2,2′-bipy ligands giving rise to discrete octanuclear tetracations $[\{Pt_2Ag_4(C{\equiv}CBu^t)_8\}\{Ag(bipy)\}_4]^{4+}$ **144**, in which the hexanuclear cluster $[Pt_2Ag_4(C{\equiv}CBu^t)_8]$ acts as octadentate bridging ligand towards four Ag(bipy) fragments [174]. In these octanuclear Pt_2Ag_8 cores (**143** and **144**), the interaction of the internal dicoordinated Ag ions with the alkynyl groups of "$Pt(C{\equiv}CBu^t)_4$" fragments is stronger and more symmetrical than those of the external tetracoordinated "AgO_2" or "Ag(bipy)" units and as a consequence, the alkynyl ligands exhibit a final asymmetrical μ_3-η^2-coordination mode (Pt-κC^α, Ag-η^2, Ag-κC^α). Surprisingly, although **139** is able to interact in a reversibly way with excess of halide ions (Br^-, Cl^-) causing partial or total destruction of the hexanuclear core [167], an unusual 1:1 cocrystallization extended 1D adduct $[Pt_2Ag_4(C{\equiv}CBu^t)_8{\cdot}(bipy)]_\infty$ **145** is generated in the presence of excess of 2,2′-bipy ligand. The crystallographic study of **145** reveals the presence of a σ-*trans*-configured bipy molecule acting as μ_4-bridging ligand. Both nitrogen atoms of the bipy ligand display very long misdirected bridging contacts (3.488 and 3.565 Å) with two adjacent Ag centers of successive clusters in the final network. Photophysical studies in the solid state reveal that both 10-nuclear systems **143** and **144** display similar green luminescence (λ_{max} 476 nm, $\tau \sim 0.35$ μs) to that observed for the hexanuclear $[Pt_2Ag_4(C{\equiv}CBu^t)_8]$ **139** cluster (Fig. 7), suggesting that the influence of the four external AgL units on the central hexanuclear chromophore is negligible [173,174].

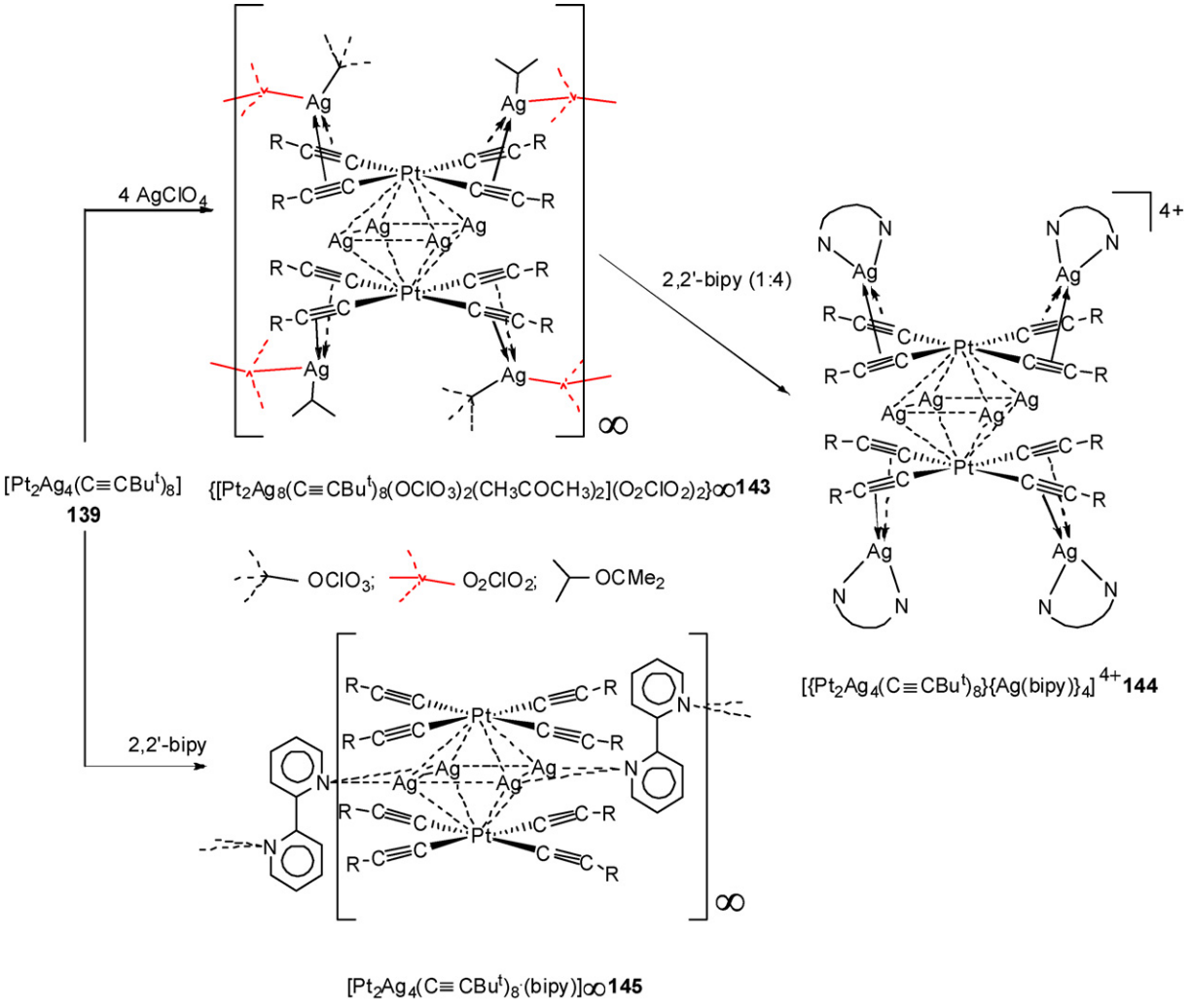

$[Pt_2Ag_4(C{\equiv}CBu^t)_8]$ **139**

$\{[Pt_2Ag_8(C{\equiv}CBu^t)_8(OClO_3)_2(CH_3COCH_3)_2](O_2ClO_2)_2\}_\infty$ **143**

$[\{Pt_2Ag_4(C{\equiv}CBu^t)_8\}\{Ag(bipy)\}_4]^{4+}$ **144**

$[Pt_2Ag_4(C{\equiv}CBu^t)_8{\cdot}(bipy)]_\infty$ **145**

Scheme 25.

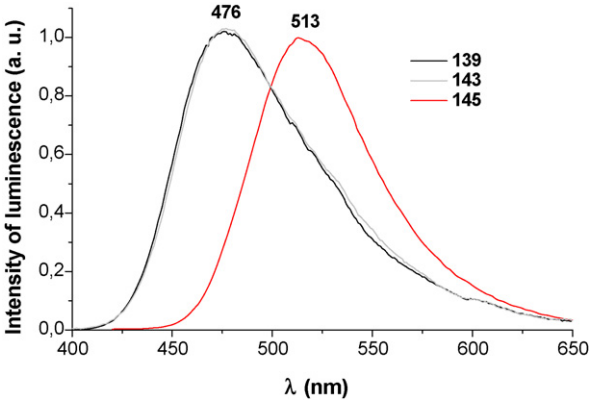

Fig. 7. Normalized emission spectra of $[Pt_2Ag_4(C{\equiv}CBu^t)_8]$ **139**, $\{[Pt_2Ag_8(C{\equiv}CBu^t)_8(acetone)_2(OClO_3)_2](O_2ClO_2)_2\}_\infty$ **143** and $[Pt_2Ag_4(C{\equiv}CBu^t)_8{\cdot}(bipy)]_\infty$ **145** in the solid state (KBr pellets) at 298 K.

However, in the extended cocrystallization 1:1 adduct **145**, the very weak interaction of the nitrogen atoms of the bipy ligand with the equatorial silver center of the Pt_2Ag_4 core seems to cause an stabilization of the emitting state and also to reduce the access to non-radiative deactivation processes. This system (**145**) exhibits a very intense luminescence (at least 3 times higher than free **139**), which is red-shifted (λ_{em} = 513 nm) with respect to that **139** (Fig. 7).

3.4. Heteronuclear platinum-group 12 metal acetylide complexes

Even though alkynyl-mercurials have been widely used as alkynyl transfer reagents to form not only platinum [57,177], but also other transition metal alkynyl complexes, the number of systems containing Hg···η^2-C≡C bonds is rather limited. The versatile behaviour of σ-alkynyl mercury derivatives [178] and their interesting photophysical properties have been recently reviewed by Wong [36] and Mingos et al. [178].

Several years ago, our group reported the first crystallographic example of a Hg···η^2(alkyne) bond [179]. Thus, in contrast to previous reported reactions between neutral *cis*-bis(alkynyl)platinum(II) complexes [*cis*-Pt(C≡CR)$_2$L$_2$] [180] or [*cis*-Pt(C≡CR)(C≡CR′)L(CO)] [181] and $HgCl_2$, which evolve with alkynyl transference, anionic substrates $[cis\text{-}PtX_2(C{\equiv}CR)_2]^{2-}$ (X = C_6F_5, C≡CR; R = Bu^t, $SiMe_3$) react with mercury halides to form stable bimetallic Pt–Hg $[\{cis\text{-}Pt(C_6F_5)_2(C{\equiv}CR)_2\}HgX_2]^{2-}$ (**146**, Chart 19) and trinuclear $PtHg_2$ $[\{Pt(C{\equiv}CR)_4\}(HgX_2)_2]^{2-}$ (**147**, Chart 19) complexes, respectively [179]. Following a similar methodology, Young and co-workers prepared the related double-tweezer 1:2 adduct $[\{Pt(OBET)_2\}(HgCl_2)_2]^{2-}$ (**148**, Chart 19) [182], and, more recently, Lang and co-workers have obtained the neutral bimetallic $[\{Pt(4,4'\text{-}Me_2bipy)(C{\equiv}CPh)_2\}HgX_2]$ (**149**, X = Cl, I) [183]. The crystal structures of complexes **146** (R = $SiMe_3$, X = Br) [179] and **148** [182] were established by X-ray. In a similar manner to the Pt–Co complexes **55** and **56** (Chart 10), in the binuclear Pt–Hg derivative **146** the $HgBr_2$ fragment is well-embedded by the 3-platina-1,4-diine fragment, giving a PtC_4Hg planar core, and the Hg is closer to the C_β atoms than to the C_α (average Δ 0.17 Å). Complex **148** exhibits a reverse asymmetry with Hg–C_α distances shorter than Hg–C_β (~0.2 Å). Taking into account the recent van der Waals radius estimated for Hg (~2.0 Å) [184,185], the measured Pt–Hg distances (3.627 Å **146**; 3.347(1) Å **148**) are shorter than the sum of the Van der Waals radii (~3.75 Å).

The ability of anionic homoleptic $[Pt(C{\equiv}CPh)_4]^{2-}$ and mixed $[Pt(R_f)_2(C{\equiv}CR)_2]^{2-}$ to stabilize unusual $\eta^2\cdots$M bonding interactions has been successfully extended by our group to the lighter Cd^{II} center. However, in these Pt/Cd systems the donor properties of the basic platinum center compete with the alkyne units, providing access to novel assemblies, which display interesting photoluminescent properties. The degree of interaction of cadmium with the alkynyl entities and the Pt^{II} center depends on the nature of the platinate and the coligands around the divalent Cd^{II}. As shown in Scheme 26, the reaction of $[Pt(C{\equiv}CPh)_4]^{2-}$ with $CdCl_2$ not only gives the expected 1:2 adduct **150**, in which the Cd^{II} completes a pseudo-tetrahedral coordination being bonded to the alkynyl entities (Cd–$C_{\alpha,\beta}$ 2.403(11)–2.670(11) Å), but also an unexpected tetranuclear dianionic Pt_2Cd_2 yellow cluster **151** (X = Cl) [186]. This cluster contains two generated cationic "$CdCl^+$" units bonded to both platinate fragments through short Pt–Cd bonds (2.960(1) Å), and μ-κC^α alkynyl bridging ligands (Cd–C_α 2.463(4) and 2.604(5) Å). This, and related clusters **151** (X = Cl, Br, CN) are alternatively obtained by treatment of the insoluble material $[PtCd(C{\equiv}CPh)_4]$ (**152**, formed

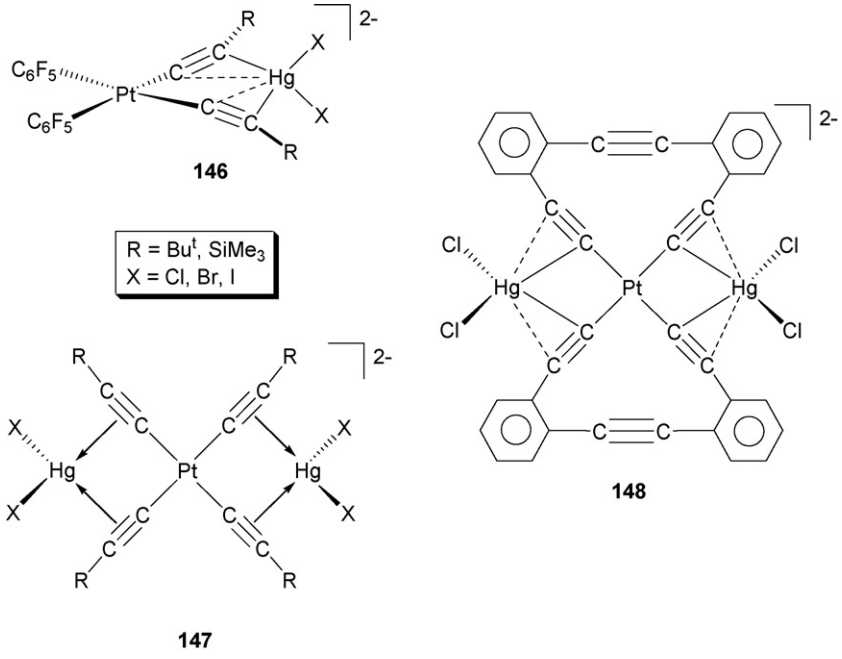

Chart 19.

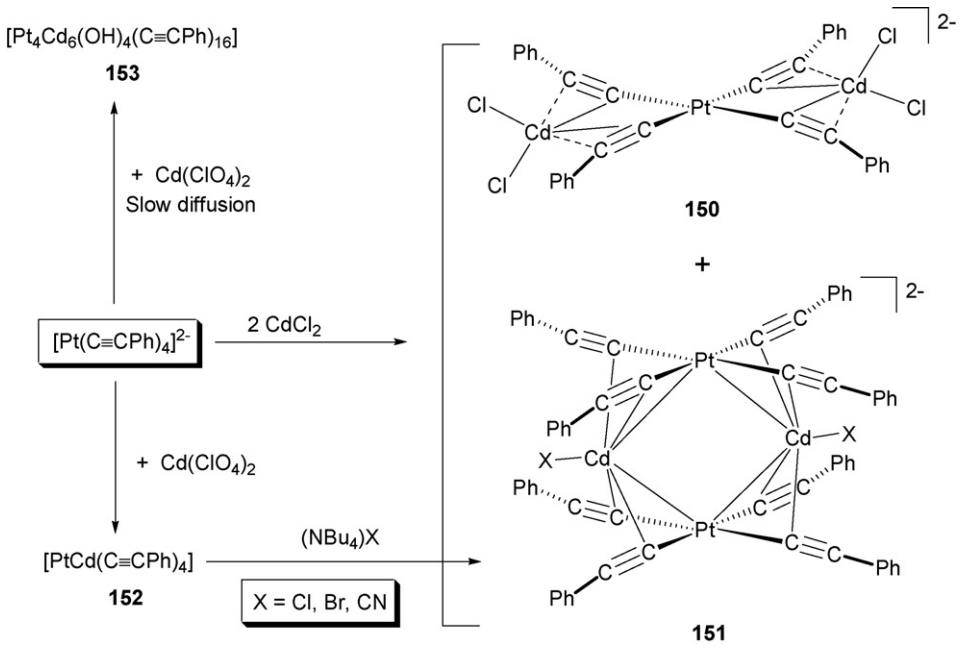

Scheme 26.

by neutralization of $[Pt(C{\equiv}CPh)_4]^{2-}$ with $Cd(ClO_4)_2$, Scheme 26) with 1 equiv. of NBu_4X [187]. The lower electronic density on the Pt center, due to the formation of the Pt → Cd bonding interactions, in clusters **151** is reflected in the ν(C≡C) absorption, which is shifted to higher frequencies (2093–2095 cm^{-1}) in relation to the precursor $[Pt(C{\equiv}CPh)_4]^{2-}$ (2075 cm^{-1}).

Interestingly, under aerobic conditions, slow diffusion of acetonic solutions of Cd^{2+} and $[Pt(C{\equiv}CPh)_4]^{2-}$ evolves with partial hydrolysis, giving rise to an unexpected decanuclear cluster Pt_4Cd_6 (**153**, Scheme 26). Crystal X-ray analysis reveals, as shown in Fig. 8, that cluster **153** is formed by a big octahedral hexanuclear cation $[Cd_6(\mu\text{-}OH)_4]^{8+}$ and four $[Pt(C{\equiv}CPh)_4]^{2-}$ anions, held together by Pt···Cd (2.8570(14)–3.2509(15) Å) and alkynyl (κC^{α} and η^2)···Cd interactions.

The trinuclear $PtCd_2$ adduct **150** [186] shows a structured emission (λ_{max} 432, 471 nm), slightly blue-shifted in relation to that of the precursor $(NBu_4)_2[Pt(C{\equiv}CPh)_4]$ (λ_{max} 447, 465 and 484 nm) [166], which is ascribed to a mixed $^3[\pi(C{\equiv}CPh) \rightarrow \pi^*(C{\equiv}CPh)]/^3$MLCT excited state. Clusters **151** are strongly emissive in the solid state and frozen solution ($CHCl_3$), displaying a red-shifted unstructured emission centered at ~495 nm. The influence of the X group coordinated to Cd in the emission maximum is negligible (X = Cl 495, Br 497, CN 498 nm), but the change in the emission profile and the clear red-shift displacement in relation to the precursor was suggested to be due to a presumed contribution of the Pt_2Cd_2 metal core (and probably also alkynyl C_{α}–Cd) to the orbitals involved in the optical transition [188].

In an effort to provide further insight about these $Cd^{II}\cdots Pt^{II}$ and $Cd^{II}\cdots$alkynyl bonding interactions and their role into the final photophysical properties, we have also investigated the behaviour of the more electrophilic mixed bis(pentafluorophenyl)bis(alkynyl)platinates $[Pt(R_f)_2(C{\equiv}CR)_2]^{2-}$ towards Cd^{II}. The *cis*-configured $[cis\text{-}Pt(R_f)_2(C{\equiv}CR)_2]^{2-}$ precursors are able to stabilize, through η^2-alkyne interactions, not only the neutral $CdCl_2$ unit, giving bimetallic Pt–Cd complexes **154** (Chart 20), but also a naked Cd^{II} ion in the trinuclear dianionic Pt_2Cd complexes **155** (Chart 20), the latter obtained by reaction with $Cd(NO_3)_2$ regardless of the molar ratio used [189]. To our knowledge, these are the only reported species in which a Cd^{II} center is only stabilized by η^2-bonding interactions. Crystal X-ray structures of the anions **154** (R = Tol) and **155** (R = Bu^t, Ph) confirm that, in all cases, the complexation of the Cd takes place

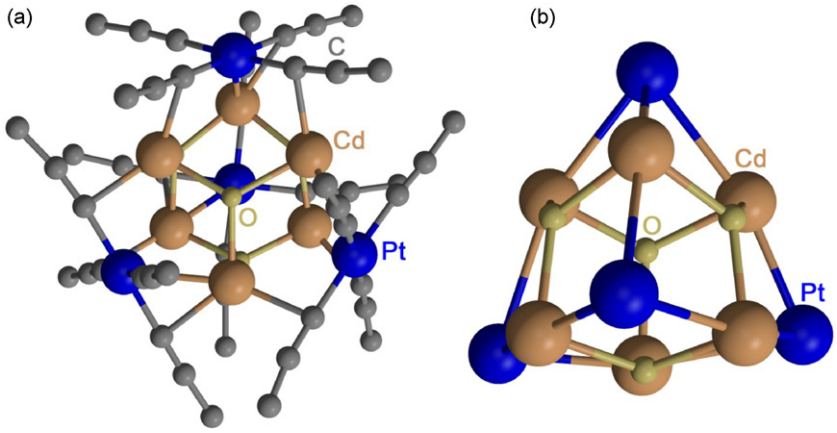

Fig. 8. (a) Crystal structure of cluster $[Pt_4Cd_6(C{\equiv}CPh)_4(\mu\text{-}C{\equiv}CPh)_{12}(\mu_3\text{-}OH)_4]$ **153** (phenyl groups have been omitted for clarity). (b) Perspective of the central $Pt_4Cd_6(\mu_3\text{-}OH)_4$ framework in **153** (Ref. [187]).

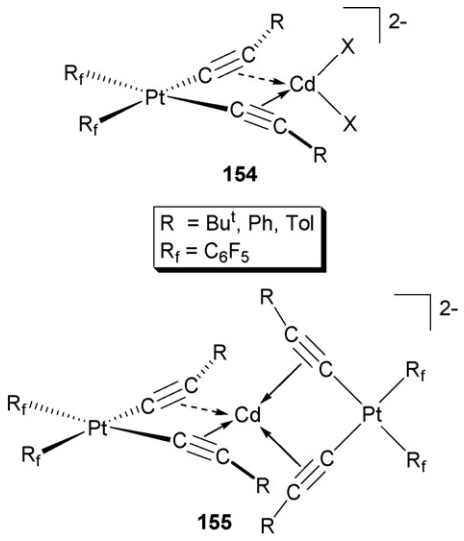

Chart 20.

in the corresponding platinum coordination plane (*in-plane*), leading to planar $Pt(C{\equiv}C)_2Cd$ cores. The η^2-alkynide linkages are asymmetrical, the Cd–C_α distances (2.365(7)–2.418(4) Å) being shorter than the Cd–C_β (2.528(12)–2.657(7) Å), and there is no evidence of significant interaction between the Pt and Cd atoms (3.1748(5)–3.2998(4) Å) when compared with the van der Waals limit (3.3 Å). Interestingly, if the reactions between [*cis*-$Pt(R_f)_2(C{\equiv}CPh)_2]^{2-}$ and Cd^{2+} takes place in the presence of the tetradentate cyclen ligand (1,4,7,10-tetraazacyclodecane), the platinum center effectively competes with the alkynyl ligands, affording the unusual bimetallic derivative **156** (Fig. 9), containing a very short Pt–Cd bond (2.764(1) Å) and retaining only a weak interaction with the C_α (2.493 Å) of one of the alkynyl fragments [190]. Although the Pt–Cd axis is not entirely perpendicular to the platinum coordination plane (34.58(9)° from the normal), a significant donation of electron density from the d_z2 orbital of Pt^{II} occurs.

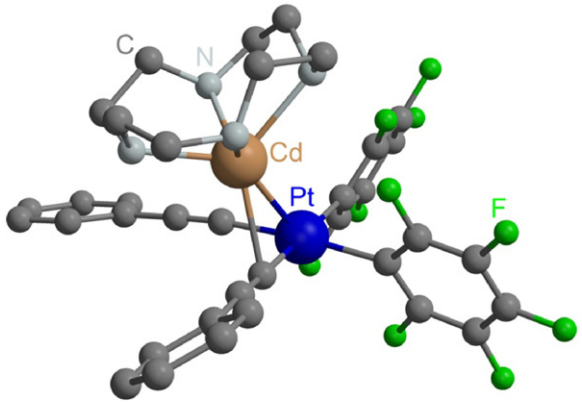

Fig. 9. X-ray structure of [*cis*-$Pt(R_f)_2(C{\equiv}CPh)_2Cd(cyclen)]$ (**156**) (Ref. [190]).

By using diimine chelating donors (N–N = bpy, dmbpy, phen) or the tridentate terpyridine (trpy) ligands (Scheme 27), the *in situ* generated dicationic units "$Cd(N{-}N)_2^{2+}$" or "$Cd(trpy)^{2+}$" form final pseudo-octahedral environments around the Cd^{II}, by connecting to both Pt–C_α bonds (**157**) and, in the case of **158**, also contacting weakly with a solvent molecule [191]. In comparison with complex **156**, the interaction of the cadmium with the C_α carbons is stronger (2.354(7)–2.554(5) Å), while the bonding interaction with the Pt center is weaker, with distances ranging from 2.999(3) to 3.1162(3) Å. Interestingly, the change from *cis*- to-*trans* geometry on the platinum substrate causes a significant preference of the "$Cd(bpy)_2^{2+}$" unit to be bonded to the platinum center. In the final complexes **159**, the [*trans*-$Pt(R_f)_2(C{\equiv}CR)_2]^{2-}$ fragments employ only one of the Pt–C_α bonds, giving rise to a distorted trigonal bipyramidal coordination, with very short Cd–C_α (2.372(10) Å) and Pt–Cd (2.8931(6) Å) bond distances (R = Tol). ^{19}F NMR spectroscopy indicates that all these complexes are dynamic in solution. For instance, in the case of complexes **156** and **159**, the dynamic behaviour involves processes such as a fast exchange of the "CdN_4^{2+}" unit between both *cis* (**156**) or *trans* (**159**) alkynyl fragments, with a very low energetic barrier in complex **159**, and, presumably, a free rotation of the

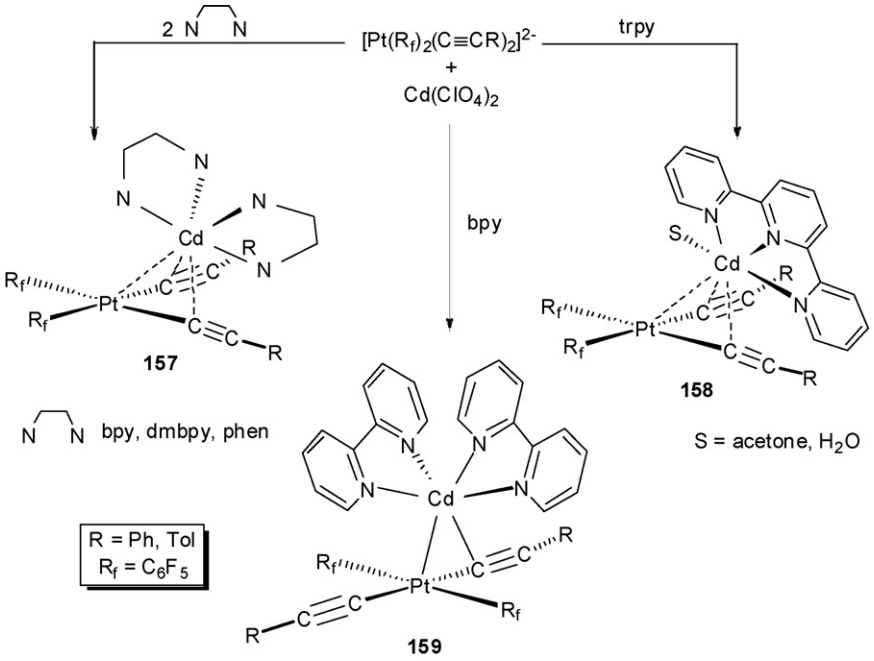

Scheme 27.

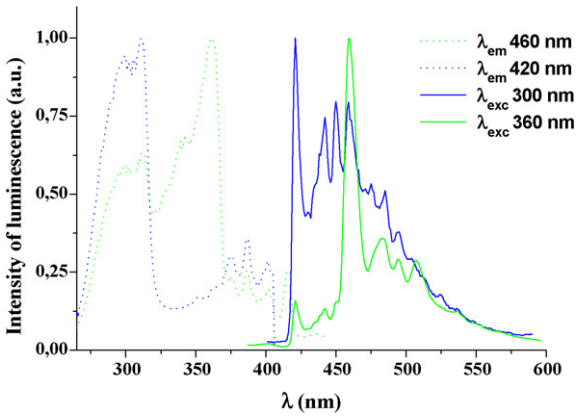

Fig. 10. Normalized excitation and emission spectra of solid $(NBu_4)_2$[*cis*-{$Pt(R_f)_2(C{\equiv}CPh)_2\}_2Cd$] (**155**) in the solid state (powder) at 77 K.

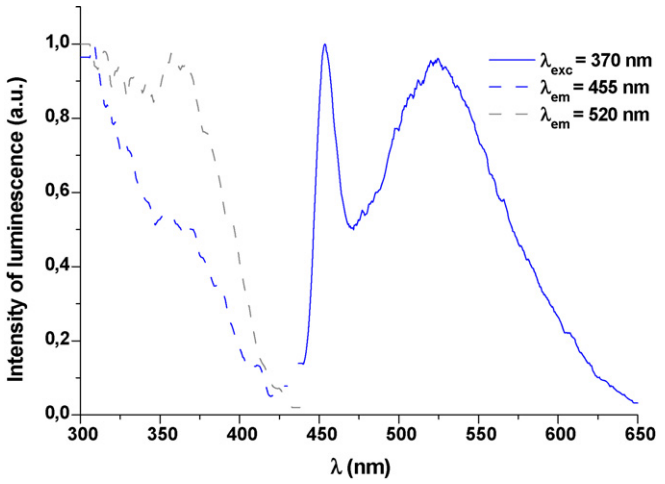

Fig. 11. Normalized excitation and emission spectra of solid [*trans*-$Pt(R_f)_2(C{\equiv}CTol)_2Cd(bpy)_2$] (**159** Tol) at 77 K.

C_6F_5 rings, but dissociation of the "CdN_4^{2+}" unit does not occur [191].

The photophysical properties of these anionic (**154**, Chart 20) and neutral (**156**–**159**, Fig. 9 and Scheme 27) bimetallic Pt–Cd and trimetallic $PtCd_2$ (**155**, Chart 20), and those of their precursors (*cis*- and *trans*-$[Pt(R_f)_2(C{\equiv}CR)_2]^{2-}$), were investigated [189–191]. The arylethynyl precursors exhibit (solid and glasses) typical structured emissions, attributed to a mixed ^{3}IL [$\pi \rightarrow \pi^*(C{\equiv}CR)$]/^{3}MLCT [$d\pi(Pt) \rightarrow \pi^*(C{\equiv}CR)$] manifold, with predominant intraligand character, which are red-shifted in the *trans*-configured complexes [191], confirming that the extent of π delocalization through the platinum is usually more efficient in *trans* type isomers [192]. Dual emissions were observed in the tolylethynyl derivatives (solid, glass for [*cis*-$Pt(R_f)_2(C{\equiv}CTol)_2]^{2-}$ and glass for [*trans*-$Pt(R_f)_2(C{\equiv}CTol)_2]^{2-}$) due to the presence of close emissive excited states (*cis*-configured) or different conformers (*trans*-configured) that no equilibrate in rigid media.

UV–vis absorption studies reveals that the incorporation of $CdCl_2$ or Cd^{2+} by η^2-alkyne interactions to [*cis*-$Pt(R_f)_2(C{\equiv}CR)_2]^{2-}$ in complexes PtCd (**154**, Chart 20) and Pt_2Cd (**155**, Chart 20) causes a clear hypsochromic shift in the low energy absorption, which is ascribed to an admixture of ^{1}IL [$\pi\pi^*(C{\equiv}CR)$]/^{1}MLCT in relation to the corresponding precursor [189]. This behaviour has been attributed to the existence of a lesser electronic delocalization on the alkynyl fragments "$Pt(C{\equiv}C{-})_2$", caused by the *in-plane* η^2-complexation of the Cd^{II}. Bathochromic shifts are usually observed in heteropolymetallic (Pt–M) η^2-alkynyl$\cdots$M(d^{10}) (d^{10} = Cu^I, Ag^I, Au^I) complexes, which exhibit *out-of-plane* η^2-complexation and intermetallic interactions [156,168,175]. These complexes exhibit structured emissions arising from ^{3}[$\pi\pi^*(C{\equiv}CR)$] ^{3}IL and/or mixed ^{3}[$\pi\pi^*$/$Pt(d\pi)(C{\equiv}CR) \rightarrow \pi^*(C{\equiv}CR)$] (^{3}MLCT) manifolds with predominant ^{3}IL character [189]. For the tolylethynyl derivatives **154** and **155** and the trimetallic phenylethynyl complex $(NBu_4)_2$[*cis*-{$Pt(R_f)_2(C{\equiv}CPh)_2\}_2Cd$] (**155**, see Fig. 10) dual emissions are observed in rigid media at low temperature (77 K) depending on the excitation wavelength, which are tentatively attributed to the fact that $^3\pi\pi^*$ and ^{3}MLCT (or mixed $^3\pi\pi^*/^3$MLCT) are not coupled.

One important property of some mixed-metal systems containing closed-shell metal$\cdots$metal contacts is that they are often intensely luminescent, making them attractive with respect to potential applications. In contrast to this behaviour, the neutral complexes [*cis*-$Pt(R_f)_2(C{\equiv}CPh)_2Cd$(cyclen)] (**156**, Fig. 9) [190] and [*trans*-$Pt(R_f)_2(C{\equiv}CR)_2Cd(bpy)_2$] (**159**, Scheme 27) [191], having very short Pt–Cd bonds and a relatively weak interaction with an alkynyl unit, are not emissive at room temperature in the solid state. Upon cooling at 77 K, complexes **159** (R = Ph, Tol) display a high energy structured emission slightly blue-shifted in relation to the precursors [448 (Ph), 455 (Tol) nm in **159** *vs.* 457 (Ph), 460 (Tol) nm in the precursor], assigned to the mixed ^{3}IL/^{3}MLCT (L = C≡CR) manifold perturbed by the donor-acceptor Pt → Cd bond, which probably stabilizes the energy of the Pt(d)/π(C≡CR) HOMO. The tolylacetylide derivative [*trans*-$Pt(R_f)_2(C{\equiv}CTol)_2Cd(bpy)_2$] exhibits an additional low energy feature (~520 nm, Fig. 11), which is absent in 2-MeTHF fluid and glass, tentatively ascribed to $\pi\cdots\pi$ stacking interactions, in accordance with the presence of very short contacts (bpy$\cdots C_6F_5$ ~3.25 Å) found in the extended lattice [191]. The luminescence of the cadmium-cyclen derivative **156** exhibits an interesting solvent-dependence, which seems to be related with the presence of channels in the lattice. The unsolvated (dried) complex is only emissive at 77 K (λ_{max} 446, 469, 481 and 492 nm). Its crystallization forms the solvate **156**·$2Me_2CO$, which has the solvent molecules located in extended channels of the lattice [190]. Interestingly, the incorporation of the solvent causes the turn-on of a blue emission at room temperature (λ_{max} 451 nm), similar (but more intense) to that of the precursor (444–515 nm), associated with the ^{3}IL/^{3}MLCT manifold of the dialkynyl platinum fragment.

In the solid state, the neutral bimetallic *cis*-configured complexes [*cis*-$Pt(R_f)_2(C{\equiv}CR)_2Cd(N\text{-}N)_2$] **157** and [*cis*-$Pt(R_f)_2(C{\equiv}CR)_2Cd(trpy)$] **158** show blue and/or green emissions (more or less structured profiles), with dual exponential decays in the milliseconds range at low temperature (77 K), which are suggested to originate from close emissive states of different nature: metal (Pt, Cd) perturbed intraligand (alkynyl, polyimine) manifolds mixed to a greater (trpy, **158**) or a lesser extent with (Pt → Cd) charge transfer (^{3}MM′CT) (Fig. 12) [191].

3.5. Heteropolymetallic alkynyl bridging platinum-main group metal complexes

Several unsolvated platinum–lithium species such as $LiPt(C{\wedge}P)(C{\equiv}CPh)_2$ [C∧P = $CH_2C_6H_4P(o\text{-tolyl})_2$-$\kappa C,P$] **160** [85] and [*cis*-$PtTlLi(R_f)_2(C{\equiv}CPh)_2$] **161** [193] have recently been reported, which presumably are stabilized by interaction of the lithium center with the alkynyl fragments. Crystallographic evidence reported by the Wrackmeyer research group, showed that dimeric tetranuclear heteroleptic complexes **162** (Eq. (20)), (R^1 = Ph, R^2 = Bu^n), are generated from neutral *trans*-dialkynylbis(triethylphosphine)platinum(II) on treatment with organolithium R^2Li reagents in hydrocarbon solvents (Eq. (20)) [194].

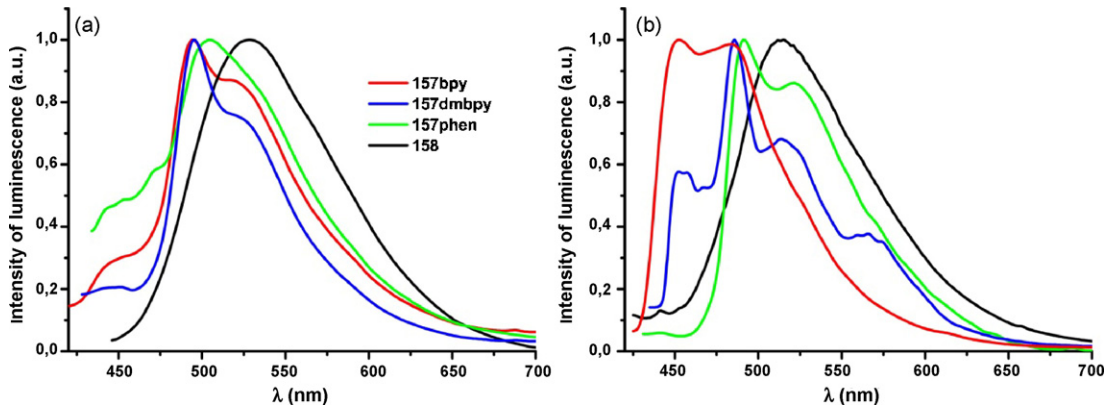

Fig. 12. Normalized emission spectra of crystalline samples of [*cis*-Pt(R_f)$_2$(C≡CTol)$_2$Cd(N–N)$_2$] (**157**, N–N = bpy, dmbpy, phen) and [*cis*-Pt(R_f)$_2$(C≡CTol)$_2$Cd(trpy)] (**158**) at (a) 298 K and (b) 77 K.

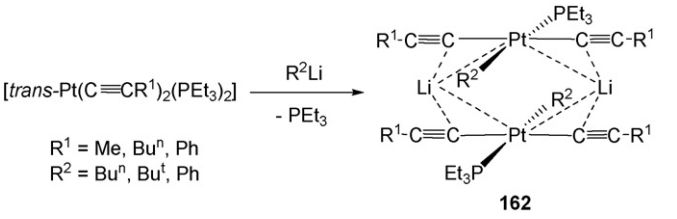

(20)

The lithium centers connect two almost parallel dialkynylplatinate(II) fragments by two rather unequal Li···C$_\alpha$ contacts [2.074(51)–2.238(69) Å] and probably very weak Pt···Li interactions [Pt···Li = 2.807(64) Å], which remains in C_6D_6 solution ($^1J^{195}$Pt–^{7}Li = 78 Hz), as has been confirmed by multi-nuclear NMR spectroscopy (^{1}H, ^{7}Li, ^{13}C, ^{195}Pt) [194]. Zwitterionic η^2-alkynylborate platinum(II) intermediate species have been proposed by the same group, in 1,1-organoboration reactions of neutral dialkynylbis(phosphine)platinum compounds, but such species have not been detected [195]. However, the intermediate alkyne Pt^0–Sn complex [Pt(PPh$_3$)$_2$(η^2-PhC≡C–SnEt$_3$)] **163** [196] could be detected in the well-known oxidative addition reaction of alkynylstannanes with bis(phosphine)platinum(0) fragments [197,198].

As commented above, one interesting feature of metal ions with closed-shell and pseudo-closed-shell electronic configurations (d^8, d^{10}, s^2) is their tendency to form weak metal–metal bonds. The interest in this topic has grown in the last years, mainly due to the role of these metallophilic bonds as a tool for crystal engineering and their interesting photophysical properties [199–206]. A particular case is constituted by the bonds between Pt^{II} and 6s^2 (Tl^I and Pb^{II}) metal centers, which arise from the overlap between the filled 5 d_z2 (Pt) and 6 s (Tl^I or Pb^{II}) and the empty set of 6p_z orbitals through appropriate configuration mixing [207–211]. A simplified molecular orbital diagram in the first reported trinuclear luminescent complex [PtTl$_2$(CN)$_4$] was suggested by Balch in 1988 (Fig. 13) [211].

In this complex, the metallophilic bonding interaction is efficiently reinforced by electrostatic attraction and the trinuclear Tl^I–Pt^{II}–Tl^I is generated instead of the expected Pt···Pt (d^8···d^8) stacked columnar structure [212]. The ability of Pb^{II} to overlap with the Pt^{II} center seems to be less effective because the related system K$_2$Pt(CN)$_4$/Pb^{2+} gave the salt K$_2$Pb[Pt(CN)$_4$]$_2$·6H$_2$O, formed by zig-zag Pt···Pt bonding columns [213]. Because C≡CR$^-$ and CN$^-$ groups are isoelectronic, we decided to examine the reactivity of alkynyl platinates towards Tl^I and also Pb^{II} aiming to investigate the possible competition between the basic platinum center and the alkynyl fragments to bond the 6s^2 metal center. With the expectation of generating interesting structures stabilized by alkynyl

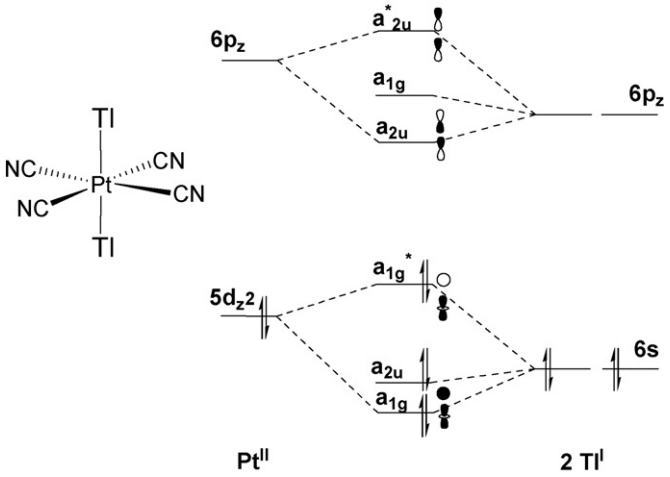

Fig. 13. Qualitative molecular orbital diagram for the Tl–Pt–Tl unit, proposed by Balch and co-workers for compound [Tl$_2$Pt(CN)$_4$] (Ref. [211]).

bridging and/or Pt^{II}–Tl^I bonding, both homoleptic [Pt(C≡CR)$_4$]$^{2-}$ and mixed [Pt(R_f)$_2$(C≡CR)$_2$]$^{2-}$ and [Pt(bzq)(C≡CR)$_2$]$^-$ precursors have been neutralized with Tl^I. As shown in Scheme 28, only when [Pt(C≡C–C$_6$H$_4$CF$_3$-4)$_4$]$^{2-}$ is used as precursor, the presence

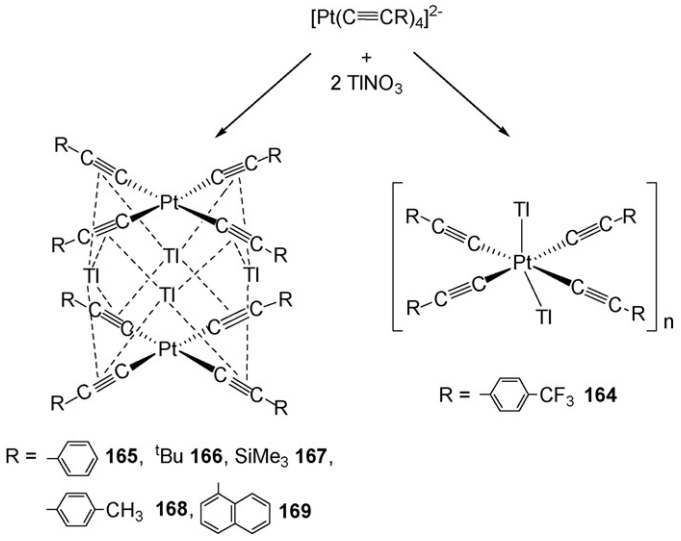

Scheme 28.

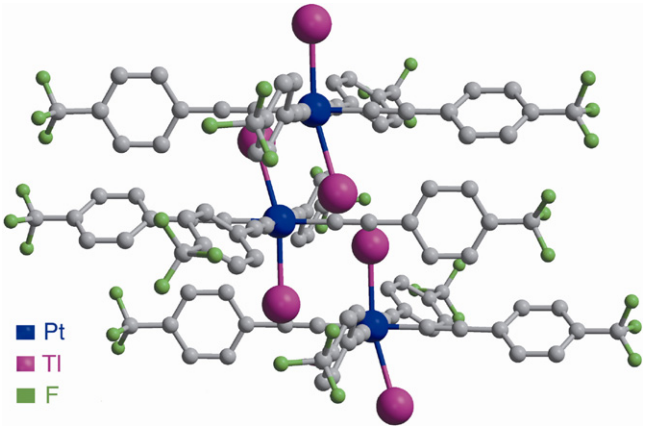

Fig. 14. Perspective view along the *a* axis of the crystalline structure of **164** showing the stacking of the $[PtTl_2(C{\equiv}CC_6H_4CF_3\text{-}4)_4]$ units (Ref. [214]).

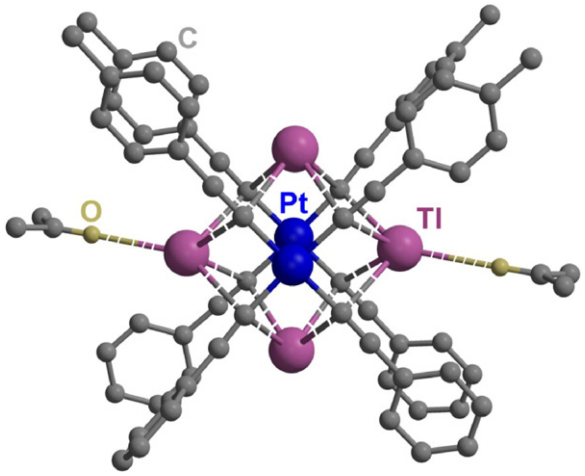

Fig. 16. Molecular structure of $[Pt_2Tl_4(C{\equiv}CTol)_8]\cdot 4$ acetone (**168**) showing the contacts of two thallium atoms with two acetone molecules (Ref. [214]).

of acceptor CF_3 substituent reduces the donor capability of the alkynyl ligands, making the platinum center the preferred bridging site [214]. In this case, trinuclear entities with two unsupported Pt–Tl [2.9355(5) and 3.0272(5) Å] bonds are formed, which self-associate through secondary Tl···π···alkynyl interactions to afford a supramolecular columnar species $[PtTl_2(C{\equiv}CC_6H_4CF_3\text{-}4)_4]$ **164** (Fig. 14). However, the reaction of $[Pt(C{\equiv}CR)_4]^{2-}$ [R = Ph, Bu^t, $SiMe_3$, Tol, 1-naphthyl (Np)] with 2 equiv. of Tl^I afforded unusual sandwich hexanuclear clusters of type $[Pt_2Tl_4(C{\equiv}CR)_8]$ (**165**–**169**) (Scheme 28), in which the Tl^I show a stronger preference for the electron rich alkynyl fragments [214,215].

The crystal structures of $[Pt_2Tl_4(C{\equiv}CR)_8]\cdot S_x$ [R = Bu^t, $S_x = HCCl_3$ **166**; R = Tol, S_x = (acetone)$_4$ **168**; R = 1-naphthyl, $S_x = (acetone)_3(H_2O)_{1/3}$ **169**] confirm that these clusters are formed by two eclipsed platinate units connected by four thallium centers (see Table 2 for structural details).

This assembly has some resemblance with those mixed Pt-d^{10} clusters $[Pt_2M_4(C{\equiv}CR)_8]$ (M = Cu, Ag, Au) previously commented, but in contrast to the linear coordination of the d^{10} ion, in this case each Tl^I center is bonded to four alkynyl fragments (one associated with each Pt fragment). The η^2-acetylenic interactions are asymmetric with the Tl–C_α distances shorter than the corresponding Tl–C_β and very close to the sum of the van der Waals radius of C (1.7 Å) and the ionic radius of Tl^+ (1.4–1.5 Å), indicating a notable ionic contribution to the bonding in this type of assembly. Curiously, while in the naphthyl derivative (**169**) the clusters are connected through weak intermolecular Tl···π(naphthyl) interactions (3.411–3.842 Å), yielding a final extended lattice having circular channels (Fig. 15) in which the acetone molecules are trapped, in the tolyl derivative (**168**) two acetones are weakly interacting [Tl···O 3.042(9) Å] with two Tl^I (Fig. 16). These acetone molecules are easily lost causing a visual change of both the color and luminescence (yellow green to yellow orange) of the cluster [214]. These clusters exhibit relatively short intramolecular Pt···Pt separations (3.520–3.8463 Å), comparable to those seen in linear chain Pt^{II} complexes [212], and Pt···Tl [3.486(7)–3.7204(4) Å] distances close to the van der Waals limit (3.68 Å) (Table 2), which presumably are involved in their emissive properties.

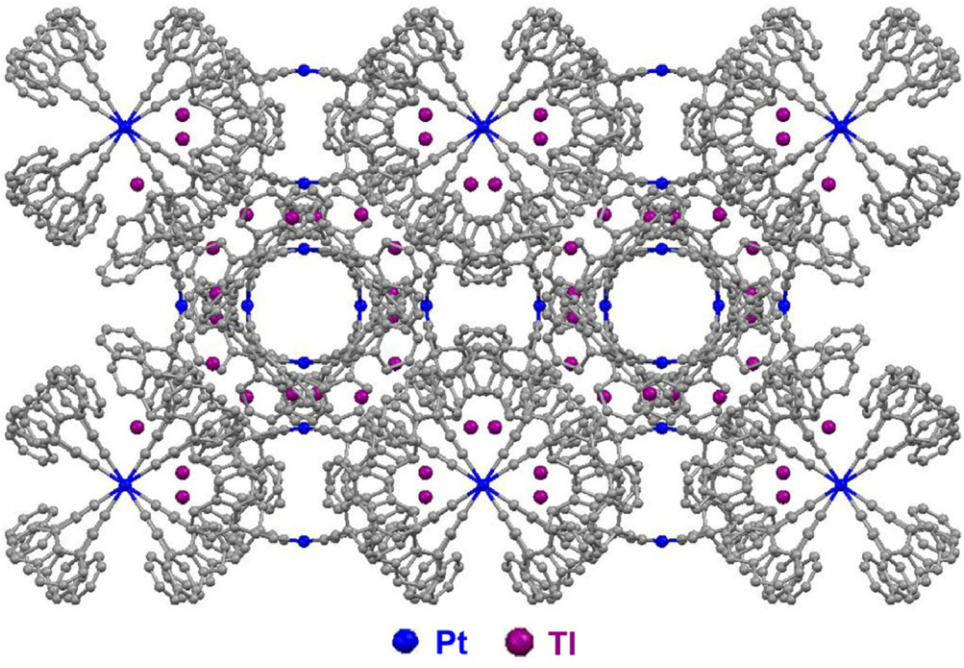

Fig. 15. Expansion of the crystalline structure for $[Pt_2Tl_4(C{\equiv}CNp)_8]\cdot 3acetone\cdot 1/3H_2O$ (**169**·3acetone·1/3H_2O) showing circular channels (Ref. [214]).

Table 2
Selected bond lengths (Å) of $[Pt_2Tl_4(C{\equiv}CR)_8]$.

	$[Pt_2Tl_4(C{\equiv}CBu^t)_8]{\cdot}HCCl_3$[a] **166**	$[Pt_2Tl_4(C{\equiv}CTol)_8]{\cdot}4$ acetone **168**	$[Pt_2Tl_4(C{\equiv}CNp)_8]{\cdot}3$ acetone$\cdot 1/3\ H_2O$ **169**
Pt–C_α	2.852(13)–2.948	2.900(7)–3.015(7)	2.91(2), 2.97(2)
Pt–C_β	3.193–3.381	3.086(7)–3.296(10)	3.21(2)–3.29(2)
Pt–Tl	3.4846(7)–3.514	3.5675(5)–3.7204(4)	3.628(1)–3.714(1)
Pt···Pt	3.573[b]	3.8463(5)	3.572(2)
Tl···Tl	4.270–4.238	4.3065(5), 4.4731(4)	4.538(1)

[a] Molecule A.
[b] 3.520 Å (at 173 K).

In the solid state these Pt_2Tl_4 clusters exhibit (except the 1-Np derivative **169**) an intense orange luminescence, which is slightly blue-shifted in the aryl derivatives [631 nm Bu^t (**166**), 635 nm $SiMe_3$ (**167**) [215] *vs.* 594 nm Ph (**165**, KBr pellets) [215]]. In the case of the tolyl derivative, the unsolvated freshly prepared $[Pt_2Tl_4(C{\equiv}CTol)_8]$ **168** powder shows site-selectivity excitation with the maximum ranging from 590 to 602 nm, which was associated with the presence of aggregate of clusters. In fluid CH_2Cl_2 solution, this emission is blue-shifted (478 nm) and structured at 77 K (475, 520 and 580 nm), being ascribed to a mixed ^{3}IL [$\pi \rightarrow \pi^*$(C≡CR)] and metal–ligand-to-metal cluster core transition ^{3}MLM′CT [$Pt(C{\equiv}CTol)_4 \rightarrow Pt_2Tl_4$] [214]. The extensive Tl···π(naphthyl) interaction and probably π···π(naphthyl) interactions in the naphthyl derivative (**169**) seem to be responsible of the quenching of the emission observed at room temperature. At 77 K, it displays structured emissions (554–655 nm) with very long lifetime (115 μs solid, 172.4 μs CH_2Cl_2, 77 K) associated with metal (or cluster) perturbed ππ* transitions on the C≡C–Np groups [214].

The supramolecular chain **164** [214] is an interesting example of system whose color (*mechanochromism*) and luminescence (*tribochromism*) change with pressure [216]. Crystalline solvate samples of $[PtTl_2(C{\equiv}CC_6H_4CF_3)_4SS']_\infty$ (S = S′ = acetone **164a**; S = acetone, S′ = dioxane **164b**) are yellow pale in color and exhibit two luminescence bands (blue 457 nm and orange 611 nm, Fig. 17), which are slightly red-shifted at 77 K. By simple grinding of the sample or by using 10 Torr pressure to make KBr pellets, the initial color change to orange and the blue emission disappears (see Fig. 17). In acetone solution, the blue emission is observed (slightly structured) in diluted concentration, while the orange emission appears by increasing the concentration ($\geq 5 \times 10^{-4}$ mol L^{-1}). By comparison with the precursor $(NBu_4)_2[Pt(C{\equiv}CC_6H_4CF_3)_4]$, the blue emission is ascribed to an intraligand [$\pi \rightarrow \pi^*$(C≡$CC_6H_4CF_3$)] excited state, while the low strong orange emission is thought to occur by lumophore aggregation of "$PtTl_2(C{\equiv}CC_6H_4CF_3)_4$" entities through Tl···π alkynyl interactions [214].

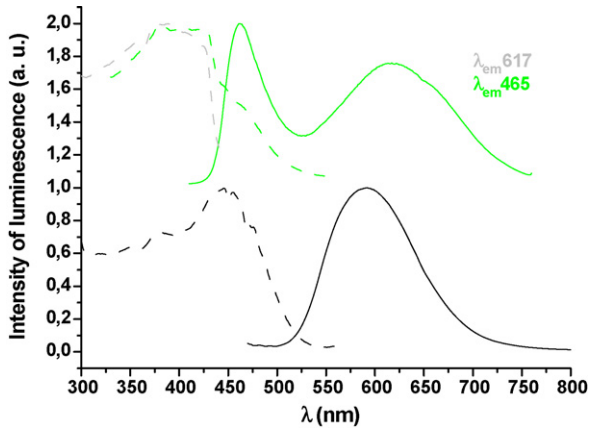

Fig. 17. Excitation and emission spectra of $[PtTl_2(C{\equiv}CC_6H_4CF_3)_4(acetone)_2]_\infty$ **164a** in the solid state (powder) at 77 K (top) and under 10 Torr pressure (KBr pellets) (bottom).

In similar reactions of Tl^+ with the heteroleptic [*trans*-$Pt(R_f)_2(C{\equiv}CBu^t)_2]^{2-}$ or [*cis*-$Pt(R_f)_2(C{\equiv}CPh)_2]^{2-}$ platinate systems, the thallium center has a higher affinity for the platinum than for the alkynyl ligands, yielding six-coordinated platinum entities with two direct platinum–thallium bonds (2.9921–3.135 Å) [193,217]. The crystal structure of the solvate [*trans*,*trans*,*trans*-$PtTl_2(R_f)_2(C{\equiv}CBu^t)_2(acetone)_2]_n$ [Tl···O(acetone) 2.83(2) Å](**170**·$2CH_3COCH_3$) reveals the formation of an extended chain of six-membered metallacycles ($Pt_2Tl_2C_{\alpha 2}$) by self-assembly of octahedral entities through short intermolecular secondary Tl···C_α(alkynyl) bonding contacts [Tl···C_α = 2.905(10) Å] (**170**, Chart 21) [217]. However, in the *cis*-configured acetone solvate [*trans*,*cis*,*cis*-$PtTl_2(R_f)_2(C{\equiv}CPh)_2(acetone)_2]_2$, one of the Tl^I is also interacting with both C_α alkynyl atoms and the trinuclear $PtTl_2$ units dimerizes by weak alkynyl–Tl contacts and two bridging acetone (**171**, Chart 21) [193].

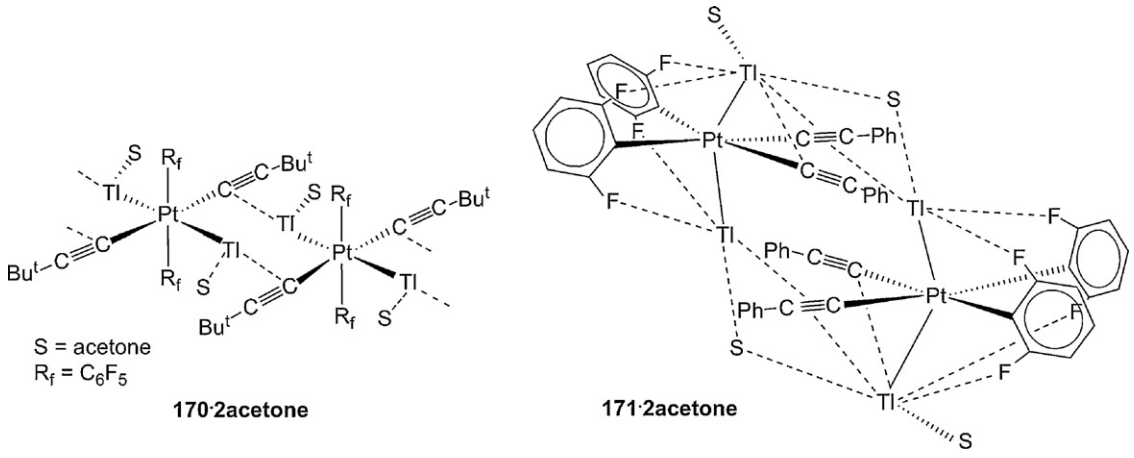

Chart 21.

In these pentafluorophenyl plantinate-thallium systems, both ^{19}F NMR spectroscopy and structural details confirm the presence of Tl···F_o bonding contacts, which contribute to their stability. One of the Tl^I centers in complex **171**·2 acetone is easily eliminated as TlCl by treatment with LiCl, yielding a mixed Pt–Tl–Li derivative [*cis*-$PtTlLi(R_f)_2(C{\equiv}CPh)_2$] **161** [193], which retains one of the Pt–Tl bonds as confirmed by ^{19}F NMR spectroscopy. Both, $PtTl_2$ (**171**) and PtTlLi (**161**) derivatives exhibit an strong and similar long-lived emission (λ_{em} 547 nm **171** and 542 nm **161**), which is attributed, on the basis of TD-DFT calculations, to charge transfer from the Tl–Pt–Tl (**171**) or Pt–Tl (**161**) units to the platinum fragment [*cis*-$Pt(R_f)_2(C{\equiv}CPh)_2]^{2-}$. In addition, the PtTlLi derivative is a relatively good ionic conductor in the solid state ($\sigma_{10\,^\circ C} = 1.28 \times 10^{-5}$ S cm^{-1}; $\sigma_{-15\,^\circ C} = 1.24 \times 10^{-6}$ S cm^{-1}).

Replacement of the pentafluorophenyl groups by a planar aromatic π-system, such as cyclometallating benzoquinolinate ligand (bzq$^-$), has a remarkable effect on the final structures and on the nature of the lowest emitting state. Thus, the neutralization reaction of $[Pt(bzq)(C{\equiv}CR)_2]^-$ (R = Ph **172**, C_6H_5N-2 **173**) with Tl^I affords a neutral bimetallic unit with a very short Pt–Tl bond [2.9266(12) Å; R = C_6H_5N-2 **173**], confirming again the low preference of Tl^I for the soft alkynyl entities. The X-ray structure of $[PtTl(bzq)(C{\equiv}CC_6H_5N\text{-}2)_2]_2$ **173** reveals that the Pt^{II}–Tl^I unit dimerizes by weak Tl···C_β (alkynyl) [3.05(2), 3.12(2) Å] and Tl···N(pyridyl) [2.85(2) and 3.01(2) Å] bonding interactions, giving tetranuclear Pt_2Tl_2 entities, which further self-associate through additional Tl···π (arene, 2-py *ca.* 3.45 Å) and π···π stacking contacts (∼3.46 Å) between adjacent bzq ligands [218] (Fig. 18). Both complexes $[PtTl_2(bzq)(C{\equiv}CR)_2]_2$ (R = Ph **172**, py-2 **173**) display in the solid state an intriguing luminescence *thermochromism* attributed to the existence of two low-lying emissive states. At 298 K, an intense low energy emission predominates (orange 625 nm R = Ph; orange-red 640 nm, R = py-2), ascribed to $^3\pi\pi^*$ excimeric emission due to extensive π···π interactions between aromatic bzq ligands. Upon cooling to 77 K, the emission is dominated by a high energy (HE) vibronic (∼1300 cm^{-1}) band, which is bathochromically shifted in relation to the corresponding precursor (R = Ph, λ_{max} 532 nm; py-2 524 nm), thus reflecting the formation of the Pt–Tl bond. This HE structured band has been assigned to a metal–metal′-to-ligand (bzq) charge transfer ^{3}MM′LCT [d/s σ*(Pt, Tl) → π*(bzq)] mixed, as in the platinum precursors, with some ligand-to-ligand (alkynyl to bzq) ^{3}LL′CT character. At room temperature, the internal conversion from this high ^{3}MM′LCT excited state to the low energy $^3\pi\pi^*$ manifold seems to be very fast [218].

The ability of alkynyl platinates to interact with heavy main metals is not limited to Tl^I. Recently, Lalinde and Forniés employed dialkynylcycloplatinate species $[Pt(bzq)(C{\equiv}CR)_2]^-$ (R = Ph, $C_6H_4CF_3$-4) bearing two different alkynyl subtituents as metalla ligands to Pb^{II} salts. They reported the successful isolation of two types of novel luminescent trinuclear Pt^{II}–Pb^{II}–Pt^{II} complexes (**174**–**176**) stabilized by Pt – Pb bonds and unusual Pb^{II}–alkynyl bonding interactions, these latter being the first report modelling a Pb^{II}–alkyne bond [219].

The reaction of $[Pt(bzq)(C{\equiv}CPh)_2]^-$ with 0.5 equiv. of $Pb(ClO_4)_2{\cdot}3H_2O$ affords the neutral trinuclear sandwich type complex $[\{Pt(bzq)(C{\equiv}CPh)_2\}_2Pb]$ **174**, in which two eclipsed and very close platinate fragments [Pt···Pt 3.5794(5) Å, bzq···bzq 3.36-3.48 Å] are connected by a lead center (Fig. 19). Curiously, the Pb^{II} exhibits a *symmetrical hemidirected* coordination, being bonded to four Pt–C_α(alkynyl) bonds [Pt–Pb 2.9182(5) Å; 2.9759(5) Å; Pb–C_α 2.619(9)–2.682(9) Å], which define the basal plane of a square pyramidal geometry, and has the $6s^2$ lone pair at the apex of the pyramide. The Pb^{II}–C_β distances (3.00–3.22 Å) are longer than the sum of the van der Waals radii of carbon (1.43 Å) and the covalent radii of lead (1.47 Å), indicating that the alkynyl are coordinated essentially in a μ-κC^α bonding mode. As shown in

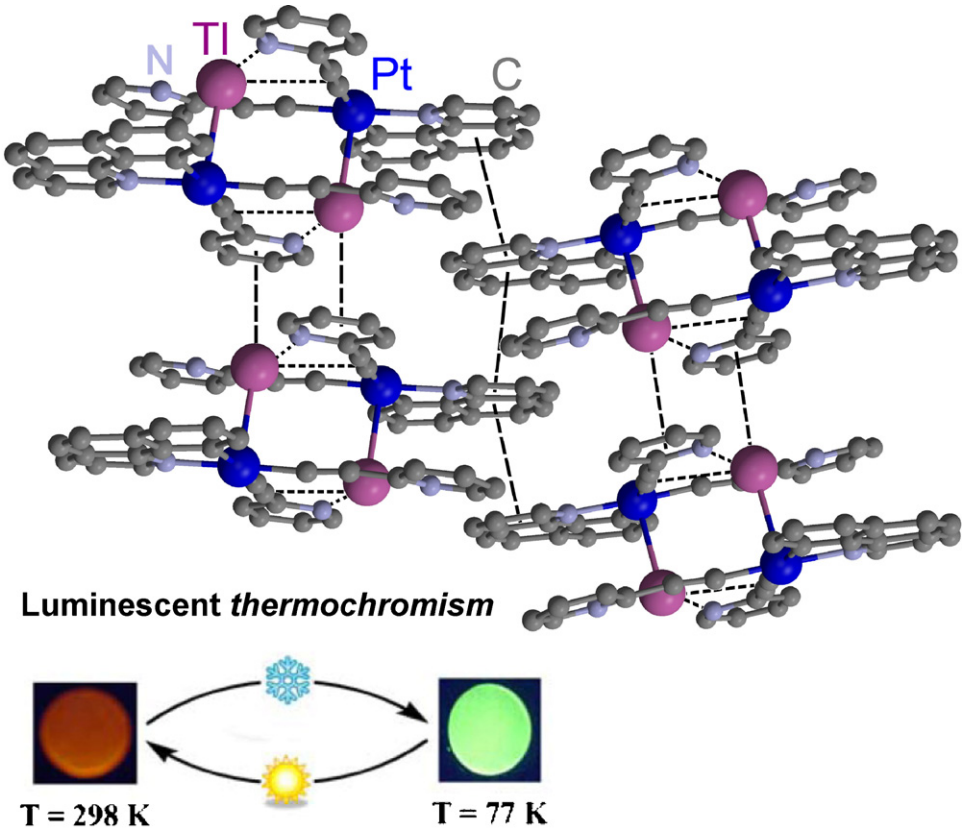

Fig. 18. Supramolecular structure of complex $[PtTl(bzq)(C{\equiv}CC_6H_5N\text{-}2)_2]_2{\cdot}2CH_2Cl_2$ **173** and a scheme of luminescent *thermochromism* behaviour (Ref. [218]).

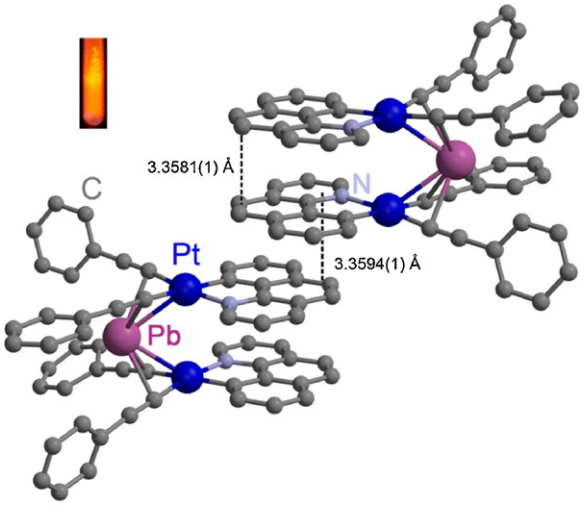

Fig. 19. π-Stacked dimers in [{Pt(bzq)(C≡CPh)$_2$}$_2$Pb] **174** and emission in the solid state at 77 K (inset) (Ref. [219]).

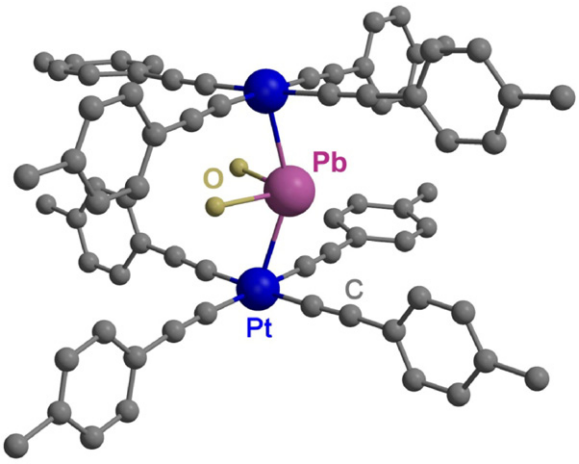

Fig. 20. Molecular structure of [{Pt(C≡CTol)$_4$}$_2$Pb(H$_2$O)$_2$]$^{2-}$ in **177** showing the *hemidirected* trigonal bipyramidal coordination of Pb^{II} (Ref. [219]).

Fig. 19, the cluster crystallizes as π-stacked dimers (3.36–3.42 Å) arranged in a head-to-tail orientation, a feature that has influence in its optical properties. Thus, this cluster **174** exhibits in the solid state a bright yellow emission (λ_{max} 575 nm) in diluted (5×10^{-5} M) CH_2Cl_2 solution, which was attributed to be derived from a ^{3}MLM′CT [Pt(d)/π(C≡CPh) → Pt(p_z)/Pb(sp)/π*(C≡CPh)] state modified by metal-metal interactions due to the short Pt···Pb and even Pt···Pt distances. Interestingly, this emission is quenched by increasing the concentration to 10^{-3} M and also in the solid state at room temperature, a feature attributed to the formation of dimers through π···π(bzq) interactions as observed in the lattice. Upon cooling to 77 K, the quenching is less effective and cluster **174** exhibits a remarkably red-shifted bright orange emission (607 nm, τ = 24 μs, Fig. 18, inset), which has been ascribed to similar ^{3}MLM′CT excited state mixed with some ^{3}ππ* excimeric character. The stability of this type of cluster strongly depends on the alkynyl substituent. Thus, as shown in Scheme 29, the analogous reaction system [Pt(bzq)(C≡CC$_6$H$_4$CF$_3$-4)$_2$]$^-$/Pb(ClO$_4$)$_2$, containing the less electron-donating C$_6$H$_4$CF$_3$-4 substituent, originates the related neutral Pt$_2$Pb cluster **175**, as an orange solid, in relatively low yield (8.5%) and the perchlorate adduct **176**, as a yellow microcrystalline solid in moderate yield (~40%).

In the anion of **176**, the platinum fragments are slightly displaced and their interaction with the Pb^{II} center is asymmetric and weaker to that in the neutral cluster **174** [Pt–Pb 2.8515(5) and 3.3136(5) Å and Pb–C$_\alpha$ 2.630(9)–2.772(10) Å]. As a consequence, the interaction with the perchlorate in an asymmetrical chelating way [Pb–O 2.880(8), 3.013(8) Å] contributes to fulfilling the requirements of the acidic Pb^{II} center. Conductivity and NMR studies in solution indicate that both Pt$_2$Pb systems (**175** and **176**) are involved in fast dissociative equilibria with bimetallic Pt–Pb species and the platinate precursor. Both complexes exhibit characteristic unstructured emission bands (yellow **176**, orange **175**, see Scheme 29) in the solid state at 77 K, ascribed to a ^{3}[Pt(d_z2)π(C ≡ CR) → Pt(p_z)/Pb(sp)/π ∗ (C ≡ CR)] excited state, probably mixed with some ^{3}ππ* excimeric character in neutral derivative **175**. Compared with the phenylethynyl Pt$_2$Pb cluster **174**, the emission in **175** is remarkably red-shifted (620 *vs.* 660 nm) in agreement with the involvement of the lower lying π*(C≡CC$_6$H$_4$CF$_3$) orbitals [better accepting than π*(C≡CPh)] in the excited state. In the same way, the remarkably shift to higher energies in the adduct **176** (600 nm) was attributed to the presence of Pb···O (O$_2$ClO$_2$) contacts, which presumably weaken the interaction of the Pb center with the C≡CC$_6$H$_4$CF$_3$-4 entities, thus increasing the energy of the π*(C≡CAryl) based LUMO.

Surprisingly, starting from the homoleptic precursor, [Pt(C≡CTol)$_4$]$^{2-}$, the related reaction with 0.5 equiv. of Pb(ClO$_4$)$_2$·3H$_2$O lead to a very unusual diaqua lead substituted (NBu$_4$)$_2$[{Pt(C≡CTol)$_4$}$_2$Pb(H$_2$O)$_2$] **177** complex, stabilized mainly through Pt–Pb bonds [2.8908(5) and 2.9109(5) Å] [219]. As shown in Fig. 20, which emphasizes the *hemidirected* trigonal

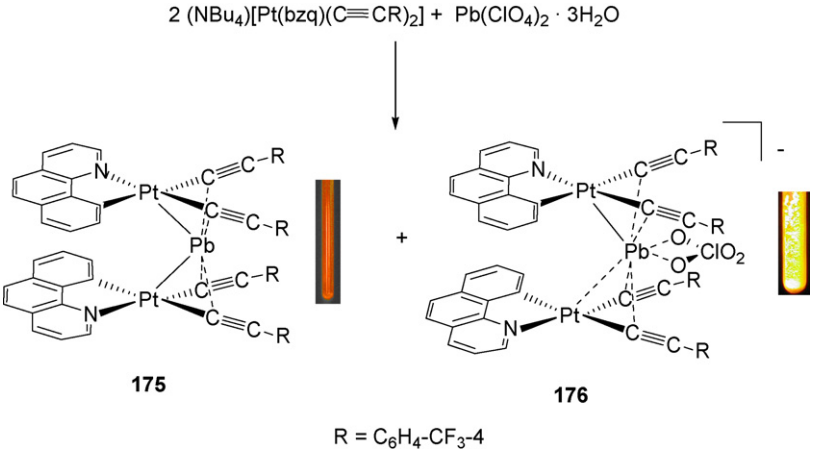

Scheme 29.

bipyramidal coordination of Pb^{II}, the displacement of the lead from the axial Pt atom could suggest a certain degree of interaction with the alkynyl ligands. However, the Pb–C_α distances range from 3.046(9) to 3.46(1) Å and are considered essentially non-bonding. In agreement with the effective $5d_z2(Pt)$-$6s^2(Pb^{II})$-$5d_z2(Pt)$ bonding interaction, this anion exhibits at 77 K an intense high energy long-lived blue emission (497 nm, τ 10 μs), attributed to a metal-centered excited state $^3(d\sigma^*p\sigma)$, related to the bent Pt^{II}–Pb^{II}–Pt^{II} entity ($^3MM'CT$). It was not emissive at 298 K, probably due to the presence of lead coordinated H_2O molecules, but exhibits an intriguing and reversible recovering of the emission upon exposure to a drop of acetone.

4. Conclusions and perspectives

This review article summarizes the chemistry of homo and heteropolynuclear platinum complexes containing alkynyl bridging ligands. The versatile bonding modes of these ligands have allowed the synthesis of a large family of organometallic compounds and supramolecular aggregates with unusual topologies and, some, with interesting optical properties.

Although different synthetic routes have been employed, one of the most successful strategies involves the combination of σ-alkynyl platinum substrates with electrophilic metal centers or derivatives having easily leaving ligands. Particularly, homoleptic $[Pt(C{\equiv}CR)_4]^{2-}$ and mixed alkynyl–platinate complexes containing pentafluorophenyl groups as auxiliary ligands are valuable building blocks to generate a wide range of polymetallic systems with only alkynyl fragments bridging the metal centers. The final σ or π (η) interaction of the alkynyl units depends on the metal fragments, with solvate d^6 (Ir^{III}, Rh^{III}) and some electrophilic d^8 (Pt^{II}, Ir^{I}) substrates, favouring the occurrence of mono or even double-alkynylation processes. However, with second-row d^8 (Pd^{II}, Rh^{I}), d^{10} (Cu^{I}, Ag^{I}, Au^{I}, Cu^{II}, Hg^{II}) or $6s^2$ (Tl^{I}, Pb^{II}) metal ions, the alkynyl groups usually remains σ-bonded to Pt^{II}, while the heterometal interacts with both, C_α and C_β (η^2) or primarily with the C_α (μ-κC_α) alkynyl carbon atoms. In some heterometallic Pt^{II}–Cd^{II} and Pt-$6s^2$ (Tl^{I}, Pb^{II}) systems, the heterometal shows a delicate compromise between its affinity to form unsupported Pt···M bonds and its stabilization by unusual η-alkynyl bonding interactions.

A wide range of homo and heterobimetallic complexes having one or two alkynyl bridging ligands have been reported, however, only a few studies related with alkynyl activation have been recorded. In particular, interesting (2C + 2C) alkynyl coupling induced by thiophenol (Section 2.2) or the successful formation of vinylidene bridging ligands (Section 2.2) will stimulate further research in this area. Some new reactivity observations found in diplatinum double-alkynide bridging systems in our group will be reported in the near future.

On the other hand, bimetallic (μ-dppm) Pt–Pt and polymetallic Pt-d^{10} and Pt-$6s^2$ (Tl^{I}, Pb^{II}) systems with μ-C≡CR ligands constitute a growing family of interesting luminescent complexes with long-lived emission energies (even in fluid solution) spanning a wide range in the visible spectrum. In the heteropolynuclear aggregates, the phosphorescence can be easily fine-tuned by alkynyl ligand substituent and the nature of the heterometal. This heterometal usually determines not only the strength of the metal–alkynyl bonding but also the presence of intramolecular Pt–M (M = d^{10}, $6s^2$, Pt^{II}) and, on occasion, intermolecular Pt···Pt metallophillic interactions, factors that also have a significant role in the nature of the emission. In this field, the introduction of additional luminophores such as cyclometallated (CN, CNC, CCN) as auxiliary ligands in the synthesis of polymetallic alkynyl bridging systems is in its infancy and will be the focus of research in the future.

Acknowledgments

This work was supported by the Spanish MICINN (Project CTQ2008-06669-C02-02/BQU). Authors thank all their co-workers involved in alkynyl chemistry for their dedication and especially to Prof. Dr. Juan Forniés for his continuous scientific and personal support.

References

[1] R. Nast, Coord. Chem. Rev. 47 (1982) 89.
[2] W. Beck, B. Niemer, M. Wieser, Angew. Chem., Int. Ed. Engl. 32 (1993) 923.
[3] J. Manna, K.D. John, M.D. Hopkins, Adv. Organomet. Chem. 38 (1995) 79.
[4] S. Lotz, P.H. van Rooyen, R. Meyer, Adv. Organomet. Chem. 37 (1995) 219.
[5] H. Lang, K. Köhler, S. Blau, Coord. Chem. Rev. 143 (1995) 113.
[6] J. Forniés, E. Lalinde, J. Chem. Soc., Dalton Trans. (1996) 2587.
[7] P.J. Stang, Chem. Eur. J. 4 (1998) 19.
[8] U. Belluco, R. Bertani, R.A. Michelin, M. Mozzon, J. Organomet. Chem. 600 (2000) 37.
[9] H. Lang, D.S.A. George, G. Rheinwald, Coord. Chem. Rev. 206–207 (2000) 101.
[10] K. Osakada, T. Yamamoto, Coord. Chem. Rev. 198 (2000) 379.
[11] D. Michel, P. Mingos, R. Vilar, D. Rais, J. Organomet. Chem. 641 (2002) 126.
[12] H. Lang, T. Stein, J. Organomet. Chem. 641 (2002) 41.
[13] T. Ren, Organometallics 24 (2005) 4854.
[14] U. Rosenthal, P. Arndt, W. Baumann, V.V. Burlakov, A. Spannenberg, J. Organomet. Chem. 670 (2003) 84.
[15] N.J. Long, C.K. Williams, Angew. Chem., Int. Ed. 42 (2003) 2586.
[16] M.I. Bruce, P.J. Low, Adv. Organomet. Chem. 50 (2004) 179.
[17] V. Rosenthal, Angew. Chem., Int. Ed. 42 (2003) 1794.
[18] T.C.W. Mak, L. Zhao, Chem. Asian J. 2 (2007) 456.
[19] P. Mathur, S. Chatterjee, V.D. Avasare, Adv. Organomet. Chem. 55 (2008) 201.
[20] M.I. Bruce, Chem. Rev. 91 (1991) 197.
[21] M.I. Bruce, M. Gaudio, G. Melino, N.N. Zaitseva, B.K. Nicholson, B.W. Skelton, A.H. White, J. Cluster Sci. 19 (2008) 147.
[22] T.C.W. Mak, X.L. Zhao, Q.M. Wang, G.C. Guo, Coord. Chem. Rev. 251 (2007) 2311.
[23] M.I. Bruce, Coord. Chem. Rev. 248 (2004) 1603.
[24] J.P. Selegue, Coord. Chem. Rev. 248 (2004) 1543.
[25] V. Rosenthal, P.M. Pellny, F.G. Kirchbauer, V.V. Burlakov, Acc. Chem. Res. 33 (2000) 119.
[26] G. Jia, Coord. Chem. Rev. 251 (2007) 2167.
[27] V. Cadierno, M.P. Gamasa, J. Gimeno, Coord. Chem. Rev. 248 (2004) 1627.
[28] H. Werner, Coord. Chem. Rev. 248 (2004) 1693.
[29] M. Akita, T. Koike, Dalton Trans. (2008) 3523.
[30] S. Szafert, J.A. Gladysz, Chem. Rev. 103 (2003) 4175;
S. Szafert, J.A. Gladysz, Chem. Rev. 106 (2006) PR1.
[31] F. Paul, C. Lapinte, Coord. Chem. Rev. 178–180 (1998) 431.
[32] N.J. Long, Angew. Chem., Int. Ed. Engl. 34 (1995) 21.
[33] S.R. Marder, in: D.W. Bruce, D. O'Hare (Eds.), Inorganic Materials, Wiley, Chichester, 1996.
[34] I.R. Whittall, A.M. McDonagh, M.G. Humphrey, Adv. Organomet. Chem. 42 (1998) 291.
[35] D.W. Bruce, in: D.W. Bruce, D. O'Hare (Eds.), Inorganic Materials, Wiley, Chichester, 1996, p. 429.
[36] W.Y. Wong, Coord. Chem. Rev. 251 (2007) 2400.
[37] P. Nguyen, P. Gómez-Elipe, I. Manners, Chem. Rev. 99 (1999) 1515.
[38] E.E. Silverman, T. Cardolaccia, X. Zhao, K.Y. Kim, K.H. Glusac, K.S. Schanze, Coord. Chem. Rev. 249 (2005) 1491.
[39] C.E. Powel, M.G. Humphrey, Coord. Chem. Rev. 248 (2004) 725.
[40] M. Hissler, J.E. McGarrah, W.B. Connick, D.K. Geiger, S.D. Cummings, R. Eisenberg, Coord. Chem. Rev. 208 (2000) 115.
[41] V.W.W. Yam, Acc. Chem. Res. 35 (2002) 555.
[42] V.W.W. Yam, K.K.W. Lo, Chem. Soc. Rev. 28 (1999) 323.
[43] V.W.W. Yam, K.K.W. Lo, K.M.C. Wong, J. Organomet. Chem. 578 (1999) 3.
[44] V.W.W. Yam, W.Y. Lo, C.H. Lam, W.K.M. Fung, K.M.C. Wong, V.C.Y. Lau, N. Zhu, Coord. Chem. Rev. 245 (2003) 39.
[45] V.W.W. Yam, J. Organomet. Chem. 689 (2004) 1393.
[46] W.Y. Wong, Dalton Trans. (2007) 4495.
[47] Z.N. Chen, N. Zhao, Y. Fan, J. Ni, Coord. Chem. Rev. 253 (2009) 1.
[48] F.N. Castellano, I.E. Pomestchenko, E. Shikhova, F. Hua, M.L. Muro, N. Rajapakse, Coord. Chem. Rev. 250 (2006) 1819.
[49] A. Harriman, R. Ziessel, Chem. Commun. (1996) 1707.
[50] R. Ziessel, M. Hissler, A. El-ghayoury, A. Harriman, Coord. Chem. Rev. 178–180 (1998) 1251.
[51] Z.N. Chen, Y. Fan, J. Ni, Dalton Trans. (2008) 573.
[52] M. Ciriano, J.A.K. Howard, J.L. Spencer, F.G.A. Stone, H. Wadepohl, J. Chem. Soc., Dalton Trans. (1979) 1749.
[53] A.T. Hutton, B. Shebanzadeh, B.L. Shaw, J. Chem. Soc., Chem. Commun. (1984) 549.
[54] N.W. Alcock, T.J. Kemp, P.G. Pringle, P. Bergamini, O. Traverso, J. Chem. Soc., Dalton Trans. (1987) 1659.
[55] V.W.W. Yam, L.P. Chan, T.F. Lai, Organometallics 12 (1993) 2197.

[56] V.W.W. Yam, P.K.Y. Yeung, L.P. Chan, W.M. Kwok, D.L. Phillips, K.L. Yu, R.W.K. Wong, H. Yan, Q.J. Meng, Organometallics 17 (1998) 2590.
[57] K.M.C. Wong, C.K. Hui, K.L. Yu, V.W.W. Yam, Coord. Chem. Rev. 229 (2002) 123.
[58] W.M. Kwok, D.L. Phillips, P.K.Y. Yeung, V.W.W. Yam, J. Phys. Chem. A 101 (1997) 9286.
[59] J.M. Casas, B.E. Diosdado, J. Forniés, A. Martín, A.J. Rueda, A.G. Orpen, Inorg. Chem. 47 (2008) 8767.
[60] J.R. Berenguer, M. Bernechea, J. Forniés, E. Lalinde, J. Torroba, Organometallics 24 (2005) 431.
[61] J.R. Berenguer, M. Bernechea, E. Lalinde, Organometallics 26 (2007) 1161.
[62] J.R. Berenguer, M. Bernechea, E. Lalinde, Dalton Trans. (2007) 2384.
[63] I. Ara, L.R. Falvello, J. Forniés, E. Lalinde, A. Martín, F. Martínez, M.T. Moreno, Organometallics 16 (1997) 5392.
[64] I. Ara, L.R. Falvello, S. Fernández, J. Forniés, E. Lalinde, A. Martín, M.T. Moreno, Organometallics 16 (1997) 5923.
[65] A. García, E. Lalinde, M.T. Moreno, Eur. J. Inorg. Chem. (2007) 3553.
[66] L.R. Falvello, S. Fernández, J. Forniés, E. Lalinde, F. Martínez, M.T. Moreno, Organometallics 16 (1997) 1326.
[67] C. Müller, R.J. Lachicotte, W.D. Jones, Organometallics 21 (2002) 1190.
[68] I. Ara, J.R. Berenguer, E. Eguizábal, J. Forniés, J. Gómez, E. Lalinde, J.M. Sáez-Rocher, Organometallics 19 (2000) 4385.
[69] I. Ara, J.R. Berenguer, J. Forniés, E. Lalinde, M.T. Moreno, Organometallics 15 (1996) 1820.
[70] J.R. Berenguer, J. Forniés, E. Lalinde, F. Martínez, E. Urriolabeitia, A.J. Welch, J. Chem. Soc., Dalton Trans. (1994) 1291.
[71] J.R. Berenguer, J. Forniés, E. Lalinde, A. Martín, B. Serrano, J. Chem. Soc., Dalton Trans. (2001) 2926.
[72] J.R. Berenguer, J. Forniés, E. Lalinde, F. Martínez, Organometallics 14 (1995) 2532.
[73] I. Ara, M. Bernechea, J. Forniés, E. Lalinde, A. Martín, J. Torroba, to be submitted.
[74] I. Ara, J.R. Berenguer, J. Forniés, E. Lalinde, M. Tomás, Organometallics 15 (1996) 1014.
[75] J.R. Berenguer, E. Eguizábal, L.R. Falvello, J. Forniés, E. Lalinde, A. Martín, Organometallics 18 (1999) 1653.
[76] K.M.C. Wong, W.H. Lam, Z.Y. Zhou, V.W.W. Yam, Chem. Eur. J. 14 (2008) 10928.
[77] J. Forniés, M.A. Gómez-Saso, E. Lalinde, F. Martínez, M.T. Moreno, Organometallics 11 (1992) 2873.
[78] L.R. Falvello, J. Forniés, J. Gómez, E. Lalinde, A. Martín, F. Martínez, M.T. Moreno, J. Chem. Soc., Dalton Trans. (2001) 2132.
[79] J.R. Berenguer, J. Forniés, F. Martínez, J.C. Cubero, E. Lalinde, M.T. Moreno, A.J. Welch, Polyhedron 12 (1993) 1797.
[80] L.R. Falvello, J. Forniés, A. Martín, J. Gómez, E. Lalinde, M.T. Moreno, J. Sacristán, Inorg. Chem. 38 (1999) 3116.
[81] G. Aullón, S. Alvarez, Organometallics 21 (2002) 2627.
[82] For derivatives with R = Bu^t, $SiMe_3$, $C(OH)Me_2$, $C_5H_4FeC_5H_5$, unpublished results.
[83] J.R. Berenguer, J. Forniés, E. Lalinde, F. Martínez, L. Sánchez, B. Serrano, Organometallics 17 (1998) 1640.
[84] W.J. Hoogervorst, C.J. Elsevier, M. Lutz, A.L. Spek, Organometallics 20 (2001) 4437.
[85] J.M. Casas, J. Forniés, S. Fuertes, A. Martín, V. Sicilia, Organometallics 26 (2007) 1674.
[86] J. Forniés, E. Lalinde, A. Martín, M.T. Moreno, J. Chem. Soc., Dalton Trans. (1994) 135.
[87] J.R. Berenguer, J. Forniés, E. Lalinde, F. Martínez, J. Organomet. Chem. 470 (1994) C15.
[88] M.I. Bruce, P.J. Low, M. Ke, B.D. Kelly, B.W. Skelton, M.E. Smith, A.H. White, N.B. Witton, Aust. J. Chem. 54 (2001) 453.
[89] H. Lang, I.Y. Wu, S. Weinmann, C. Weber, B. Nuber, J. Organomet. Chem. 541 (1997) 157.
[90] J.R. Berenguer, J. Forniés, E. Lalinde, A. Martín, Angew. Chem., Int. Ed. Engl. 33 (1994) 2083.
[91] J.R. Berenguer, L.R. Falvello, J. Forniés, E. Lalinde, M. Tomás, Organometallics 12 (1993) 6.
[92] W. Frosch, S. Back, M. Köhler, H. Lang, J. Organomet. Chem. 601 (2000) 226.
[93] A. Blagg, A.T. Hutton, P.G. Pringle, B.L. Shaw, Inorg. Chim. Acta 76 (1983) L265.
[94] A. Blagg, A.T. Hutton, P.G. Pringle, B.L. Shaw, J. Chem. Soc., Dalton Trans. (1984) 1815.
[95] S.W. Carr, P.G. Pringle, B.L. Shaw, J. Organomet. Chem. 341 (1988) 543.
[96] R.J. Blau, M.H. Chisholm, K. Folting, R.J. Wang, J. Am. Chem. Soc. 109 (1987) 4552.
[97] R.J. Blau, M.H. Chisholm, K. Folting, J. Chem. Soc., Chem. Commun. (1985) 1582.
[98] M.I. Bruce, K. Costuas, J.F. Halet, B.C. Hall, P.J. Low, B.K. Nicholson, B.W. Skelton, A.H. White, J. Chem. Soc., Dalton Trans. (2002) 383.
[99] P. Blenkiron, G.D. Enright, A.J. Carty, J. Chem. Soc., Chem. Commun. (1997) 483.
[100] P. Ewing, L.J. Farrugia, Organometallics 8 (1989) 1246.
[101] L.J. Farrugia, N. McDonald, R.D. Peacock, J. Cluster Sci. 5 (1994) 341.
[102] L.J. Farrugia, N. MacDonald, R.D. Peacock, J. Chem. Soc., Chem. Commun. (1991) 163.
[103] P. Ewing, L.J. Farrugia, J. Organomet. Chem. 320 (1987) C47.
[104] L.J. Farrugia, Organometallics 9 (1990) 105.
[105] W.Y. Wong, F.L. Ting, W.L. Lam, Eur. J. Inorg. Chem. (2001) 623.
[106] S. Yamazaki, Z. Taira, T. Yonemura, A.J. Deeming, Organometallics 24 (2005) 20.
[107] S. Yamazaki, Z. Taira, T. Yonemura, A.J. Deeming, A. Nakao, Chem. Lett. (2002) 1174.
[108] J. Lewis, B. Lin, P.R. Raithby, Trans. Met. Chem. 20 (1995) 569.
[109] S. Back, R.A. Gossage, M. Luz, I. del Río, A.L. Spek, H. Lang, G. van Koten, Organometallics 19 (2000) 3296.
[110] I. Ara, J.R. Berenguer, J. Forniés, E. Lalinde, Inorg. Chim. Acta 264 (1997) 199.
[111] A.T. Hutton, C.R. Langrick, D.M. McEwan, P.G. Pringle, B.L. Shaw, J. Chem. Soc., Dalton Trans. (1985) 2121.
[112] D.M. McEwan, D.P. Markham, P.G. Pringle, B.L. Shaw, J. Chem. Soc., Dalton Trans. (1986) 1809.
[113] D.H. Cao, P.J. Stang, A.M. Arif, Organometallics 14 (1995) 2733.
[114] I. Ara, J.R. Berenguer, E. Eguizábal, J. Forniés, E. Lalinde, A. Martín, F. Martínez, Organometallics 17 (1998) 4578.
[115] J.R. Berenguer, E. Eguizábal, L.R. Falvello, J. Forniés, E. Lalinde, A. Martín, Organometallics 19 (2000) 490.
[116] I. Ara, J.R. Berenguer, E. Eguizábal, J. Forniés, E. Lalinde, F. Martínez, Organometallics 18 (1999) 4344.
[117] I. Ara, J.R. Berenguer, E. Eguizábal, J. Forniés, E. Lalinde, Organometallics 20 (2001) 2686.
[118] I. Ara, J.R. Berenguer, J. Forniés, E. Lalinde, Organometallics 16 (1997) 3921.
[119] J. Forniés, J. Gómez, E. Lalinde, M.T. Moreno, Chem. Eur. J. 10 (2004) 888.
[120] J.R. Berenguer, J. Forniés, E. Lalinde, F. Martínez, Organometallics 15 (1996) 4537.
[121] K. Osakada, M. Hamada, T. Yamamoto, Organometallics 19 (2000) 458.
[122] H. Lang, A. del Villar, J. Organomet. Chem. 670 (2003) 45.
[123] D.E. Smith, A.J. Welch, I. Treurnich, R.J. Puddephatt, Inorg. Chem. 25 (1986) 4616.
[124] L. Manojlovic-Muir, K.W. Muir, I. Treurnich, R.J. Puddephatt, Inorg. Chem. 26 (1987) 2418.
[125] L. Manojlovic-Muir, A.N. Henderson, I. Treurnich, R.J. Puddephatt, Organometallics 8 (1989) 2055.
[126] S. Yamazaki, A.J. Deeming, M.B. Hursthose, K.M.A. Malik, Inorg. Chim. Acta 235 (1995) 147.
[127] H. Lang, A. del Villar, B. Walfort, G. Rheinwald, J. Organomet. Chem. 689 (2004) 1464.
[128] S. Yamazaki, A.J. Deeming, D.M. Speel, D. Hibbs, M.B. Hursthose, K.M.A. Malik, Chem. Commun. (1977) 177.
[129] H. Lang, A. del Villar, B. Walfort, Inorg. Chem. Commun. 7 (2004) 694.
[130] V.W.W. Yam, L.P. Chan, T.F. Lai, J. Chem. Soc., Dalton Trans. (1993) 2075.
[131] Q.S. Li, F.B. Xu, D.J. Cui, K. Yu, X.S. Zeng, X.B. Leng, H.B. Song, Z.Z. Zhang, Dalton Trans. (2003) 1551.
[132] G.Q. Yin, Q.H. Wei, L.Y. Zhang, Z.N. Chen, Organometallics 25 (2006) 580.
[133] Q.H. Wei, G.Q. Yin, Z. Ma, L.X. Shi, Z.N. Chen, Chem. Commun. (2003) 2188.
[134] V.W.W. Yam, K.L. Yu, K.M.C. Wong, K.K. Cheung, Organometallics 20 (2001) 721.
[135] V.W.W. Yam, C.K. Hui, K.M.C. Wong, N. Zhu, K.K. Cheung, Organometallics 21 (2002) 4326.
[136] H. Lang, A. del Villar, G. Rheinwald, J. Organomet. Chem. 587 (1999) 284.
[137] C.J. Adams, P.R. Raithby, J. Organomet. Chem. 578 (1999) 178.
[138] C.J. Adams, N. Fey, Z.A. Harrison, I.V. Sazanovich, M. Towrie, J.A. Weinstein, Inorg. Chem. 47 (2008) 8242.
[139] R. Packheiser, B. Walfort, H. Lang, Organometallics 25 (2006) 4579.
[140] D. Fortin, S. Clément, K. Gagnon, J.F. Bérubé, M.P. Stewart, W.E. Geiger, P.D. Harvey, Inorg. Chem. 48 (2009) 446.
[141] S. Yamazaki, A.J. Deeming, J. Chem. Soc., Dalton Trans. (1993) 3051.
[142] H. Lang, A. del Villar, B. Walfort, G. Rheinwald, J. Organomet. Chem. 682 (2003) 155.
[143] A. Jakob, P. Ecorchard, K. Köhler, H. Lang, J. Organomet. Chem. 693 (2008) 3479.
[144] W.Y. Wong, G.L. Lu, K.H. Choi, J. Organomet. Chem. 659 (2002) 107.
[145] I. Ara, J.R. Berenguer, J. Forniés, E. Lalinde, M.T. Moreno, J. Organomet. Chem. 510 (1996) 63.
[146] H. Lang, P. Zoufalá, S. Klaib, A. del Villar, G. Rheinwald, J. Organomet. Chem. 692 (2007) 4168.
[147] H. Lang, A. del Villar, T. Stein, P. Zoufalá, T. Rüffer, G. Rheinwald, J. Organomet. Chem. 692 (2007) 5203.
[148] P. Espinet, J. Forniés, F. Martínez, M. Sotés, E. Lalinde, M.T. Moreno, A. Ruiz, A.J. Welch, J. Organomet. Chem. 403 (1991) 253.
[149] J. Forniés, J. Gómez, E. Lalinde, M.T. Moreno, Inorg. Chim. Acta 347 (2003) 145.
[150] I. Ara, J.R. Berenguer, E. Eguizábal, J. Forniés, E. Lalinde, A. Martín, Eur. J. Inorg. Chem. (2001) 1631.
[151] J. Forniés, E. Lalinde, F. Martínez, M.T. Moreno, A.J. Welch, J. Organomet. Chem. 455 (1993) 271.
[152] J. Forniés, M.A. Gómez-Saso, F. Martínez, E. Lalinde, M.T. Moreno, A.J. Welch, New J. Chem. 16 (1992) 483.
[153] I. Ara, J.R. Berenguer, E. Eguizábal, J. Forniés, J. Gómez, E. Lalinde, J. Organomet. Chem. 670 (2003) 221.
[154] I. Ara, J. Forniés, E. Lalinde, M.T. Moreno, M. Tomás, J. Chem. Soc., Dalton Trans. (1995) 2397.
[155] I. Ara, J. Forniés, E. Lalinde, M.T. Moreno, M. Tomás, J. Chem. Soc., Dalton Trans. (1994) 2735.
[156] J. Forniés, S. Fuertes, A. Martín, V. Sicilia, E. Lalinde, M.T. Moreno, Chem. Eur. J. 12 (2006) 8253.
[157] A. Díez, A. García, E. Lalinde, M.T. Moreno, Eur. J. Inorg. Chem. (2009) 3060.

[158] S.M. AlQaisi, K.J. Galat, M. Chai, D.G. Ray III, P.L. Rinaldi, C.A. Tessier, W.J. Youngs, J. Am. Chem. Soc. 120 (1998) 12149.
[159] J. Manna, C.J. Kuehl, J.A. Whiteford, P.J. Stang, D.C. Muddiman, S.A. Hofstadler, R.D. Smith, J. Am. Chem. Soc. 119 (1997) 11611.
[160] J.A. Whiteford, C.V. Lu, P.J. Stang, J. Am. Chem. Soc. 119 (1997) 2524.
[161] C. Müller, J.A. Whiteford, P.J. Stang, J. Am. Chem. Soc. 120 (1998) 9827.
[162] J.A. Whiteford, P.J. Stang, S.D. Huang, Inorg. Chem. 37 (1998) 5595.
[163] D. Pellico, M. Gómez-Gallego, P. Ramírez-López, M.J. Mancheño, M.A. Sierra, M.R. Torres, Chem. Eur. J. 15 (2009) 6940.
[164] S. Tanaka, Y. Yoshida, T. Adachi, T. Yoshida, K. Onitsuka, K. Sonogashira, Chem. Lett. (1994) 877.
[165] P. Espinet, J. Forniés, F. Martínez, M. Tomás, E. Lalinde, M.T. Moreno, A. Ruiz, A.J. Welch, J. Chem. Soc., Dalton Trans. (1990) 791.
[166] J. Benito, J.R. Berenguer, J. Forniés, B. Gil, J. Gómez, E. Lalinde, Dalton Trans. (2003) 4331.
[167] J. Forniés, E. Lalinde, A. Martín, M.T. Moreno, J. Organomet. Chem. 490 (1995) 179.
[168] B. Gil, J. Forniés, J. Gómez, E. Lalinde, A. Martín, M.T. Moreno, Inorg. Chem. 45 (2006) 7788.
[169] V.W.W. Yam, K.L. Yu, K.K. Cheung, J. Chem. Soc., Dalton Trans. (1999) 2913.
[170] V.W.W. Yam, C.K. Hui, S.Y. Yu, N. Zhu, Inorg. Chem. 43 (2004) 812.
[171] J. Gómez, Universidad de La Rioja, Ph.D. Thesis, 2000.
[172] H.V.R. Dias, J.A. Flores, J. Wu, P. Kroll, J. Am. Chem. Soc. 131 (2009) 11249.
[173] I. Ara, J. Forniés, J. Gómez, E. Lalinde, R.I. Merino, M.T. Moreno, Inorg. Chem. Commun. 2 (1999) 62.
[174] I. Ara, J. Forniés, J. Gómez, E. Lalinde, M.T. Moreno, Organometallics 19 (2000) 3137.
[175] J.P.H. Charmant, J. Forniés, J. Gómez, E. Lalinde, R.I. Merino, M.T. Moreno, A.G. Orpen, Organometallics 18 (1999) 3353.
[176] This transition is believed to involve a platinum-based HOMO corresponding to a dσ* function formed by overlapping d_z2 orbitals, which are antibonding with regard to the axial Pt–Pt bond, whereas the LUMO should be located on Pt(*pz*) and the ligands (π*C≡CPh).
[177] C.R. Langrick, D.M. McEwan, P.G. Pringle, B.L. Shaw, J. Chem. Soc., Dalton Trans. (1983) 2487.
[178] D.M.P. Mingos, R. Vilar, D. Rais, J. Organomet. Chem. 641 (2002) 126.
[179] J.R. Berenguer, J. Forniés, E. Lalinde, A. Martín, M.T. Moreno, J. Chem. Soc., Dalton Trans. (1994) 3343.
[180] R.J. Cross, M.F. Davidson, J. Chem. Soc., Dalton Trans. (1986) 1987.
[181] R.J. Cross, J. Gemmill, J. Chem. Soc., Dalton Trans. (1984) 199.
[182] D. Zhang, D.B. McConville, C.A. Tessier, W.J. Youngs, Organometallics 16 (1997) 824.
[183] W. Frosch, A. del Villar, H. Lang, J. Organomet. Chem. 602 (2000) 91.
[184] K.R. Flower, V.J. Howard, S. Naguthney, R.G. Pritchard, J.E. Warren, A.T. McGown, Inorg. Chem. 41 (2002) 1907.
[185] S.S. Batsanov, J. Chem. Soc., Dalton Trans. (1998) 1541.
[186] J.P.H. Charmant, L.R. Falvello, J. Forniés, J. Gómez, E. Lalinde, M.T. Moreno, A.G. Orpen, A. Rueda, Chem. Commun. (1999) 2045.
[187] J. Forniés, J. Gómez, E. Lalinde, M.T. Moreno, Inorg. Chem. 40 (2001) 5415.
[188] EHMO calculations on $[Pt(C{\equiv}CPh)_4CdCl]_2^{2-}$ gave: HOMO π*Pt(*d*, 36%)-π(C≡CPh), LUMO πPt(*pz*, 10%)-π*(C≡CPh), Cd.(*sp* 4%).
[189] J. Fernández, J. Forniés, B. Gil, J. Gómez, E. Lalinde, M.T. Moreno, Organometallics 25 (2006) 2274.
[190] J. Forniés, S. Ibáñez, A. Martín, B. Gil, E. Lalinde, M.T. Moreno, Organometallics 23 (2004) 3963.
[191] J.R. Berenguer, B. Gil, J. Fernández, J. Forniés, E. Lalinde, Inorg. Chem. 48 (2009) 5250.
[192] K. Haskins-Glusac, I. Ghiviriga, K.A. Abboud, K.S. Schanze, J. Phys. Chem. B 108 (2004) 4969.
[193] J.P.H. Charmant, J. Forniés, J. Gómez, E. Lalinde, R.I. Merino, M.T. Moreno, A.G. Orpen, Organometallics 22 (2003) 652.
[194] A. Sebald, B. Wrackmeyer, C.R. Theocharis, W. Jones, J. Chem. Soc., Dalton Trans. (1984) 747.
[195] B. Wrackmeyer, A. Sebald, J. Organomet. Chem. 544 (1997) 105.
[196] G. Butler, C. Eaborn, A. Pidcock, J. Organomet. Chem. 210 (1981) 403.
[197] C. Cauletti, C. Furlani, A. Sebald, Gazz. Chim. Ital. 118 (1988) 1.
[198] M. Herberhold, U. Steffl, W. Milius, B. Wrackmeyer, Chem. Eur. J. 4 (1998) 1027.
[199] P. Pykkö, Angew. Chem., Int. Ed. 43 (2004) 4412.
[200] M.J. Katz, K. Sakai, D.B. Leznoff, Chem. Soc. Rev. 37 (2008) 1884.
[201] V.W.W. Yam, E.C.C. Cheng, Chem. Soc. Rev. 37 (2008) 1806.
[202] B.M. Anderson, S.K. Hurst, Eur. J. Inorg. Chem. 21 (2009) 3041.
[203] C.M. Che, S.W. Lai, Coord. Chem. Rev. 249 (2005) 1296.
[204] E. Fernández, A. Laguna, J.M. López-de-Luzuriaga, Dalton Trans. (2007) 1969.
[205] L.R. Falvello, J. Forniés, E. Lalinde, B. Menjón, M.A. García-Monforte, M.T. Moreno, M. Tomás, Chem. Commun. (2007) 3838.
[206] K. Matsumoto, K. Sakai, Adv. Inorg. Chem. 49 (2000) 375.
[207] L.R. Falvello, J. Forniés, R. Garde, A. García, E. Lalinde, M.T. Moreno, A. Steiner, M. Tomás, I. Usón, Inorg. Chem. 45 (2006) 2543.
[208] J. Forniés, A. García, E. Lalinde, M.T. Moreno, Inorg. Chem. 47 (2008) 3651.
[209] J.R. Stork, M.M. Olmstead, J.C. Fettinger, A.L. Balch, Inorg. Chem. 45 (2006) 849.
[210] W. Chen, F. Liu, D. Xu, K. Matsumoto, S. Kishi, M. Kato, Inorg. Chem. 45 (2006) 5552.
[211] J.K. Nagle, A.L. Balch, M.M. Olmstead, J. Am. Chem. Soc. 110 (1988) 319.
[212] G. Gliemann, H. Yersin, Struct. Bonding 62 (1985) 87.
[213] A.L. Balch, E.Y. Fung, J.K. Nagle, M.M. Olmstead, S.P. Rowley, Inorg. Chem. 32 (1993) 3295.
[214] J.R. Berenguer, J. Forniés, B. Gil, E. Lalinde, Chem. Eur. J. 12 (2006) 785.
[215] J.R. Berenguer, J. Forniés, J. Gómez, E. Lalinde, M.T. Moreno, Organometallics 20 (2001) 4847.
[216] A.L. Balch, Angew. Chem., Int. Ed. 48 (2009) 2641.
[217] I. Ara, J.R. Berenguer, J. Forniés, J. Gómez, E. Lalinde, R.I. Merino, Inorg. Chem. 36 (1997) 6461.
[218] J. Forniés, S. Fuertes, A. Martín, V. Sicilia, B. Gil, E. Lalinde, Dalton Trans. (2009) 2224.
[219] J.R. Berenguer, A. Díez, J. Fernández, J. Forniés, A. García, B. Gil, E. Lalinde, M.T. Moreno, Inorg. Chem. 47 (2008) 7703.